UNIVERSITÀ
DEGLI STUDI
DI PADOVA

Head Office: Università degli Studi di Padova

Department of Pharmaceutical and Pharmacological Sciences

Ph.D. COURSE IN: MOLECULAR SCIENCES
CURRICULUM: PHARMACEUTICAL SCIENCES
SERIES: XXXII

DEVELOPMENT OF TRANSDERMAL DELIVERY SYSTEMS FOR INNOVATIVE CLINICAL APPLICATIONS OF CANNABINOIDS

Coordinator: Ch.mo Prof. Leonard Prins
Supervisor: Ch.mo Prof. Nicola Realdon
Co-supervisor: Ch.mo Prof. Giovanni Marzaro

Ph.D. student: Elisa Vettorato

Table of contents

List of abbreviations

11-OH-THC: 11-hydroxy-Δ^9-tetrahydrocannabinol
2-AG: 2-arachidonylglicerol
5-HT: 5-hydroxytryptamine, serotonin
5-$HT_{1–2A}$: serotonin type 1 or 2A receptor
5-HT_3: serotonin type 3 receptor
90G: phospholipid Phospholipon® 90G
ACMPR: Access to Cannabis for Medical Purposes Regulations
AD: anno Domini
AEA: N-arachidonylethanolamide, anandamide
AUC: area under the curve
AVPC: 9-antrivinyl labeled analog of phosphatidylcholine
$BF_3 \cdot Et_2O$: boron trifluoride diethyl etherate
CE: cyclohexane
CBC: cannabichromene
CB1: cannabinoid receptor type 1
CB2: cannabinoid receptor type 2
CBD: cannabidiol
CBDA: cannabidiolic acid
CBG: cannabigerol
CBGA: cannabigerolic acid
CBN: cannabinol
$CDCl_3$: deuterated chloroform
CFR: Code of Federal Regulations
CH_2Cl_2, DCM: dichloromethane
CH_2CN, ACN: acetonitrile
CH_3COOH: acetic acid
$CHCl_3$: chloroform
CLSM: Confocal Laser Scanning Microcopy
COX-2: cyclooxygenase-2
CSA: Controlled Substance Act
CuI: copper iodide
CYP2C: cytochrome P450 isozyme 2C
CYP3A: cytochrome P450 isozyme 3A
DDW: double distilled water

DH-CBD: desoxycannabidiol, deoxycannabidiol
DIPEA: *N,N*-diisopropylethylamine
DLS: Dynamic Light Scattering
DM: *Decreto Ministeriale* (Ministerial Decree)
DMF: *N,N*-dimethylformamide
DPR: *Decreto del Presidente della Repubblica* (Presidential Decree)
DSC: Differential Scanning Calorimetry
EMA: European Medicine Agency
Et_3N: triethylamine
EtOAc: ethyl acetate
EtONa: sodium ethoxide
EtOH: ethanol
EU: European Union
FAAH: Fatty Acid Amide Hydrolase
FDA: United States Food and Drug Administration agency
FITC: fluorescein isothiocyanate
FITC-Bac: fluorescein isothiocyanate-labeled bacitracine
GABA: γ-aminobutyric acid
GC-MS: gas chromatography-mas spectrometry
Gly-R: glycine receptor
GMP: Good Manufacturing Practices
GPCRs: G-protein Coupled Receptors
H_2O: water
H_2O_2: hydrogen peroxide
HBr: hydrobromic acid
HCl: hydrochloric acid
HCOOH: formic acid
HPLC: High Performance Liquid Chromatography
HPLC-DAD: High-Performance Liquid Chromatography with Diode-Array Detection
I_{Gly}: glycine flux
K_B: equilibrium dissociation constant of a competitive agonist
LC-DAD-ESI-MS: Liquid Chromatography with Diode-Array Detection coupled with Electrospray Ionization Mass Spectrometry
LGS: Lennox-Gastaut syndrome
MAA: Marketing Authorization Application
m-CPBA: m-chloroperbenzoic acid
MeOH: methanol
mQ: ultrapure milliQ water

MS: multiple sclerosis
MWCO: molecular weight cut-off
Na_2CO_3: sodium bicarbonate
$NaHCO_3$: sodium bicarbonate
Na_2SO_3: sodium sulfite
Na_2SO_4: sodium sulfate
NaCl: sodium chloride
NaOH: sodium hydroxide
NBS: N-bromosuccinimide
n-BuLi: n-butyllithium
NH_3: ammonia
NH_4Cl: ammonium chloride
NH_4OH: ammonium hydroxide, ammonia solution
NMR: Nuclear Magnetic
OA: oleic acid
OMC: Office of Medicinal Cannabis
OO: olive oil
PC: phosphatidylcholine
PdI: polydispersity index
Pd(OAc): palladium(II) acetate
PG: propylene glycol
Ph_3P: triphenylphosphine
pK_a: acid dissociation constant
PTFE: polytetrafluoroethylene
PTSD: post-traumatic stress disorder
REV: Receptor Essential Volume
R_f: retention factor
RR: rhodamine red-dihexadecanoylglycerophosphoethanolamine
RT: room temperature
S100: phospholipid Lipoid S100
SC: stratum corneum
SCFM: *Stabilimento Chimico Farmaceutico Militare di Firenze* (Military Pharmaceutical Chemical Works of Florence)
TEM: Transmission Electron Microscopy
Tf_2O: trifluoromethanesulfonic anhydride
THCA-A: delta-9-tetrahydrocannabinolic acid subtype A
THCA-B: delta-9-tetrahydrocannabinolic acid subtype B
THCV: tetrahydrocannabivarin

THP: trihexyphenidyl hydrochloride
TLC: thin layer chromatography
T_m: transition temperature in DSC analysis
TMS: tetramethylsilane
TRIS: tris(hydroxymethyl)aminomethane
TRPA1: Transient Receptor Potential cation channel subfamily A
TRPM8: Transient Receptor Potential cation channel subfamily M
TRPV1: Transient Receptor Potential Vanilloid V1
TSC: Tuberous Sclerosis Complex
USA: United Stated of America
UV-Vis: ultraviolet-visible spectroscopy
Δ^9-THC, THC: delta-9-tetrahydrocannabinol
Δ^9-THCA: delta-9-tetrahydrocannabinolic acid

NMR PEAKS
d: doublet
dd: doublet of doublets
ddd: doublet of doublets of doublets
dquart: doublet of quartets
dt: doublet of triplets
m: multiplet
quint: quintet
s: singlet
s br: broad singlet
t: triplet

Abstract

The use of cannabis for medicinal purposes is deeply rooted in history, dating back to ancient times. Once recommended by many physicians for numerous diseases, through millennia this plant has lived several revivals and new falls, driven by different factors rather than by science alone. In the past century, new analytical techniques could unveil the chemistry and biochemistry of cannabis main compounds, thus increasing its potential therapeutic applications. While there has been a strong push for legalizing medicinal cannabis and research, conclusive evidence regarding the short- and long-term health effects (harms and benefits) of cannabis use remains elusive. Poorly designed scientific research studies have resulted in a lack of information on the health implications of cannabis use. Very scarce guidelines can help healthcare practitioners and patients as they make choices regarding the issues of if, when, where, and how to use cannabis safely and effectively for therapeutic purposes. Among the major concerns in cannabis use, there is a lack of knowledge about pharmacokinetic and pharmacodynamic properties of cannabinoids, modes of delivery, effects of different concentrations, and the dose-response relationships. These limitations could be overcome by controlling the delivered dose to the patient, minimizing the variability coming from the plant extraction products. Transdermal delivery of cannabinoids could allow a constant, defined release of these active ingredients. Due to the high lipophilicity of cannabinoids, innovative transdermal delivery systems are needed to overcome the skin barrier. Scientific research on cannabis, though, cannot be easily pursued, because its acquisition and detention have been restricted by narcotic laws. In Italy, both plant-derived and synthetic cannabinoids ("substances obtained by synthesis or semi-synthesis amenable for chemical structure or pharmaco-toxicological effect to tetrahydrocannabinol") are restricted by the DPR 1990, n° 309.

The main goal of this project was to develop innovative pharmaceutical forms in order to ensure a constant release of cannabinoids to the patient, avoiding the variability coming from a massive first-pass effect when administered orally, and the intoxicating effects coming from inhalation of cannabinoids. For the restrictions mentioned above, a model molecule was chosen for the development of these pharmaceutical forms, searching compounds with similar behavior and solubility of the most abundant and effective cannabinoid, Δ^9-tetrahydrocannabinol (THC), but without its intrinsic psychotropic effects. From a peculiar analysis of the structure-activity relationship of THC, and the literature available on cannabinoids, the choice was desoxy-CBD, a CBD-derivative which has been studied during the last years for its interesting actions in the regulation of the glycinergic spinal system, involved especially in pain signaling. The great advantage of this molecule is the absence of psychoactivity, dramatically reducing the risk of addiction. This molecule, although, is not easily available on the market; thus, it was

synthesized as described in Chapter 2. The synthetic pathway was improved in terms of efficiency and stereoselectivity by synthesis and condensation of two synthons, *m*-pentylphenol and *p*-mentha-2,8-dien-1-ol, from 3-methoxybenzylbromide and R-(+)-limonene. A semisynthetic pathway was then used, by a reductive dehydroxylation of CBD itself, enhancing the total yield from 6% to 50%.

Once synthesized, desoxy-CBD was characterized and purified, and formulated into vesicular drug delivery systems. These systems were based on the technology of ethosomes: soft, deformable vesicles composed mainly of phospholipidic multilayers enclosing a hydroethanolic core. Ethosomes were patented by Prof. Elka Touitou in 1998, and their unique features were studied over the last 20 years. Their soft structure, small size, negative ζ-potential, and high entrapment efficiency improve the skin penetration of the loaded drugs compared to other rigid vesicular systems. The properties and technology of ethosomes have been studied in a secondment into the laboratory of Prof. Touitou at the Hebrew University of Jerusalem (Israel), and the results are reported in Chapter 3.

Innovative vesicular systems containing propylene glycol or oleic acid were developed in the laboratories of Pharmaceutical technology in Padova. Systems with different concentrations of ethanol, phosphatidylcholine, propylene glycol or oleic acid, and aqueous phase were performed and tested in terms of stability, particle size, pH when necessary. The most stable systems were then loaded with cannabidiol or desoxy-CBD, and their properties were compared. Vesicles containing cannabinoids were incorporated into hydrogels to improve their stability and a future application onto the patients' skin. Loaded hydrogels were then studied for their rheological profile and, in the case of vesicles with propylene glycol, tested for their release properties. The main results of PG-containing systems are reported in Chapter 3, while for vesicles containing OA are described in Chapter 4. As the main goal of this project was the delivery of cannabinoids coming from cannabis flowering tops, preliminary studies on the extractions of cannabis in olive oil and ethanol were performed. The extracts were then formulated into the most stable vesicular systems containing propylene glycol or oleic acid, which were further characterized in terms of particle size, pH and stability, and the main results are reported in Chapter 4.

Riassunto

L’uso della cannabis a scopo terapeutico ha radici molto profonde nella storia. Mentre un tempo veniva prescritta da molti medici per un vasto numero di patologie, nel corso dei millenni la cannabis e il suo uso in medicina hanno vissuto numerosi ritorni e cadute, spesso dipendenti da fattori non sempre legati alla scienza. Nell’arco dell’ultimo secolo, sono state utilizzate nuove tecniche analitiche per investigare la chimica e la biochimica dei comporti preponderanti della cannabis, ed in tal modo è aumentato anche il potenziale terapeutico di questo prodotto. Nonostante ci sia stato un forte impulso verso la legalizzazione dell’uso terapeutico della cannabis e la ricerca a riguardo, rimangono tuttora sfuggenti le evidenze scientifiche riguardanti gli effetti a breve o lungo termine, sia in termini di tossicità che di efficienza terapeutica. Gli studi scientifici a riguardo sono molteplici, tuttavia la scarsa qualità della loro progettazione è ciò che ancora oggi rende limitate le informazioni a disposizione riguardanti gli effetti sulla salute dei pazienti. Sono poche le linee guida che possono aiutare i professionisti del settore sanitario per scegliere se prescrivere la cannabis, quale tipo, quando e come usarla per il trattamento di uno stato patologico. Tra le maggiori problematiche nell’uso di questo farmaco vi è la mancanza di conoscenza dettagliata sulla farmacocinetica e farmacodinamica dei cannabinoidi, sulla via di somministrazione più efficace, gli effetti riscontrabili a diverse concentrazioni e la relazione dose-risposta. Questi punti potrebbero essere superati tramite il controllo della dose somministrata, minimizzando la variabilità che intrinsecamente un prodotto vegetale porta con sé. La somministrazione transdermica dei cannabinoidi potrebbe assicurare un rilascio costante, definito e prolungato nel tempo. A causa dell’elevata lipofilicità dei cannabinoidi, sono necessari sistemi di somministrazione transdermica innovativi per superare la barriera cutanea ed evitare l’accumulo nello strato corneo. La ricerca sui cannabinoidi, tuttavia, non può essere eseguita facilmente, poiché regolata dalle norme sulle sostanze stupefacenti e psicotrope: in Italia, tale normativa prevede la regolamentazione sia dei prodotti vegetali (Tabella II) che delle sostanze di sintesi o semisintesi riconducibili per struttura chimica o attività farmaco-tossicologica al tetraidrocannabinolo (Tabella I) all’interno del DPR 1990, n°309.

L'obiettivo principale di questo progetto è stato lo sviluppo di forme farmaceutiche innovative al fine di garantire un rilascio costante di cannabinoidi per il paziente, evitando la variabilità derivante da un massiccio effetto di primo passaggio tipico della somministrazione orale, e la tossicità derivante dall'inalazione. Per le restrizioni sopra menzionate, è stata scelta una molecola modello per lo sviluppo di queste forme farmaceutiche, ricercando composti con proprietà chimiche e solubilità simili al Δ^9-tetraidrocannabinolo (THC), ma senza i suoi intrinseci effetti psicotropi. Da un'analisi peculiare della relazione struttura-attività del THC e

dalla letteratura disponibile sui cannabinoidi, la scelta è stata desossi-CBD, un derivato del CBD che è stato studiato negli ultimi anni per le sue interessanti azioni nella regolazione del sistema glicinergico situato nel midollo spinale, il quale è coinvolto soprattutto nelle vie di segnalazione del dolore. Il grande vantaggio di questa molecola è l'assenza di psicoattività, che riduce drasticamente il rischio di dipendenza. Tuttavia, questa molecola non è facilmente disponibile sul mercato, e per questo motivo è stata sintetizzata come descritto nel Capitolo 2. La via sintetica di letteratura è stata migliorata in termini di efficienza e stereoselettività, mediante la sintesi e la condensazione di due sintoni, *m*-pentilfenolo e *p*-menta-2,8-dien-1-olo, rispettivamente a partire da 3-metossibenzilbromuro e R-(+)-limonene. Successivamente è stata utilizzata una via semisintetica, mediante una deidrossilazione riduttiva del CBD stesso, aumentando la resa totale di reazione dal 26,0% al 41,0%.

Una volta sintetizzato, il desossi-CBD è stato caratterizzato e purificato, e formulato in sistemi vescicolari. Questi sono stati basati sulla tecnologia degli etosomi: vescicole non rigide e deformabili, composte principalmente da multistrati di fosfolipidi che racchiudono un nucleo idroetanolico. Gli etosomi sono stati brevettati dalla Prof. Elka Touitou nel 1998 e le loro caratteristiche uniche sono state studiate negli ultimi 20 anni. La loro struttura deformabile, le loro dimensioni ridotte, il loro potenziale *z* negativo e l'elevata efficienza di intrappolamento, migliorano la permeazione cutanea dei farmaci caricati, rispetto ad altri sistemi vescicolari rigidi. Le proprietà e la tecnologia degli etosomi sono state studiate in un periodo di visita nel laboratorio della Prof. Touitou presso la Hebrew University of Jerusalem (Israele), e i risultati ottenuti sono riportati nel Capitolo 3.

Nei laboratori di tecnologia farmaceutica di Padova sono stati sviluppati innovativi sistemi vescicolari contenenti glicole propilenico o acido oleico. Sistemi con diverse concentrazioni di etanolo, fosfatidilcolina, glicole propilenico o acido oleico, e fase acquosa sono stati eseguiti e testati in termini di stabilità, dimensione delle particelle e pH quando richiesto. I sistemi più stabili sono stati quindi caricati con cannabidiolo o desossi-CBD e le diverse proprietà sono state confrontate tra loro. Le vescicole contenenti cannabinoidi sono state incorporate in idrogeli per migliorare la loro stabilità, così come una futura applicazione sulla cute dei pazienti. Gli idrogel caricati sono stati quindi studiati per il loro profilo reologico e, nel caso di vescicole con glicole propilenico, sono stati testati per le loro proprietà di rilascio. I principali risultati dei sistemi contenenti PG sono riportati nel Capitolo 3, mentre per le vescicole contenenti OA sono descritti nel capitolo 4. Poiché l'obiettivo principale di questo progetto era la veicolazione di cannabinoidi provenienti da infiorescenze di cannabis, sono stati eseguiti studi preliminari sulle estrazioni di cannabis in olio d'oliva ed etanolo. Gli estratti sono stati quindi formulati nei sistemi vescicolari più stabili contenenti glicole propilenico o acido oleico, che sono stati ulteriormente caratterizzati in termini di dimensione delle particelle, pH e stabilità, e dei quali i principali risultati sono riportati nel Capitolo 4.

Chapter 1

Introduction on cannabis

1.2 CANNABIS AND CANNABINOIDS

Cannabis is among the world's oldest cultivated plants (1). Classified in the family *Cannabaceae* alongside with *Humulus lupulus*, cannabis is generally considered as a multitypic genus with at least two putative species, *Cannabis sativa* and *Cannabis indica* (2).
From the ancient times this plant was exploited for human use, and existing evidence suggests that its use in Europe and East Asia started in the early Holocene (3). Its properties were employed for medical and religious purposes, most notably in China and India (4). Great civilizations of the past, such as Ancient Egypt or Roman Empire, were believed to use cannabis especially for its fibers and seeds, but limited evidence suggests some therapeutic uses of this plant. Few medical Egyptian papyri indicate it was administered orally, as bandaging onto the skin or by fumigation (1, 5). On the other side, Galen and Ephippus described how the seeds may be cooked and eaten as a delicacy. Pliny the Elder (Gaius Plinius Secundus, c. 23–79 AD) mentioned cannabis in his Naturalis Historia of 77 AD (6): the cultivation, harvest and preparation were described, as well as its use for producing rope or material (7). In another volume of this same work, some indications of medical uses of cannabis were reported, and special warnings about its potency were given as well (8, 9). A renewed interest in Cannabis medical properties arose in the 19th century. In this period of colonial expansion into Africa and Asia, Cannabis found its way back to Europe, and many practitioners introduced its use in Western medicine. Described as "Indian hemp", it was known for its "intoxication symptoms", as well as a treatment for tetanus and other convulsive diseases (10), as well as a treatment for mental disorders (11).

Nowadays an extensive investigation about the characteristics of this ambiguous and disputed plant is available. Despite its extreme variability and the differences between each breed, all cannabis plants are easily recognized by certain distinct common botanical characteristics. Cannabis is generally dioecious, presenting male plants bearing staminate flowers and female plants bearing pistillate flowers. Only female flowers can eventually develop into the fruit and seeds. Specific breeds can be monoecious, and this condition is particularly frequent in varieties developed for industrial hemp production. Virtually every aerial part of the cannabis plant is covered in minute trichomes, either simple hairs (covering trichomes) or glandular trichomes

containing a resin. The latter type of trichomes, *i.e.*, capitate glandular trichomes, can be typically found on the bracts and floral leaves only. These trichomes have been proven to contain phytocannabinoids, the unique phytochemicals of cannabis, some of which are bioactive molecules responsible for both therapeutic and intoxicant properties of the plant. Within the trichomes, cannabinoids are present as a resinous substance. The phytocannabinoids content of trichomes can be highly variable according to the position on the same plant, with higher concentration in the apical inflorescences (12).

To present date, more than more than four hundred compounds belonging to a variety of phytochemical groups have been reported to occur in the plant, only few of them have been investigated for their pharmacological activities, and more than 104 psychoactive cannabinoids have been identified (2, 9, 12). Several studies demonstrated the extreme variability in the quali-quantitative profile of phytocompounds between cannabis varieties and in different cultivation conditions (13).

The phytochemistry of Cannabis sativa has been extensively researched. Over 7000 scientific papers had been published on cannabis, its constituents and their pharmacological activities by 1980 (14). The first isolation of one of the major compounds, cannabidiol, occurred between late 1930s and early 1940s by Roger Adams and co-workers (15, 16). Many detailed descriptions of the chemistry of cannabis have been published during ‘70s, such as those of Mechoulam (17) and Razdan (18). The psychoactive effects of cannabis and its preparations have been ascribed in the main to the presence of tetrahydrocannabinols (THCs), in particular the compound Δ^9-tetrahydrocannabinol (Δ^9-THC), which was first isolated in 1942 (19) and identified in 1964 thanks to the development of nuclear magnetic resonance imaging (20). Δ^9-THC is one of a group of mostly C21 compounds known as cannabinoids, which appear to be unique to Cannabis sativa (9).

It was only years after the investigation of THC chemistry that the effects of this compound found biochemical basis with the discovery of the cannabinoid receptors in 1988 (21), and anandamide in 1992 (22). This scientific foundation led to the re-emergence of cannabis as a modern medicine in the last decades (1).

1.2.1 CANNABINOID RECEPTORS AND ENDOCANNABINOIDS

The pharmacological action of cannabinoids is mainly due to their interaction with receptors and ion channels inside the human body, especially with the endocannabinoid system and the cannabinoids receptors, discovered in 1988 (1). The endocannabinoid system is widely distributed in the brain and spinal cord and assumes a crucial role in many regulatory physiological processes including neural development, synaptic plasticity and learning, pain,

memory, immune function, inflammation, appetite regulation, metabolism, cardiovascular function, digestion, psychomotor behavior, and regulation of stress and emotion (23).

The cannabinoid receptor 1 (CB1) and 2 (CB2) are members of the super family of G-protein-coupled receptors (GPCRs) (24) and were cloned for the first time in 1990 and 1993, respectively (25, 26). Both receptor types are coupled through G proteins to adenylyl cyclase and mitogen-activated protein kinase (27). In the last decades, CB1 receptors were found to be located primarily in central and peripheral neurons, while CB2 receptors predominantly in peripheral tissues and immune cells. CB1 receptors were also discovered in non-neuronal cells, including immune cells, whereas CB2 receptors can be present in some neuronal cells. The endocannabinoid system is believed to have a fundamental role in regulating neurotransmitters release, in order to prevent excessive neuronal activity in the central nervous system (24). This theory was supported by several studies on the location of the cannabinoid receptors: as pre-synaptic receptors, their activation causes the opening of potassium channel, and consequently inducing hyperpolarization of the pre-synaptic terminal. In addition, calcium channels are subsequently closed, inhibiting the release of a wide number of different excitatory and inhibitory neurotransmitters including acetylcholine, noradrenaline, dopamine, 5-hydroxytryptamine (5-HT), γ-aminobutyric acid (GABA) and others (28, 29). CB2 receptor activation can induce the release of cytokines from immune cells and, in addition, affect immune function by modulating immune cell migration both within and outside the central nervous system (30-32). CB1 and 2 receptors are also involved in anti-inflammatory processes. CB1-mediated effects are suspected to be secondary to inhibition of arachidonic acid conversion by cyclooxygenase (33). On the other hand, CB2 receptors induce immunosuppression, which leads to reduced inflammation (27).

Endogenous ligands of these receptors, generally named “endogenous cannabinoids”, were also discovered in last decades. Two of them are historically considered the main compounds, N-arachidonoylethanolamine (anandamide, or AEA), and 2-arachidonoylglycerol (2-AG), isolated from the brain in 1992 and from peripheral tissues in 1995, respectively (22, 34). A multitude of other endogenous mediators continue to be discovered even in these days (35). AEA is a partial agonist at CB receptors, and its affinity to CB1 receptors is slightly higher as compared to CB2 receptors. Similar behavior is registered in the affinity of 2-AG (26, 36). Anandamide and 2-AG are not stored in vesicles, but evidence was provided of on-demand synthesis from membrane phospholipid precursors when most needed (23). In the synthetic on-demand process, a crosstalk between eicosanoid and endocannabinoid pathways can occur (36, 37). The production of AEA and 2-AG occurs post-synaptically, while their action is mainly pre-synaptic, serving as fast retrograde synaptic messengers (26). Generally, endocannabinoids are rapidly removed from the intrasynaptic space by a membrane transport process (38). AEA is hydrolyzed to arachidonic acid and ethanolamine by fatty acid amide hydrolase (FAAH), while 2-AG is hydrolyzed both by FAAH and by monoacyl hydrolases. After suppression these

enzymes, a prolonged activity of endocannabinoids can be obtained (39). AEA and other cannabinoid agonists can also provide inhibitory effects on serotonin type 3 ($5HT_3$) receptors, and this could be connected to the anti-emetic and analgesic effects of exogenous cannabinoids (40).

1.2.2 TETRAHYDROCANNABINOL AND CANNABIDIOL

As previously stated, phytocannabinoids showed interesting pharmacologic activity mediated especially by interaction with CB1 and CB2 receptors. The two major compounds Δ^9-THC and CBD were extensively studied in their interactions with cannabinoid receptors. Δ^9-THC binds to CB1 and CB2 receptors with K_i values in the low nanomolar range. Its affinity to CB1 and partial agonist activity resulted very close to anandamide behavior, although its efficacy both at CB1 and CB2 resulted lower than the endogenous cannabinoids (24). CBD lacks detectable psychoactivity (41). In the first times it was demonstrated its capability to bind to CB1 and CB2 receptors at concentrations in the micromolar range. Such low affinity for these receptors led the pharmacological research with CBD to CB1- and CB2-independent modes of action. In recent times, however, evidence has emerged that CBD can interact with cannabinoid receptors at reasonably low concentrations. CBD resulted capable of antagonizing cannabinoid CB1/CB2 receptor agonists with apparent K_B values in the low nanomolar range (42).

Considering the results over experimentations on the interactions between Δ^9-THC and CBD with cannabinoids receptors, a reason of such different *in vivo* effects of these compounds could hardly be found. However, an explanation of this behavior can be given considering that neuronal CB1 receptors are targeted less selectively from exogenous compounds, which are metabolized over several hours (27), than anandamide itself, synthesized only when most needed and then rapidly removed (43, 44). Instead of promoting an inhibitory effect on neurotransmitter release from the neuron where they are located, these receptors when activated *in vivo* can enhance the release of transmitters from other neurons. In particular, there is evidence of an increased release of acetylcholine in rat hippocampus, of acetylcholine, glutamate and dopamine in rat prefrontal cortex, and of dopamine in mouse and rat nucleus accumbens (45–48). This last effect, *i.e.*, dopamine release in nucleus accumbens, could be the explanation to the "reward" effect given by Δ^9-THC, and partly to the ability of this phytocannabinoid to incentive to eat, and hence food intake (42). The mixed effect of Δ^9-THC, inhibitory and stimulatory, can be considered one of the reasons why this molecule causes both excitant and depressant effects in behavioral bioassays (27). This dual action is not only responsible of uncertain efficacy of Δ^9-THC, but also of a number of effects accounted as "psychoactivity", such as euphoria, dysphoria, dizziness, anxiety. Cognitive disturbance especially affecting short-term memory is registered in people assuming Δ^9-THC (27).

On the other side, CBD shows a duality too, but especially as agonist or inverse agonist of cannabinoid receptors, in particular CB2 receptors. CBD does interact with more than one target behaving as a CB2 receptor inverse agonist, and this is likely a consequence of its well-documented anti-inflammatory properties (41). In fact, it was demonstrated that inverse agonism of CB2 receptors can inhibit immune cell migration and reduce signs of inflammation. In some studies CBD showed significant inhibition of migration both of murine microglial cells and macrophages (49, 50) and of human neutrophils (51), but it has several other actions over different targets, some of which could lead to reduce inflammatory states (24). Among the several non-cannabinoid targets of CBD, fatty acid amide hydrolase and 5-lipoxygenase enzymes have been recognized to be downregulated by this molecule (52). CBD can bind to transient receptor potential vanilloid 1 (TRPV1) (53) and 5-$HT_{1–2A}$ receptors (54). These interactions, especially with 5-$HT_{1–2A}$ receptors, could be a possible explanation for some therapeutic effects of CBD not yet fully understood, most likely the anti-epileptic effect (55).
Widening the knowledge on the bioactivity of cannabinoids, the therapeutic effects of these molecules must be considered together with the strong side effects that are inevitable when assuming cannabinoids. These can be very deeply impacting, and long-term effects such as addiction can be registered in several cases. Short-term effects are the most evident and well investigated. During acute cannabis intoxication, subjective effects such as enhanced sociability, sensitivity to stimuli, appetite for sweet and fatty foods, and distorted perception of time are often registered (56). Other effects usually include short-term memory, dry mouth, and impaired perception and motor skills. With very high blood levels of Δ^9-THC, panic attacks, paranoid thoughts, and hallucinations may be experienced (57). Intensity and duration of acute cannabis intoxication can be influenced not only by Δ^9-THC dosage, but also from individual differences in the rate of absorption and metabolism of this compound, and the loss of sensitivity to its pharmacological actions. Sustained use of cannabis causes prolonged CB1 receptor occupation, which in turn triggers a process of desensitization, down-regulation of CB1 receptors and tolerance to cannabinoid agonists, as demonstrated in animals (58) and in humans, where the process can be reversed by abstinence (59).

1.2.2.1 ROUTES OF ADMINISTRATION AND METABOLISM

Self-administration of cannabinoids was pursued for medical as well as recreational purposes for centuries, resulting in different onset and duration of the effects according to the chosen modality. Generally, smoked or vaporized cannabis causes the fastest onset of action, *i.e.*, within minutes, due to the lipophilicity of Δ^9-THC. It results in higher cannabinoid blood levels and shorter duration of effects compared to all other routes (60). The psychotropic side effects start in a very short time, as well, with a peak in 15-30 minutes and ending within 2-3 hours. The bioavailability of Δ^9-THC can vary from 2% to 56% based on puff duration, breath hold

duration, and depth of inhalation, with an average of 25-27% in normal conditions (61). Vaporization is a relatively recent technique especially designed to heat cannabis to a temperature where active cannabinoid vapors form, but below the point of combustion where smoke and associated toxins are produced (62). Vaporization is preferable to smoking, due to less toxic byproducts such as tar, polycyclic aromatic hydrocarbons, and carbon monoxide, and to a more efficient extraction of Δ^9-THC (62,63).

Oral administration is the second major route. Bioavailability and blood peak of Δ^9-THC are much lower compared to smoking and vaporization (5-6 times lower) (64). The onset of action is much slower, with delayed psychotropic effects beginning in 30-90 minutes, a peak at 2-3 hours, and longer duration of action and effects lasting 4-12 hours (60). Such low values of bioavailability with oral administration of cannabinoids is mainly due to an extensive first-pass metabolism. The majority of cannabinoid metabolism occurs in the liver, with variable levels of different metabolites, dependent on the route of administration (60, 65). One of the most abundant metabolites is 11-hydroxy-Δ^9-tetrahydrocannabinol (11-OH-THC), which is a product of hepatic cytochrome P450 family. Further oxidation of this product leads to inactivation of the molecule, obtaining 11-nor-9-carboxy-Δ^9-tetrahydrocannabinol (66). Hepatic uptake occurs also for CBD, which behaves as a powerful inhibitor of many cytochrome P450 isozymes, including CYP2C and CYP3A (55). Similar pharmacokinetics and cannabinoid blood levels can be achieved with oral mucosal formulations (67). Intramuscular and intravenous administrations of Δ^9-THC alone were evaluated in few studies, and results suggested a more complete bioavailability as compared with the oral route (68).

Topical transdermal formulations have been developed in the last decades, although no clinical studies are available so far. Permeation studies over a dermal patch showed good results, suggesting the utility for development of a transdermal therapeutic system (69). Also, rectal formulations have been developed and showed promising results in the delivery of the prodrug Δ^9-THC hemisuccinate, with higher bioavailability of Δ^9-THC as compared to the oral route (70).

1.2.2.2 RECOGNIZED PARMACOLOGY

Considering the high variability on the cannabinoids amount coming from a natural product, the great number of their pharmacological targets, the still unknown *in vivo* effects of these molecules, and the differences in the pharmacokinetics according to the route of administration and the type of cannabinoid administered (whether from a natural or synthetic source), very little is the knowledge about the real therapeutic effect of cannabis and cannabinoids. Several studies were performed aiming to demonstrate the efficacy of this product, or the lack thereof, in the treatment of many pathologic conditions.

Conclusive evidence of benefit from cannabis and cannabinoids could be found in a range from modest to moderate effect in the treatment of chronic pain, chemotherapy-induced nausea and vomiting, and symptoms of spasticity associated with multiple sclerosis. Differences in efficacy was registered between routes of administration: oral route was more efficient in nausea and vomiting, and in spasticity associated with multiple sclerosis. On the other side, better management of chronic pain was achieved with smoked or vaporized cannabis (2). For many other conditions, such as symptoms of irritable bowel syndrome, epilepsy, spasticity in patients with paralysis due to spinal cord injury and motor system symptoms associated with Parkinson's disease or the levodopa-induced dyskinesia, there is insufficient or no evidence upon which to base conclusions about therapeutic effects (2).

The recognized evidence in cannabis efficacy was reflected into the development of a number of medications containing cannabinoids. The active ingredients can be synthesized or extracted from vegetable sources. Research in the 1960s and early 1970s led to the development of synthetic cannabinoids (71), thus introducing into the clinic of Δ^9-THC (dronabinol, Marinol®, Solvay Pharmaceuticals, Brussels, Belgium) and of one of its synthetic analogues, nabilone (Cesamet®, Valeant Pharmaceuticals, Aliso Viejo, CA, USA). Marinol® is available since 1992 in USA, when it was approved by FDA as 2.5 mg, 5 mg, or 10 mg Δ^9-THC tablets for nausea/vomiting associated with chemotherapy, and for acquired immune deficiency syndrome (AIDS)-associated anorexia and weight loss. It is typically used once to twice daily, and dose ranges vary from 2.5 to 40 mg/day (23, 24). Nabilone was approved by FDA as 0.25, 0.5, and 1 mg Δ^9-THC tablets. It is used once to 3 times daily, with a dose ranging from 0.2 to 6 mg/day, for the suppression of nausea and vomiting produced by chemotherapy (24, 72).
In recent times, another single-cannabinoid product recently approved by the European Medicines Agency (EMA) is an oral formulation of cannabidiol, Epidiolex© (GW Pharmaceuticals, Cambridge, United Kingdom). This oral solution of highly purified plant-derived cannabidiol received Orphan Drug Designation from FDA for the treatment of severe, drug-resistant epilepsy syndromes such as Dravet and Lennox-Gastaut syndromes (LGS), and from EMA for the treatment of LGS, Dravet syndrome, West syndrome and Tuberous Sclerosis Complex (TSC). Phase 3 clinical trials for these conditions ended in the last 2 years, and for the treatment of TSC are still ongoing. The company has also submitted a Marketing Authorization Application (MAA) to the EMA with positive decision obtained in July 2019 (73).
Another interesting formulation called Nabiximols (Sativex®) is available in Canada since 2005, and few years later it was approved also in Europe. It is an oromucosal spray made of cannabis extract containing Δ^9-THC and CBD in a 1:1 ratio, together with minor cannabinoids and other non-cannabinoid components. It is approved as an adjunct treatment for neuropathic pain in multiple sclerosis, and for moderate to severe cancer-related pain for patients who have failed the highest tolerated opiate dosing (23, 74).

The combination of Δ^9-THC (often shortened to "THC") and CBD in therapy showed some benefits as compared to the use of THC alone. CBD was reported to lower some of adverse events of THC, such as anxiety and paranoid symptoms (75). In addition, CBD can modulate the metabolism of THC by inhibiting the conversion to 11-OH-THC (76), and adjuvate the analgesic effect of THC with its anti-inflammatory and immunomodulatory effect (77). Moreover, many benefits in the administration of cannabis extract instead of synthetic cannabinoids were noted. Major and minor cannabinoids, terpenoids and flavonoids available in cannabis phytocomplex apparently have a synergistic effect, enhancing the therapeutic action (78) and reducing some side effects of THC. The interactions between cannabis compounds can be recognized as "entourage effects" (35, 79), since the combination of the bioactivities of these compounds results much more beneficial than the action of a single component. The differences in quantity and availability of specific terpenoids and flavonoids are nowadays well established and correlated to a specific strain of cannabis. The possibility of sophisticated crossbreed of specific strains to obtain standardized compositions of cannabinoids, terpenes, and other phytochemicals is now available, leading to safe, standardized vegetable products on the market (35). One of the main companies that achieved standardization in cannabis production is Bedrocan® (Bedrocan International, Veendam, Netherlands). Whole, dried female flowers top called *cannabis flos* are collected and show a distinct chemical profile for each variety. The same amount of THC, CBD, and terpenes is guaranteed in every batch (74). Meanwhile, the largest authorized importer, exporter, and distributor of cannabis in the European Union is Aurora Europe GmbH, subsidiary of Aurora Cannabis (Edmonton, Alberta, Canada), leader in German market since 2005 (80).

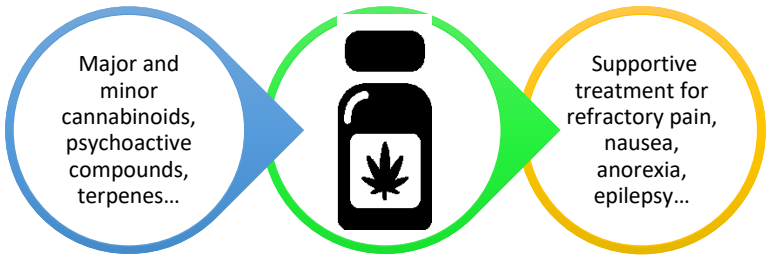

Figure 1.1 – Summary of cannabis-based medicine. The advantages coming from the use of a plant-derived product can mitigate side effects coming from isolated compounds.

1.3 ADVANCED CANNABIS LAWS AND ACTS

Cannabis is historically known as a psychotropic plant and it is distinguished from the industrial hemp, which is used for its fibers. Many pharmacological applications have been suggested through centuries, but the safety and efficacy profiles are still to be fully understood. Several attempts were made in the past to regulate the prescription of cannabis from physicians. In the following paragraphs will be given an overview on the most advanced legislation for the medical prescription and regulation of cannabis worldwide.

1.3.1 NORTH AMERICA

1.3.1.1 UNITED STATES OF AMERICA

In USA, the third edition of the Pharmacopoeia included cannabis for the first time in 1851, and subsequently some revisions included extraction methods and tinctures from dried flowers (1, 81). However, in 1942 was definitively removed from the 12th edition of U.S. Pharmacopeia after the period of federal prohibition of the drugs in 1937 (82, 83). Legal restrictions were then extended to the isolated THC in 1968, and the Comprehensive Drug Abuse Prevention and Control Act was introduced in 1970 (9). Since the promulgation of this Act, cannabis is listed as a schedule I drug (94). Nowadays, the legislation about medical prescription of cannabis or cannabinoids in USA is controversial. Cannabis itself is not approved by the U.S. Food and Drug Administration agency (FDA) as a safe and effective drug for any indication [FDA website (85). Two synthetic pharmaceutical versions of oral Δ^9-THC are approved: Dronabinol (Marinol® and Syndros®), listed in Schedule III, and Nabilone (Cesamet®), listed in Schedule II (86–88).

As of cannabis-derived products, one specific drug product containing cannabidiol was FDA-approved for the treatment of seizures associated with Lennox-Gastaut syndrome or Dravet syndrome in patients 2 years of age and older (85).

In addition, different states singularly enabled the use of medical cannabis in a strict or comprehensive way. The lack of FDA regulations for determined drugs, such as medical cannabis, means that the purity and potency of the drug can be highly variable (85) and no standardization in the doses and ingredients is available (89). The independent initiative of single states brought to a great heterogeneity in the access to medical cannabis. Since 1996, 34 states, the District of Columbia, Guam, Puerto Rico and US Virgin Islands have approved the medical use of cannabis. The prescription and supply are part of comprehensive programs, which include protection from criminal penalties for using cannabis as medication, possibility of home cultivation or availability of dispensaries, and different cannabis strains for medical purpose (90).

State dispensaries are authorized to provide herbal cannabis, cannabis-derived products and medical devices for cannabis administration. Each state authorized different delivery routes for cannabis, but the most common are oral and pulmonary, using oils, capsules and vaporization. Smoking medical cannabis is prohibited in several states (91).

1.3.1.2 CANADA

Since October 17, 2018, the Cannabis Act SOR/2018-144 legalizes cannabis use in Canada, replacing the regulations of Access to Cannabis for Medical Purposes Regulations (ACMPR). With these new regulations, patients authorized by a health care provider can choose between buying cannabis for medical purposes from a federally licensed seller, registering with Health Canada to produce a limited amount of cannabis for their own medical purposes, or designating someone to produce it for them. The possession of cannabis in public places of a registered patient can be up to 150 g of dried cannabis, or to an amount equal to 30 days of treatment considering the fixed daily amount indicated in the registration documents. Similar amounts are allowed when cannabis is received as inpatient or outpatient of a hospital. Medical documents given by a healthcare practitioner must indicate the duration of the prescription, which can last maximum one year. Strict quality controls are requested to licensed cannabis sellers, including analysis of solvent residues, microbial and chemical contaminants, dissolution and disintegration tests, and it is mandatory to specify the amount or percentage of THC, CBD and their carboxylated forms (92, 93). Some cannabis-based medications are approved on the market. Nabiximols had an approval for the treatment of multiple sclerosis associated spasticity, for symptomatic relief of neuropathic pain in adult patients with multiple sclerosis, and as adjunctive analgesic treatment for cancer-related refractory pain. Nabilone is approved for severe chemotherapy-induced nausea and vomiting. Dronabinol was approved for AIDS-related anorexia associated with weight loss and for severe nausea and vomiting associated with cancer chemotherapy, but it was withdrawn from the Canadian market by the manufacturer in February 2012 (94, 95).

1.3.2 ISRAEL

In Israel the regulations of medical cannabis are in charge to the Medical Cannabis Unit of the Ministry of Health. This agency provides for cannabis regulations for medical and research use, with different internal committees for indications and clinical recommendations, growing of a good quality medical product, and advancement of research (96). The unit deals with physicians, other government bodies, and patients treated with medical cannabis issuing them with permits to use cannabis for medical purposes. All the activities of this unit are strictly in accordance to the provisions of the Dangerous Drugs Ordinance [New Version] 1973, and the provisions of the Single Convention on Narcotic Drugs 1961, including the amendments of

1972 (97). Since the discovery of THC by Mechoulam, Israel improved the research on cannabis and cannabinoids becoming an international leader in this field, partly thanks to a huge percentage of financial resources devoted to research (98, 99). Nowadays, patients have access to herbal cannabis supplied as an oil extract, to be used for oral or sublingual administration, or as dried flowers, for smoking or vaporizing. Since March 2013, the Medical Cannabis Unit approved a procedure that allows the use of medical cannabis for the treatment of oncologic pain, inflammatory bowel disease, neuropatic pain, severe AIDS cachexia, multiple sclerosis (MS)-related spasticity, Parkinson's disease-related pain, Tourette disease, and post-traumatic stress disorder (PTSD). The access to this treatment is permitted only after fully utilizing (presumably unsuccessfully) all other recognized forms of treatment. Nabiximols (Epidiolex) is approved in Israel for the treatment of moderate to severe painful spasticity in multiple sclerosis patients, and as adjunctive treatment for adult patients with advanced cancer who experience moderate-to-severe pain during the highest tolerated dose of strong opioid therapy. Other synthetic cannabinoids (dronabinol, nabilone) are not available in Israel (96).

1.3.3 EUROPE

In Europe, Cannabis was first placed under international control by the Second Opium Convention of 1925 (League of Nations, 1925), including only the dried or fruiting tops of the pistillate (female) plant. In few decades, new guidance of United Nations controlled drugs limitedly to "medical and scientific purposes", so in 1961 a system of controls was described for the cultivation of "any plant of the genus Cannabis" that is not for industrial or horticultural purposes. Ten years later, in the 1971 Convention the controls over THC were assessed. Nowadays, each European country has different rules toward cannabis and where approved, authorized medicines may include THC in capsules (Dronabinol and Nabilone), cannabis extract as a mouth spray, and dried cannabis flowers for vaporizing or making 'tea'. One of the approved medicinal products is an oromucosal formulation containing approximately equal quantities of THC and CBD from two cannabis extracts, under the name Sativex (GW Pharmaceuticals). This product has been authorized in 17 European Union (EU) Member States and Norway for the treatment of muscle spasticity from multiple sclerosis (100).

1.3.3.1 THE NETHERLANDS

Since 2001, the Netherlands gave the monopoly on supplying medical cannabis to the governmental agency "Office of Medicinal Cannabis (OMC)". The OMC is in charge of supplying different varieties of cannabis to pharmacies and general practitioners, making available products with different amounts of THC (from less than 1% to approximately 22%) and CBD (from less than 1% to approximately 9%). Cannabis products can be prescribed for symptomatic treatment of multiple sclerosis, HIV/AIDS, cancer, long-term neurogenic pain,

and tics associated with Tourette's syndrome. The manufacturer does not recommend smoking cannabis products, preferring inhalation via vaporizers and infusion in tea (100).

1.3.3.2 ITALY

In Italy, herbal cannabis is classified under the Presidential Decree (*Decreto del Presidente della Repubblica,* DPR) 309/1990 as part of Table II, together with products containing cannabis and preparations thereof. Medications derived from cannabis are classified as part of Table V, section B. On the other hand, synthetic or semi-synthetic cannabinoids obtained from THC or showing similar chemical structure or toxicological activity are classified as part of Table I, indicating very restrictive limits of possession and handling of these substances (101). Until 2015, preparations obtained from herbal cannabis could be prepared starting only from products imported by Holland, in accordance to Cannabis Bureau Holland, having access to few products with different percentages of cannabinoids (102). After the 2015 Presidential decree, a pilot program for the national selection and growth of cannabis in the Military Pharmaceutical Chemical Works of Florence (*Stabilimento Chimico Farmaceutico Militare di Firenze,* SCFM) was established, as a combined act of the Ministry of Health and the Ministry of Defense. In this site, cannabis can be produced according the GMP (Good Manufacturing Practices) guidelines. The choice of a national production was made after the need of guaranteed access to therapies, conjugating the military safety and reliability to the chemical-pharmaceutical expertise of this factory (102). As to 2019, cannabis products of SCFM are FM2 and FM1, available from December 2016 and July 2018, respectively. Details about these products are summarized in Table 1.1 (103).

Table 1.1 – Concentrations of the major cannabinoids in FM cannabis products. Values are expressed as a range of percentage on dried product.

PRODUCT	THC (%)	CBD (%)
FM2	5.0–8.0	7.5–12.0
FM1	13.0–20.0	<1.0

The selected cannabis strains also contain less than 1% cannabigerol, cannabichromene and tetrahydrocannabivarin. Strains were selected to guarantee therapeutic continuity to the treatment with Bedrocan® varieties, in particular FM2 has a similar composition of Bediol phytocomplex, while FM1 is close to Bedrocan, Bedrobinol and Bedica compositions.
Physicians can prescribe the magistral preparation of a cannabis medication indicating the desired vegetable source, posology in weight of cannabis, treatment needs, and patient's anonymous personal information, such as age and sex (102). The information must be registered in a specific Schedule according to the Phytomonitoring system.

Pharmacists are allowed to buy active substances of cannabis plant origin with a special request in triplicate, and in the narcotic register must be recorded any movement of incoming or outgoing cannabis product. Cannabis cannot be distributed directly to the patients, but the pharmacist makes the required magistral preparation following the Good Manufacturing Practices (GMP). The herbal product is divided by the pharmacist in dosage and form of medicament, according to the posology and administration modality indicated by the healthcare prescriber. Cannabis can be assumed as decoction or inhaled using vaporizers. Assumption of cannabis oil is not forbidden, but each product must be analyzed with sensible methods such as liquid or gas chromatography–mass spectrometry (GC-MS), and the extraction method must be authorized by law.

The use of cannabis cannot be considered as a proper treatment, but as a symptomatic treatment to be used in a narrow panel of pathologies when standard treatments failed in managing the condition, or the side effects cannot be tolerated, or require a very high increment of the dosage. This was stated after considering the lack of conclusive evidence in the efficacy of cannabis for medical use in a vast number of pathologies. Scientific evidence supporting the use of cannabis has poor or modest quality, with inconclusive or conflicting results; in addition, the risks/benefits ratio is not advantageous for cannabis use. However, researches in this field are encouraged in order to get stronger evidence in favor or against cannabis medical treatment. Taking these considerations into account, the pilot project is meant to be a tool for monitoring cannabis use, its efficacy and adverse effects, in order to reconsider the real efficacy of cannabis for medical purpose after adequate evidence will be given by rigorous clinical trials (102).

Cannabis is then approved for the palliative treatment of painful spasticity in MS or spinal cord; analgesia in chronic pain where non-steroidal anti-inflammatories or steroidal or opioid drugs resulted ineffective; anti-kinetosic and anti-emetic in chemotherapy, radiotherapy and HIV therapy-induced nausea and vomit not managed by conventional treatments; appetite stimulating in cachexia, anorexia, loose of appetite in oncologic patients or affected by AIDS or nervous anorexia, resistant to standard treatments; hypotensive in resistant glaucoma; and reduction of tics and involuntary spasms in Gilles de la Tourette syndrome not managed by standard treatments (103). Considering cannabis-based medications, Sativex is available on the market from 2013, while Epidiolex is currently under approval after positive resolution of EMA of summer 2019.

1.4 NATIONAL ACADEMIES RECOMMENDATIONS

As stated in the previous paragraphs, lack of good quality scientific evidence is one of the most critical points in cannabis use for medical purposes. In 2017, the National Academies of Sciences, Engineering, and Medicine (private, non-profit institutions providing expert advices in USA (104) published a report about more than 10,000 scientific abstracts on cannabis health research. In this paper, all the available scientific evidence was evaluated, and 100 conclusions are reported regarding health issues with cannabis administration. In addition, some recommendations were suggested to improve cannabis research (2, 90). In this paragraph, the main conclusions and recommendations are briefly reported.

According to the Academies, there are several study limitations in cannabis research which make very difficult to find conclusive evidence in its safety and efficacy. There are common themes in the type of study limitations, most frequently a poor quality of the study design (lack of appropriate control groups or long-term follow-ups), small sample sizes and absence of a deep investigation of the potential therapeutic benefits of different forms of cannabis. These findings highlight the necessity to improve the research efforts on cannabis investigation, in order to provide comprehensive and conclusive evidence on the therapeutic effects of cannabis and cannabinoids.

Many barriers and challenges are encountered when investigating on cannabis. Firstly, the specific regulatory barriers being a narcotic substance make the handling very limited. Secondly, when permissions are given to researchers to acquire and possess cannabis-based products, it is very difficult to gain access to the right quantity, quality, and type of product necessary to the specific aim of the designed research. Moreover, improvements and standardization in research methodology are severely needed, in order to develop conclusive evidence on short- and long-term health outcomes.

Three main recommendations can be seen as general rules to be followed by the international community of scientists in studying cannabis health outcomes, especially in terms of gaps to address, quality to improve, and barriers to overcome.

1.4.1 FOCUS ON RESEARCH GAPS

The main goal of research on cannabis for medical use should be to maximize the knowledge on benefits and harms associated with the acute and chronic use of cannabis and cannabinoids. A strong collaboration and coordination among research groups, and supporters at local and national levels are strongly recommended and needed to share the knowledge on different research streams, including clinical and observational research. Some specific health effects have still unknown mechanisms underlying, when cannabis is administered. Basic research is still needed, and a knowledge transfer from bench to bedside is encouraged to fulfill the requirements of health care practices, public health priorities, national and state policy, and

public safety standards. This wide network should support and improve statistical associations identified in epidemiological research.

Prioritized research streams and objectives should include, but need not be limited to: investigate pharmacokinetic and pharmacodynamic properties of cannabis, modes of delivery, different concentrations, including the dose-response relationships of THC and other cannabinoids, evaluate understudied cannabis products such as topicals, develop well-controlled trials on the variations given by different administration routes of cannabis, characterize the health effects in understudied health endpoints, identify models for sustainable funding for national and local public health surveillance systems, identify gaps in the cannabis-related knowledge and skills of health care professionals, and provide continuous education programs.

1.4.2 IMPROVE RESEARCH QUALITY

Conclusive, actionable evidence is strongly needed in cannabis research. This requires carefully designed and well conducted research studies, and the obtained data must be accurately and comprehensively reported. Uniformity in research design and reporting requires the development of general guidelines, standardized terminology, and a minimum dataset for epidemiological studies. The guidelines should include a methodology for assessing the cannabis dosage, such as blood or urine test, and not only rely on patients' self-report or the practitioners' prescriptions.

The majority of epidemiological research on cannabis use does not differentiate between oral, topical, or inhalatory administration, so the health effects of cannabis use are generally applied from the most common diffusion of cannabis, *i.e.*, illegal smoking of uncontrolled herbal product, which has a highly variable concentration of cannabinoids, and could be contaminated with heavy metals and pesticides. Research on the use of medical cannabis should allow to collect data based on the route of administration and distinguish between different strains of carefully characterized cannabis.

In conclusion, a network between local and national authorities is needed to create a set of research standards and benchmarks to guide and ensure the production of high-quality cannabis research.

1.4.3 ADDRESS RESEARCH BARRIERS

Considering the limitations in cannabis investigation, one of the major barriers in USA is the classification of these substances under the 5 schedules of the Controlled Substance Act (CSA), updated annually in Title 21 Code of Federal Regulations (CFR) from 1308.11 through 1308.15 (105). An evidence-based report should be produced to fully characterize the impacts of regulatory barriers to cannabis research and propose strategies for supporting cannabis research

agenda. Some of the objectives should include proposing strategies for expanding access to research-grade marijuana, identifying funding sources and mechanisms to support cannabis research, and investigating strategies for improving the quality, diversity, and external validity of research-grade cannabis products (2).

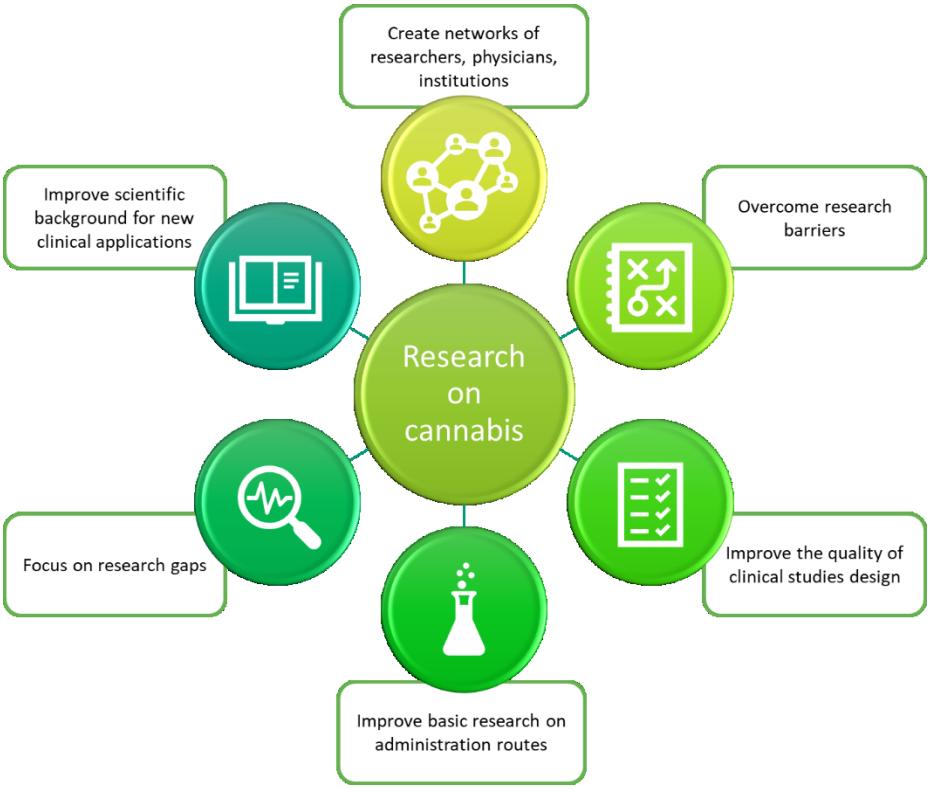

Figure 1.2 – Main recommendations on cannabis research suggested by the National Academies of Science, Engineering and Medicine.

1.5 CONCLUSIONS

The therapeutic use of cannabis is being pursued since ancient times. The knowledge over cannabis phytochemistry and physiological interaction has been improved in the last decades, although several limitations in the investigations were encountered, and some unclear aspects lead to uncertainties in the pharmacology of cannabinoids. The discovery of the endocannabinoid system and its interactions with the major phytocannabinoids, *i.e.*, cannabidiol and tetrahydrocannabinol, opened the possibility to the therapeutic use of isolated compounds for the symptomatic treatment of neuropathic or cancer-related pain, loss of appetite and weight in HIV/AIDS syndromes, and as a supportive treatment for painful refractory pathologies. Despite the recognized clinical applications of isolated compounds, several drawbacks can be encountered during the treatment with THC and its synthetic derivatives. The use of plant-based medicine could mitigate the main psychotropic side effects of THC, hence the necessity of improving the scientific investigation on cannabis-based medicines. Although necessary and fascinating, this pathway cannot be easily pursued because of the limitations imposed by narcotic laws. These limitations can vary according to the countries in which the investigations are carried on, leading to severe drawbacks on a systematic investigation over cannabis effects, both harmful and therapeutic. The scientific literature is heavily fragmented and shows a heterogeneous design of tests, especially on the used type of cannabis. The evaluation of cannabis and cannabinoids effect on human health was often performed without a neat division between administration of plant-derived products or synthetic compounds, comparing the effects of different dosages, routes of administration, and without explicitly specifying whether the subjects were frequent users of cannabis or not. Moreover, the efficacy of cannabis use was often evaluated with self-reports from patients, instead of assessing cannabis usage with, *e.g.*, blood tests. This vast jigsaw composing the scientific literature, combined with the lack of systematic investigation on the medical use of different cannabis breeds, with the variability coming from a natural product, and with the little knowledge over the interaction among major cannabinoids and minor compounds in the human body, is the composition of the framework of cannabis-based medicine. This complex world needs clear guidelines on the development of rigorous scientific literature which could overcome the pressing restrictions on cannabis use in therapy, allowing health care practitioners and patients to evaluate and carefully choose which medicinal product could be more appropriate for an appropriate treatment.

The scientific activity of this work aimed, therefore, to move the first steps toward the correct understanding of the differences coming from a synthetic derivative of cannabis and a natural plant extract, by developing innovative vesicles for the delivery of cannabinoids. Due to the strong first-pass effect on cannabinoids administered orally, it is often difficult to quantify the absorption of cannabinoids, while vaporization does not allow to obtain homogeneous administered doses. Transdermal delivery of cannabinoids could allow a constant release of

these active ingredients, with a defined administered dose for a prolonged time. Thus, in this work, innovative systems were studied and developed for the efficient delivery of cannabinoids. These compounds tend to accumulate in the outmost layer of the skin, *i.e.*, stratum corneum, due to their high lipophilicity. These studies were performed by using a model molecule with similar physicochemical behavior to THC but lacking its psychotropic effects: desoxy-CBD (DH-CBD), which is a promising molecule acting on pain signaling. This molecule is not readily available on the market; therefore, a synthetic pathway was pursued and will be further explained in Chapter 2.

Chapter 2

Medicinal chemistry development

2.1 CANNABINOIDS AND DESOXY-CBD

In the last decades, the scientific community struggled to find an unequivocal terminology to define cannabinoids. Originally referred to a structurally homogenous class of meroterpenoids typical of cannabis, the name "cannabinoid" has evolved to the definition of molecules with a similar biological effect to THC. This led to a shift from a structural meaning to the indication of molecules showing affinity to the cannabinoid receptors, CB1 and CB2, including also the so-called "endogenous cannabinoids". These compounds are endogenously produced biological analogues of THC, thus gaining the definition of endocannabinoids. Therefore, it was logical to refer to cannabis terpenoids, their analogues, or generally cannabis-derived secondary metabolites as "phytocannabinoids" and introducing the definition of "cannabinoids" as molecules capable of either directly activating CB1 and CB2 receptors or sharing chemical similarity with cannabinoids, or both (12, 106). The discovery of new non-CB targets of cannabinoids in the human body and the intricated connections between activated targets and physiological response led to a new concept of "endocannabinoid system" and to the definition in 2010 of "endocannabinoidome", with which in turn a wide variety of natural-derived compounds named "phytocannabinoidome" can interact (107). In this context, the definition of synthetic cannabinoids is usually referred to cannabis-derived cannabinoids and other synthetic molecules with cannabinoid-like structure (107).

Due to the restrictions of Italian narcotic laws, the first part of this study faced the need of using a model molecule with similar characteristics of the major phytocannabinoids, without mimicking the structure or the pharmacological effects of tetrahydrocannabinol, *i.e.* interactions with CB1 receptors. Thus, in this chapter the main features of phytocannabinoids and the experimental procedures for the synthesis of a promising model molecule will be illustrated.

2.1.1 PHYTOCANNABINOIDS

Phytocannabinoids are terpene-phenolic compounds, with a 21 carbon atoms substructure. More than 144 cannabinoids were discovered up to 2016 in the phytocomplex (12). Although this number appears very high, the real number of naturally occurring cannabinoids could have been inflated by the poor oxidative stability of some of the major phytocannabinoids, especially Δ^9-THC. In fact, many investigations were conducted on aged samples of ground cannabis or hashish. Moreover, most phytocannabinoids were characterized in the 1960s and 1970s, when the analytical techniques were less sensitive and not always appropriate to fully characterize molecules of natural sources. After a three-decade gap, new structural types have been discovered, and the technological advancement, together with the availability of new cannabis breeds, are expected to further expand the current inventory of these compounds.
Generally, phytocannabinoids are composed of a resorcinyl core bearing para-oriented terpenyl and pentyl groups, but different degrees of isoprenylation (prenyl, sesquiterpenyl) or shortened alkyl groups (frequently methyl or propyl) can be naturally found. Phytocannabinoids derived from aliphatic ketide starters are typical of cannabis and of limited distribution in nature (12).
Together with the most abundant cannabinoids, THC and CBD, other compounds can be frequently found in cannabis strains: cannabinol (CBN), cannabigerol (CBG), cannabicromene (CBC), and tetrahydrocannabivarine (THCV) (108). In the following paragraphs, the chemical and physical properties of the major cannabinoids will be illustrated.

2.1.1.1 TETRAHYDROCANNABINOL (Δ^9-THC)

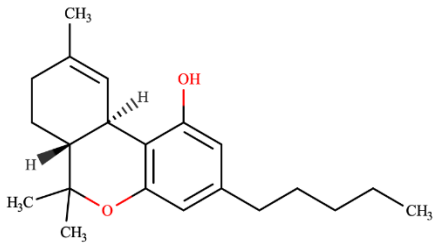

Figure 2.1 – Chemical structure of Δ^9-tetrahydrocannabinol.

Tetrahydrocannabinol was first isolated and characterized by Gaoni and Mechoulam in 1964 (20). Its chemical name is 3-pentyl-6,6,9-trimethyl-6a,7,8,10a-tetrahydro-6*H*-dibenzo-[*b*,*d*]pyran-1-ol according to the dibenzopyrane numbering system. It was historically called with different numerations. The use of the terpene numbering system gives the name Δ^1-tetrahydrocannabinol, originally developed in Europe following the biochemical nature of cannabinoids. The dibenzopyrane numbering system, which stands in agreement with the IUPAC rules, leads to the name Δ^9-tetrahydrocannabinol and is commonly used in North America (109).

When purified, THC is a pale-yellow resinous oil which becomes sticky at room temperature. It is a highly lipophilic molecule, poorly soluble in water (less than 3 µg/ml) with a LogP value of 7.0 (110), and a bitter taste but without smell. This molecule is very sensitive to light, air, and acidic solutions, but resistant to high temperatures: his boiling point is 200°C at 0.02 mmHg. Due to its chiral centers at C-6a and C-10a, different stereoisomers can form, but only (–)-*trans*-Δ^9-THC is found in the cannabis plant (109). Other isomers can be obtained according to the position of the double bond in the terpenoid ring, and the most important are the Δ^9-isomer and the Δ^8-isomer. Δ^9-THC is naturally accompanied by its homologous compounds containing a propyl side chain (*e.g.*, tetrahydrocannabivarin, THCV, THC-C3) (109).

2.1.1.2 CANNABIDIOL (CBD)

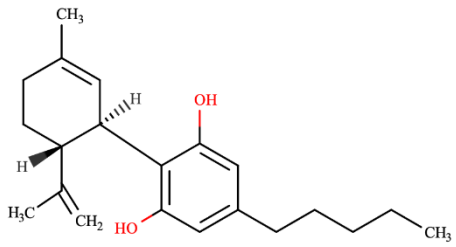

Figure 2.2 – Chemical structure of cannabidiol.

Isolated for the first time in 1940 by Adams *et al.*, but structurally identified by Mechoulam in 1963 (111), the IUPAC name of cannabidiol is 2-[(1S, 6R)-3-methyl-6-prop-1-en-2-yl-1-cyclohex-2-enyl]-5-pentyl-benzene-1,3-diol. This lipophilic molecule has a LogP value of 6.5 (112) and its structure is terpene-phenolic but not benzopyranic. Variations in the side chain can naturally occur, giving different compounds: as an example, the propyl side chain-substituted CBD is known as cannabidivarin (CBDV) (109). CBD is sensible to acidic conditions: in simulated gastric fluid (pH = 1), CBD underwent cyclisation yielding a mixture of Δ^9 and Δ^8-THC, and the reaction was 98% complete after 2 hours (12).

2.1.1.3 TETRAHYDROCANNABINOLIC ACID (Δ^9-THCA)

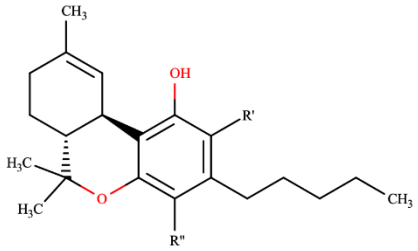

Figure 2.3 – Chemical structure of tetrahydrocannabinolic acid A (when carboxylic acid is in R') and B (when carboxyl group is in R").

Inside the glandular trichomes of cannabis Δ^9-THC is not directly available. Its acidic form, the tetrahydrocannbinolic acid (THCA), is almost exclusively found. There are two isomers of THCA. The first has its carboxylic function at position C-2 and is named 2-carboxy-Δ^9-THC or THCA-A. It was extracted for the first time by Korte et al., and isolated by Nishioka in the mid 1960s. The second has the carboxylic function at position C-4 and is named 4-carboxy-Δ^9-THC or THCA-B, isolated in 1968 by Mechoulam. THCA shows no psychotropic effects, but its decarboxylation can occur within seconds by heating above 200°C, providing the active substance Δ^9-THC (109). Both THCA-A and B are partial agonists of TRPV1 channels and antagonists of TRPM8 (111).

2.1.1.4 CANNABIDIOLIC ACID (CBDA)

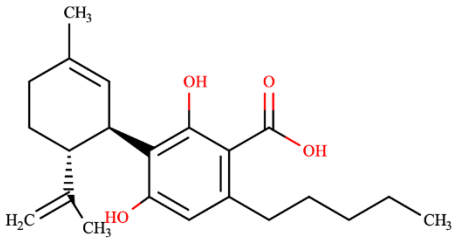

Figure 2.4 – Chemical structure of cannabidiolic acid.

Isolated in 1955 by Krejci and Santavy, cannabidiolic acid is the acidic form of CBD. It is the second major cannabinoid in cannabis species besides Δ^9-THC. It was generally believed that CBDA was a precursor for THCA biosynthesis. Further studies indicated that both CBDA and THCA appear to be formed from the same precursor, cannabigerolic acid (CBGA), and the synthesis of THCA from CBDA is unlikely in the cannabis plants (109).
CBDA acts as COX-2 selective inhibitor, activates TRPA1 and TRPV1 channels and antagonizes TRPM8 (111).

2.1.2 DESOXY-CBD (DH-CBD)

Considering the definition of cannabinoids as previously described and the chemical and biochemical properties of THC, the model molecule chosen for this project had to bear similar chemical behavior of the major cannabinoid but lacking psychotropic effects and a benzopyranic structure. Looking at the traditional cannabinoids structure-activity relationship, a free hydroxyl group on C1 and an alkyl side chain at C3 are required for CB1 receptor mediated activity (113). In particular, the phenolic residue is fundamental in the interactions with CB1, presumably for the formation of a hydrogen bond with a lysine (Lys12) side chain in transmembrane helix 3 of the receptor (114). Considering these requirements to be avoided and taking into account the low interaction between CBD and CB1 receptor even meeting the two requirements previously described, the attention was focused on a synthetic molecule with a structure very similar to CBD but keeping the lipophilicity of THC.
The designated molecule is desoxycannabidiol (DH-CBD), with the IUPAC name of 2-[(1R,6R)-3-methyl-6-(1-methylethenyl)-2-cyclohexen-1-yl]-5-pentylphenol.

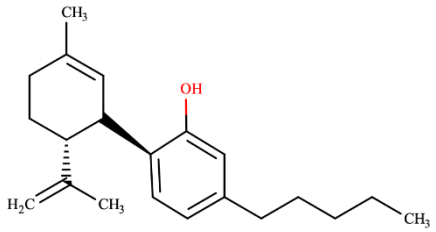

Figure 2.5 – Chemical structure of desoxycannabidiol.

The main difference with cannabidiol itself is the absence of a resorcinol nucleus, replaced by a phenolic moiety and a pentyl side chain in para-position to the terpenyl group. This highly lipophilic molecule has a LogP value of 6.9 (115), very close to the value of THC, but the absence of the resorcyl group dramatically decreases the affinity of the molecule for CB receptors, leading to the absence of psychoactive or sedative effects even at high concentration as proved by Xiong et al. (116). This molecule was developed during several computational studies on the capability of CBD to clear the Receptor Essential Volume (REV) of CB1 receptor. In 2011 it was demonstrated that desoxy-CBD, THC and didesoxy-THC (a molecule with the same benzopyranic structure of THC without the free phenolic hydroxyl group) strongly bind to the α1 and α3 subunits of spinal glycine receptors (116).

2.1.2.1 PROPOSED MECHANISM OF ACTION OF DH-CBD

In their study, Xiong et al. (116) investigated the mechanisms and behavioral implication of cannabinoid-GlyR (glycine receptors) interaction. Inhibitory glycine receptors have a key role in the in regulation of neuromotor activity, pain sensation, muscle relaxation and anxiety.

Glycinergic dorsal horn neurons receive sensory input from myelinated primary sensory neurons, and their silencing induces localized mechanical, heat and cold hyperalgesia, and itching behavior in rodents (117). Glycinergic interneurons were also found in the retina, hearing system and other areas linked to sensory systems (118). Glycine receptors are pentameric complexes composed by subunits α and β, of which are known four and two isoforms, respectively (119). Their pseudo-symmetric structure forms an ion channel for the permeation of chloride anions, therefore hyperpolarizing the neuronal membrane and reducing the responsiveness of the neuron itself. Different isoforms of subunit α are expressed in the nervous system: α1 is typically found in motoneurons and sensory neurons of the brain stem, while α3 is fundamental in the inhibition of nociception and inflammatory pain sensation, and it is located in the II lamina of the dorsal horn of the spinal cord. Many studies proved a direct interaction between cannabinoids and glycinergic signaling (120-123). In particular, the most recent studies focused on pain sensation modulated by glycinergic receptors (GlyRs). Xiong et al. (116) demonstrated that both THC and DH-CBD increased response latencies in the tail-flick reflex test in C57BL/6J mice, and the analgesic effect of these compounds were completely cancelled after administration of strychnine, which is a selective GlyR antagonist. Furthermore, the effect could not be prevented by administration of a selective CB1 receptor antagonist, AM251. The same parameter was evaluated in genetically modified mice, showing a reduced analgesic effect in heterozygous α3 mice and completely absent effect in α3 knockout mice. On the contrary, analgesia in CB1 and CB2 knockout mice remained unchanged after administration of THC or DH-CBD as compared to wild-type mice. Typical side effects induced by THC, such as hypothermia, were not induced by DH-CBD (116).

In cellular models expressing the α3 GlyRs, DH-CBD was more efficient than CBD in potentiating the glycine flux, I_{Gly}. Consistent with the observations, the *in vivo* tests demonstrated the superiority of DH-CBD over CBD in alleviating heat pain hypersensitivity. Rats were treated with a complete Freund's adjuvant to simulate an inflammatory model, and intraperitoneal or intrathecal (50 μg) injections of DH-CBD caused a significant increase in paw withdrawal latency; the same results were obtained multiple times within the same day or the following day. This suggests that there is no apparent tolerance with DH-CBD–induced analgesia (123).

In conclusion, DH-CBD could be an enticing cannabinoid for the treatment of inflammatory and chronic pain, as selective potentiator of I_{Gly}, fundamental in reducing pain signaling. This is even more appealing due to the lack of affinity for CB1 receptors, thus avoiding psychotropic effects generally given by THC, and without tolerance at least in the short time as could be registered with traditional drugs prescribed for the management of moderate to severe pain.

2.1.2.2 SYNTHESIS OF DH-CBD

Although the fascinating features of DH-CBD previously described, its building is not easily performable. The total synthesis of this compound was first proposed by Reggio (124), as a condensation between two synthons: *p*-mentha-2,8-dien-1-ol and *m*-pentylphenol. The condensation via DMF-dineopental acetal was performed according to Petrzilka's method for the synthesis of CBD (125). This reaction gave two predominant products: DH-CBD and a less polar compound, identified as *p*-mentha-1,8-dien-3-yl-3-n-pentylphenyl ether. Wilkinson et al. in 2013 (126) reported the very few alternative synthetic pathways for the synthesis of this compound, including photosensitized O_2-transfer to (+)-limonene (127) and a stepwise synthetic approach from (+)-limonene via a selenoxide elimination to install the alkene (128). None of them led to DH-CBD with high yields. The novel approach of Wilkinson, Price and Kassiou includes an improved process to obtain the two synthons, where *p*-mentha-2,8-dien-1-ol was obtained by Cope elimination from *R*-(+)-limonene, and *m*-pentylphenol was synthesized via alkylation of *m*-cresol following the indication of Reggio (124). The final coupling was performed with the Lewis acid boron trifluoride diethyl etherate, which resulted more efficient than the DMF-dineopental acetal approach, used both by Reggio in 1995 and Xiong and coworkers in 2011 (116).

In this project, the Wilkinson approach was performed but, as described in the following paragraphs, DH-CBD was obtained with very low yields. Stereoselectivity of the reactions were the major concern limiting the total yield of the pathway, thus in the laboratory of Prof. Giovanni Marzaro the process was improved by including another step in the synthesis to enhance the stereoseectivity. In order to potentiate DH-CBD production methods, a semisynthetic pathway was tested starting from pure CBD. Previous studies reported the synthesis of DH-THC through the deoxygenation of THC. The same route could not be utilized for the synthesis of DH-CBD due to the presence of two phenol groups on the aromatic ring. Therefore, it was performed a selective dehydroxylation by triflation and reduction of one triflate via palladium(II)-catalyzed reaction, and the processes will be described in Paragraph 2.2.

2.2 RESULTS AND DISCUSSION

2.2.1 TOTAL SYNTHESIS OF DH-CBD

The first method was perfectioned starting from the Wilkinson, Price and Kassiou pathway. Wilkinson et al. (126) proposed the synthesis of DH-CBD by using a Lewis acid for the condensation of two synthons: *p*-mentha-2,8-dien-1-ol and *m*-pentylphenol. This pathway was first tested in our laboratories, showing a very low yield for the synthesis of the first synthon. The amounts obtained were insufficient for the subsequent formulation of desoxy-CBD in vesicular systems.

The limiting step was the synthesis of the specific diastereomer, from which *p*-mentha-2,8-dien-1-ol could be obtained. This led to the development of a more efficient pathway, using stereoselective reactions.

The synthesis of *m*-pentylphenol was obtained following the method described by Petrzilka et al. (125) for the production of olivetol.

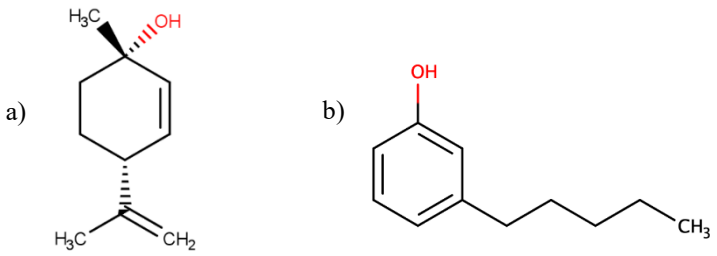

Figure 2.6 – Chemical structures of p-*mentha-2,8-dien-1-ol (a) and* m-*pentylphenol (b).*

2.2.1.1 SYNTHESIS OF 1*S*,4*R*-4-ISOPROPENYL-1-METHYL-CYCLOHEX-2-EN-1-OL (*p*-MENTHA-2,8-DIEN-1-OL)

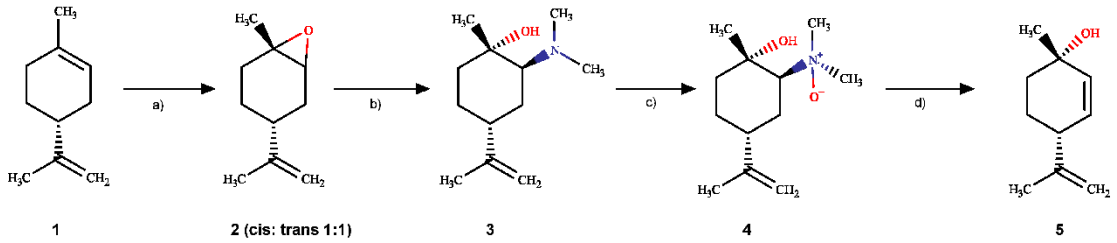

***Scheme 1**. Synthesis of p-mentha-2,8-dien-1-ol from Wilkinson, Price, Kassiou. Reagents and conditions:*

a) m-CPBA, $CHCl_3$, -10°C 30 minutes, RT 1 h, yield 56.8%;

b) Dimethylamine aqueous solution 40%, 80°C, 2 h, yield 35%;

c) H_2O_2, CH_2CN, H_2O, RT, 2 h, yield 99.7%;

d) 1 mmHg, 180°C, yield 60%.

The synthesis of compound **5** was performed starting from R-(+)-limonene oxide, **1**. The tri-substituted alkene was epoxidized to compound **2** via Prilezhaev reaction: the peracid *m*-CPBA brings a highly electrophile oxygen, which reacts with the alkene. This reaction formed an equimolar mixture of *cis*- and *trans*- limonene epoxide that was resolved by treatment of compounds **2** (cis:trans 1:1) with an aqueous solution of dimethylamine, good nucleophile. Thus, the compound **3** in *trans*- state was predominantly obtained. This was a consequence of the reaction kinetics: the **2** *trans*-limonene oxide was proven to have a chair-like conformation, while the **2** *cis*- isomer favors the boat-like conformation (129). The first isomer is more likely attacked by the nucleophile, so the **3**-*trans* species is the first to be formed in the reaction mixture. Diminishing the reaction time and keeping the reaction temperature below 100°C, the enantio-selectivity is improved obtaining **3** (129).

The *trans*-amino alcohol was then oxidized with H_2O_2 to obtain **4.** The *trans*- isomer resulted more stable than the *cis*- form, so that compound **4** was obtained as a 100% pure stereoisomer. In fact, the *trans*- isomer showed an axial conformation of isopropenyl group, creating a hydrogen intramolecular bond between the *N*-oxide and the hydroxyl group, and forming a crystalline structure with water molecules, leading to a hemihydrate form (126).

Using a Kugelrohr oven, the compound 5 was obtained by Cope elimination from 4: the presence of a β hydrogen allows the decomposition of amino-oxides under high vacuum and elevated temperatures, leading to the formation of the desired alkene and a *N,N*-dialkylhydroxylamine.

Improving the synthesis of *p*-mentha-2,8-dien-1-ol

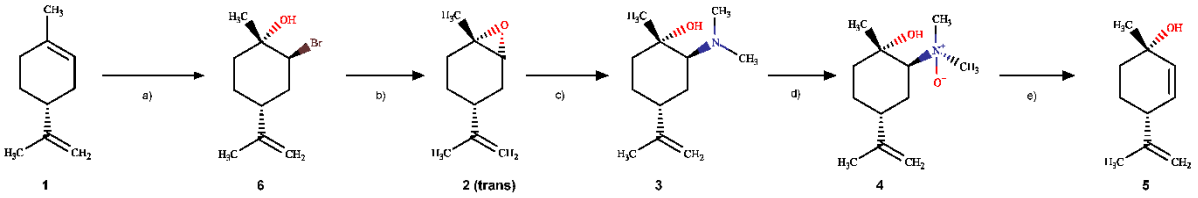

***Scheme 2**. Improved synthetic pathway of p-mentha-2,8-dien-1-ol. Reagents and conditions:*

a) NBS, H_2O, acetone, 0°C, 30 minutes, yield 90.0%;

b) EtONa, 0°C, distillation, yield 72.7%;

c) Dimethylamine aqueous solution 40%, reflux, 21 h, yield 80.9%;

d) H_2O_2, CH_2CN, H_2O, RT, 2 h, yield 99.7%;

e) 10^{-2} mmHg, 120°C, yield 90%.

The synthetic pathway proposed by Wilkinson et al. was successfully replicated in the laboratory, but the overall yield was too low to obtain compound **5** in sufficient amounts. The critical points were mainly two: the formation of an equimolar mixture of *cis*- and *trans*-limonene oxide and, consequently, a reduced efficiency in the production of compound **3**. Moreover, the purification of the two enantiomers using a separation column was not easily performed, showing overlapped retention factors (R_f) with many eluent mixtures.

Improving the first steps was crucial to raise the overall yield. An enantioselective reaction was inserted: starting from **1**, the brominating agent *N*-bromosuccinimide in aqueous ambient and at low temperature led to the formation of **6**. In this step, a 100% *trans*- bromohydrin was obtained with a very high yield (130).

The epoxide **2** was quickly obtained from **6** using a strong base, sodium ethoxide (EtONa). In this reaction, the alkoxide ion bound to the bromine-linked carbon, causing the leaving of bromine and the subsequent epoxidation. Compound **2** was purified after this step by distillation at 40-60 °C and treated with aqueous dimethylamine under reflux instead of using a sealed vial. This improved the yield of **3** to 81% against 35% in the previous synthetic pathway.

After oxidizing **3** with hydrogen peroxide to **4** with a quantitative yield, compound **5** was obtained via Cope elimination in Kugelrohr oven, with a yield over 90%.

It is important to underline that these improvements, although inserting another step in the pathway, led to a relevant improvement in the overall yield. In the previous pathway, in fact, the yield was 12%; with the new method, the overall yield improved to 48%.

2.2.1.2 SYNTHESYS OF *m*-PENTYLPHENOL

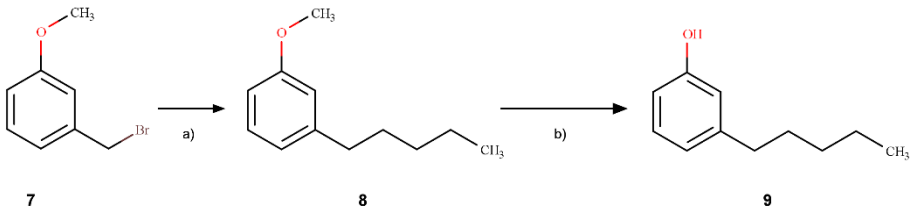

7 8 9

Scheme 3. *Synthesis of m-pentylphenol. Reagents and conditions:*

a) n-BuLi, CuI, anhydrous diethyl ether, 0°C, 4 h, yield 52.8%;

b) HBr, CH_3COOH, 130°C, 7,5 h, yield 86.8%.

The synthesis of **9** was performed starting from 3-methoxybenzyl bromide following the method described by Petrzilka et al. (125) for the synthesis of olivetol from 3,5-dimethoxy-benzylbromide.

Compound **8**, 3-methoxypentylphenol, was obtained by treating **7** with the Gilman reactant. This was obtained using copper (I) iodide and two equivalents of *n*-butyllithium. The so formed lithium dibutylcuprate, in anhydrous diethyl ether environment, forms a dimer with eight-members cycle structure, where the two lithium atoms are coordinated by two butyl groups. In the end, the Gilman reactant attacks bromine and substitute it with a butyl group.

In the last step, the methyl group in position **3** is eliminated with a mixture of HBr and CH_3COOH, obtaining compound **9**.

2.2.1.3 SYNTHESIS OF 2-[(1R,6R)-3-METHYL-6-(1-METHYLETHENYL)-2-CYCLOHEXEN-1-YL] -5-PENTYLPHENOL (DESOXY-CBD)

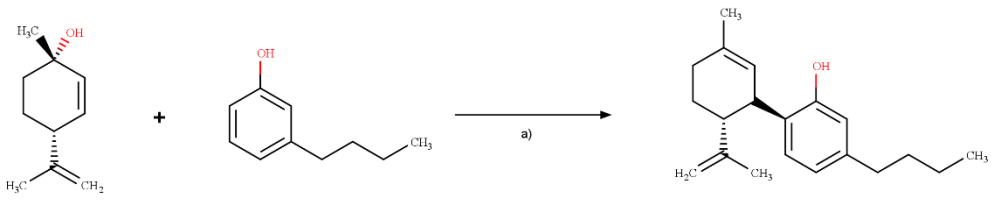

5 9 10

Scheme 4. *Synthesis of desoxy-CBD. Reagents and conditions:*

a) $BF_3{\cdot}Et_2O$, CH_2Cl_2, -78°C, 4h, yield 25.8%.

Compound **10** was obtained by condensation of synthons **5** and **9** with a Lewis acid, namely boron trifluoride diethyl etherate. This Friedel-Crafts condensation must be performed at very low temperature (-78°C) and a maximum concentration of the catalyst of 0.5%. These parameters are essential to slow down the reaction kinetics and the high reactivity of BF_3. Thus, the formation of cyclized byproducts, similar in chemical structure to THC, was avoided.

2.2.2 SEMISYNTHESIS OF DH-CBD

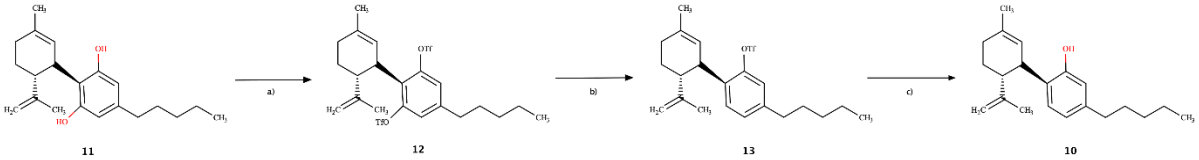

Scheme 5. *Semisynthesis of desoxy-CBD starting from CBD. Reagents and conditions:*

a) Tf_2O, DIPEA, CH_2Cl_2, -78°C, 4h, quantitative;

b) $Pd(OAc)_2$, Ph_3P, Et_3N, HCOOH, DMF, N_2 atmosphere, 40-60°C, 30 min, yield 50.1;

c) MeOH, dioxane, NaOH 1M, RT, 3h, quantitative yield.

Starting from pure CBD crystals, kindly provided by Enecta®, trifluoromethanesulfonic anhydride was added to a solution in anhydrous mixture of CH_2Cl_2 and diisopropylethylamine. The bis-triflate CBD was then selectively reduced with palladium acetate, triphenylphosphine, triethylamine and formic acid in DMF. The final product was obtained after basic hydrolysis and chromatographic column (eluent: CE/EtOAc, 98/2). Thus, desoxy-CBD synthesis was improved with a total yield of 50%, compared to the maximum total yield of 6% obtained with the total synthesis pathway.

2.3 MATERIALS AND METHODS

2.3.1 MATERIALS

The used products and reagents (Acros and Merck) were used without purification.
Organic solvents (Carlo Erba) purity was of analytical grade.
Deuterated solvents for NMR (Sigma-Aldrich and Merck) had an isotopic purity of minimum 99.5%.
Thin layer chromatography was performed on silica gel panels 60 F254 (0.22 mm, Merck), with the indicated eluents.
Column chromatography was performed with silica gel 60 (0.063 – 0.100 mm, Merck) eluting as described each time.

2.3.2 INSTRUMENTS

1H-NMR spectra were performed with Bruker 300-AMX spectrometer, using TMS as internal standard ($\delta = 0$) and deuterated solvent indicated each time; absorbance values are expressed as δ and constants in Hz.
Flash chromatography was performed with an automated system (ISOLERA Biotage) with automatic calculation of elution gradient starting from R_f values obtained from TLC.

2.3.3 TOTAL SYNTHESIS OF DH-CBD

2.3.3.1 SYNTHESIS OF 1*S*,4*R*-4-ISOPROPENYL-1-METHYL-CYCLOHEX-2-EN-1-OL

Synthesis of (+)-limonene oxide via *m*-chloroperbenzoic acid

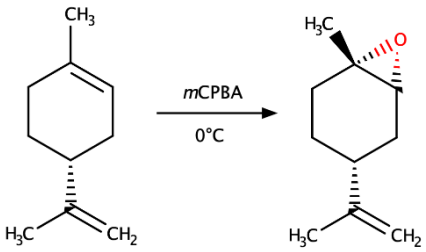

In a two-neck round bottomed, flask (+)-limonene (5.0 g, 36.7 mmol) was dissolved in chloroform (40 ml) and the reaction mixture was cooled in an ice bath. The *m*-chloroperbenzoic acid (6.4 g, 36.9 mmol) was then dissolved in chloroform (100 ml) and added dropwise to the reaction mixture within 30 minutes.

After complete addition, the system was left to -10°C for 30 minutes and RT for 1 hour. (TLC: CE/EtOAc, 90/10 + vanillin).

The mixture was treated with NaOH 1M (40.0 ml) and the organic phase was washed with 2 × Na_2CO_3 5% and 1 × brine. The organic phase was then treated with anhydrous Na_2SO_4 and filtered, and the solvent was evaporated by rotatory evaporation. Thus, *R*-(+)-limonene oxide was obtained (3.2 g, yield 56.8% of cis:trans 1:1 mixture).

^{1}H-NMR ($CDCl_3$-*d*) for *trans*- isomer: 4.67 (d, J=0.99, 4H), 2.98 (d, J=5.32, 1H); 2.07-1.98 (m, 4H), 1.89-1.75 (m, 4H), 1.74-1.60 (m, 2H), 1.66 (s, 3H), 1.31 (s, 3H).

Synthesis of 1*S*,2*S*,4*R*-2-(dimethylamine)-4-isopropenyl-1-methylciclohexanol

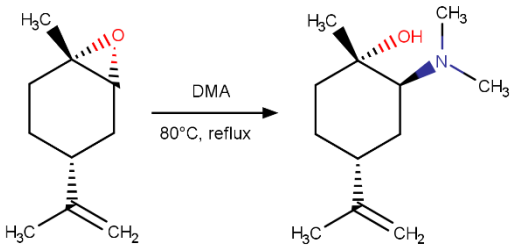

FIRST METHOD

In a screw-cap vial, *R*-(+)-limonene oxide (4.6 g, 30 mmol) and 40% aqueous solution of dimethylamine (18 ml) were weighted, and the vial was heated in an oil bath at 80°C for 2 hours. The vial was cooled in an ice bath and the reaction was quenched by opening the cap (TLC: $CHCl_3$/MeOH, 90/10 + vanillin). The product was extracted with 3 × EtOAc, then the organic phase was washed one time with a saturated solution of NH_4Cl, dehydrated by Na_2SO_4 and filtered. The solvent was removed by rotatory evaporation. The product was purified by chromatographic column (eluent: CH_2Cl_2/EtOAc/MeOH/NH_3 = 70/10/20/1), thus obtaining 1*S*,2*S*,4*R*-2-(dimethylamine)-4-isopropenyl-1-methylciclohexanol (1.6 g, yield 35.0%).
The low reaction yield and the formation of byproducts led to the development of a second reaction method.

SECOND METHOD

In a round bottomed flask *R*-(+)-limonene oxide (38.4 g, 38.4 mmol) and the 40% dimethylamine aqueous solution (22.7 ml) were mixed and refluxed for 21 hours.
The vial was cooled in an ice bath and the reaction was quenched by opening the cap (TLC: $CHCl_3$/MeOH, 90/10 + vanillin). The product was extracted with 3 × EtOAc, then the organic phase was washed one time with a saturated solution of NH_4Cl, dried with anhydrous Na_2SO_4 and filtered. The solvent was removed by rotatory evaporation. The product was purified by chromatographic column (eluent: CH_2Cl_2/EtOAc/MeOH/NH_3 = 70/10/20/1), thus obtaining a yellow viscous liquid of 1S,2S,4R-2-(dimethylamine)-4-isopropenyl-1-methylciclohexanol (34.2 g, yield 89.0%).

^{1}H-NMR ($CDCl_3$-*d*): 4.91 (d, J=1.5, 1H), 4.84 (1H, s), 3.52 (s, 1H), 2.47 (dd, J=13.0, J=3.4, 1H), 2.35 (m, 1H), 2.24 (s, 6H), 2.05 (ddd; J=13.5, J=5.5, J=2.5, 1H), 1.92 (m, 1H), 1.73 (s, 3H), 1.56-1.41 (m, 4H), 1.21 (s, 3H).

Synthesis of 1*S*,2*S*,5*R*-*N*,*N*,2-trimethyl-2-hydroxy-5-isopropenylcyclohexamine oxide hemihydrate

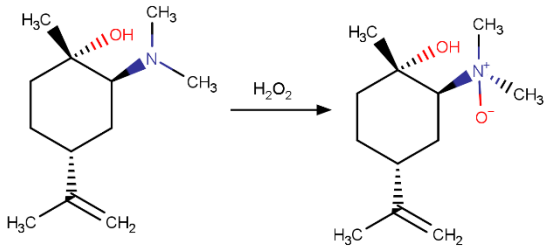

In a round bottomed flask, 1*S*,2*S*,4*R*-2-(dimethylamine)-4-isopropenyl-1-methylcyclohexanol (1.2 g, 6.1 mmol) was diluted with acetonitrile (30.5 ml) and water (24.6 ml) and cooled on an ice bath while mixing for 10-15 minutes. Hydrogen peroxide (30% solution, 60.9 mmol) was added dropwise, then the ice bath was removed, and the system was mixed for 2 hours at RT (TLC: $CHCl_3$/MeOH, 75/25 + vanillin).

The reaction was cooled in an ice bath and sodium sulfite (Na_2SO_3, 61.0 mmol) was added. The peroxide was deemed quenched when a colorless solution was obtained when a droplet of reaction mixture was mixed with a droplet of aqueous sodium iodide. The excess of salts was filtered and washed with $CHCl_3$. The filtrate and washings were combined and separated, then the aqueous layer was washed with fresh 2 × $CHCl_3$. The organic layers were dried with Na_2SO_4 and filtered. The solvent was evaporated under reduced pressure to yield an off-white, hygroscopic, crystalline solid of 1*S*,2*S*,5*R*-*N*,*N*,2-trimethyl-2-hydroxy-5-isopropenylcyclohexamine oxide hemihydrate (1.3 g, quantitative yield).

^{1}H-NMR ($CDCl_3$-*d*): 5.01 (s, 1H), 4.84 (s, 1H), 3.49 (dd, J=13.4, J=3.2, 1H), 3.23 (s, 3H), 3.14 (s, 3H), 2.57 (s, 1H), 2.54 (s, 1H), 2.09 (dq, J=-13.1, J=5.4, J=2.5, 1H), 1.94 (m, 1H), 1.77 (ddd, J=-13.3 Hz, J=13.3, J= 5.3 Hz, 1H), 1.74 (s, 3H), 1.69 (m, 1H), 1.63-1.54 (m, 1H), 1.57 (s, 3H), 1.50 (m, 1H).

Synthesis of 1*S*,4*R*-4-isopropenyl-1-methyl-ciclohex-2-en-1-ol (*p*-mentha-2,8-dien-1-ol)

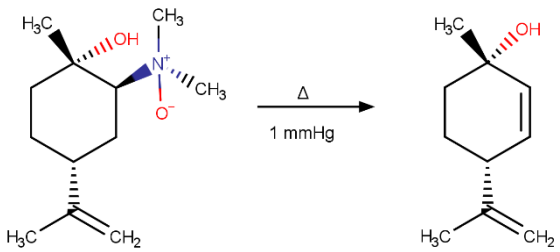

1*S*,2*S*,5*R*-*N*,*N*,2-Trimethyl-2-hydroxy-5-isopropenylcyclohexamine oxide hemihydrate (0.5 g, 2.3 mmol) was heated in a Kugelrohr oven at 120°C under high vacuum (10^{-2} mmHg) until complete pyrolysis of the solid. The colorless distillate was collected with acetone and the solvent removed under reduced pressure, giving a colorless resin of *p*-mentha-2,8-dien-1-ol (0.45 g, yield 90.0%).

^{1}H-NMR ($CDCl_3$-*d*): 5.70 (ddd, J=10.0, J=2.4, J=1.4, 1H), 5.65 (ddd, J=9.9, J=2.3, J=0.8, 1H), 4.78 (q, J=1.6, 1H), 4.74 (q, J=0.9, 1H), 2.65 (m, 1H), 1.88-1.73 (m, 2H), 1.73 (s, 3H), 1.66-1.51 (m, 3H), 1.29 (s, 3H).

2.3.3.2 SYNTHESIS OF *m*-PENTYLPHENOL

Synthesis of 3-methoxypentylphenol

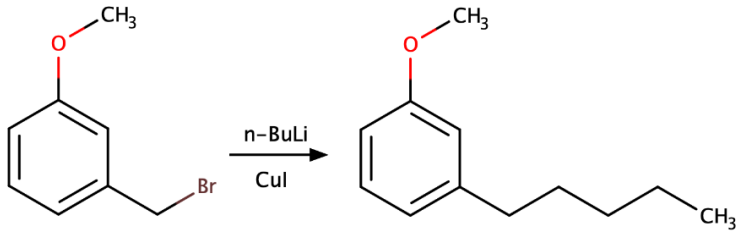

3-Methoxybenzylbromide (10.2 g, 50 mmol) was dissolved in anhydrous diethyl ether (1L) and CuI (9.5 g, 50.0 mmol) was subsequently added. The system was refrigerated on an ice bath and n-butyllithium (68.8 ml, 110.0 mmol) was added for the formation of Gilman reactant. The system was kept at 0°C for 4 hours (TLC: CE/EtOAc, 80/20 + vanillin), then the reaction was quenched by addition of an aqueous solution of NH_4Cl and NH_4OH. The product was extracted with 3 × diethyl ether, dried on Na_2SO_4 and the solvent was evaporated under reduced pressure. The product was purified with chromatographic column (eluent: CE/EtOAc, 95/5) yielding 3-methoxypentylphenol (4.7 g, yield 52.8%).

^{1}H-NMR ($CDCl_3$-*d*): 7.18 (t, J=7.6, 1H), 6.78 (d, J=7.6, 1H), 6.79-6.74 (m, 2H), 3.8 (s, 1H), 2.57 (t, J=7.5, 2H), 1.72 (m, 2H), 1.66-1.56 (m, 4H), 0.89 (t, J=6.8, 3H)

Synthesis of *m*-pentylphenol

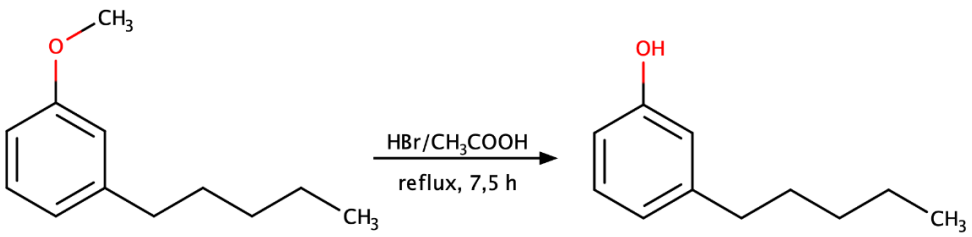

3-Methoxypentylphenol (0.7 g, 4.0 mmol) was mixed with HBr 48% (20 ml) and glacial acetic acid (CH_3COOH, 20 ml), and refluxed for 7 hours not continuatively (TLC: CE/EtOAc, 50/50 + vanillin). The reaction was quenched with $NaHCO_3$, and the product was extracted with 3 × EtOAc. The organic layer was dried with Na_2SO_4, filtered and evaporated under reduced pressure to yield *m*-pentylphenol (0.6 g, yield 86.8%).

^{1}H-NMR ($CDCl_3$-*d*): 7.15 (t, J=7.6, 1H), 6.75 (d, J=7.6, 1H), 6.68-6.63 (m, 2H), 5.28 (s, 1H), 2.55 (t, J=7.5, 2H), 1.60 (m, 2H), 1.38-1.29 (m, 4H), 0.92 (t, J=7.0, 3H).

2.3.3.3 IMPROVED SYNTHESIS OF (+)-LIMONENE OXIDE

Synthesis of 2-bromo-4-isopropenyl-1-methylcyclohexanol

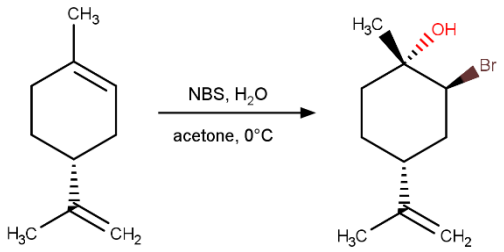

R-(+)-limonene (4.1 g, 30 mmol) was dissolved in a mixture of acetone (15.4 ml) and H_2O (3.4 ml). The system was cooled on an ice bath and *N*-bromosuccinimide (5.9 g, 33.0 mmol) was added in portions over 30 minutes (TLC: CE/EtOAc, 90/10 + vanillin). Acetone was then removed under reduced pressure, and the aqueous layer was diluted with an aqueous solution of $NaHCO_3$. The product was extracted with 3 × EtOAc and the organic layer was dried over Na_2SO_4. The solvent was removed under reduced pressure to yield 2-bromo-4-isopropenyl-1-methylcyclohexanol (9.5 g, quantitative yield).

^{1}H-NMR ($CDCl_3$-*d*): 4.76 (d, J=9.1), 4.20 (s, 1H), 2.48 (s br, 1H), 2.1-1.8 (m, 4H), 1.85 (s, 3H), 1.42 (s, 3H), 1.26 (d, J=4.7, 1H)

Synthesis of (+)-limonene oxide

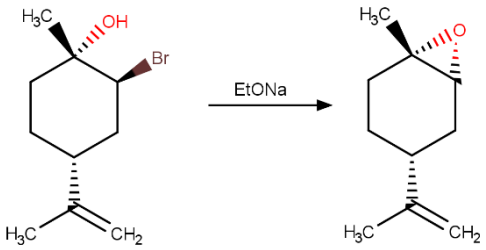

A solution of EtONa 1M (60 ml) was freshly prepared by solubilization of sodium in EtOH previously cooled in an ice bath. To this solution, 2-bromo-4-isopropenyl-1-methylcyclohexanol (9.5 g, 30.0 mmol) was added dropwise, while continuously mixing.
The reaction was quenched by addition of a saturated aqueous solution of NH_4Cl. The substance was extracted with 3 × EtOAc, the organic layer was dried over Na_2SO_4 and the solvent was evaporated under reduced pressure.
The product was purified by distillation at 45°C and high vacuum (10^{-2} mmHg) to yield (+)-limonene oxide (2.3 g, yield 50.7%).

^{1}H-NMR ($CDCl_3$-*d*): 4.67 (d, J=1.0, 4H), 2.98 (d, J=5.3, 1H); 2.07-1.98 (m, 4H), 1.89-1.75 (m, 4H), 1.74-1.60 (m, 2H), 1.66 (s, 3H), 1.31 (s, 3H).

2.3.3.4 SYNTHESIS OF 2-[(1*R*,6*R*)-3-METHYL-6-(1-METHYLETHENYL)-2-CYCLOHEXEN-1-YL]-5-PENTYLPHENOL (DESOXY-CBD)

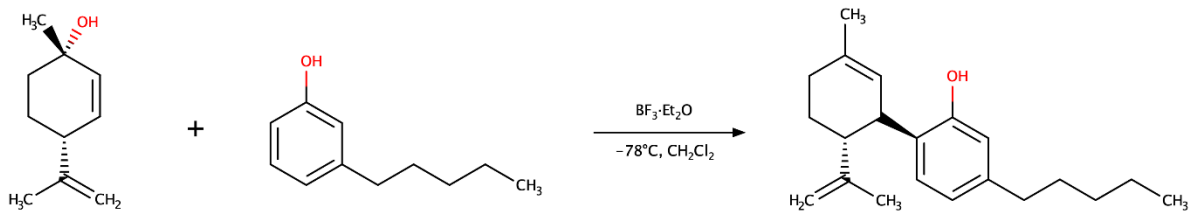

To a solution of *p*-mentha-2,8-dien-1-ol (1.5 g, 9.9 mmol) and *m*-pentylphenol (1.6 g, 9.9 mmol) in CH_2Cl_2 (100 ml) was added anhydrous Na_2SO_4 (1.5 g) and the system was purged with nitrogen. The mixture was cooled to -78°C with stirring, then fresh $BF_3 \cdot Et_2O$ (500 µL) was added dropwise, and the reaction was slowly warmed to -10°C over 1.5 hours (TLC: CE/EtOAc, 80/20 + vanillin).

The reaction was quenched with anhydrous Na_2CO_3, the salts were filtered, and the filtrate was evaporated by reduced pressure. The final product was purified with flash chromatography (eluent: CE/EtOAc, 80/20) yielding 2-[(1*R*,6*R*)-3-methyl-6-(1-methylethenyl)-2-cyclohexen-1-yl]-5-pentylphenol, desoxy-CBD (1.3 g, yield 43.3%).

^{1}H-NMR ($CDCl_3$-*d*): 6.87 (d, J=8.1, 1H), 6.64-6.61 (m, 2H), 5.52 (s, 1H), 5.44 (s, 1H), 4.67 (t, J=1.7, 1H), 4.56 (s, 1H), 3.40 (m, 1H), 2.51 (t, J=7.5, 3H), 2.32 (m, 1H), 2.21 (m, 1H), 2.06 (dt, J=17.7, J=2.5, 1H), 1.85-1.70 (m, 2H), 1.77 (s, 3H), 1.60-1.55 (m, 2H), 1.59 (s, 3H), 1.37-1.24 (m, 4H), 0.88 (t, J=6.8, 3H).

2.3.4 SEMISYNTHESIS OF DH-CBD

2.3.4.1 SYNTHESIS OF CBD TRIFLATE

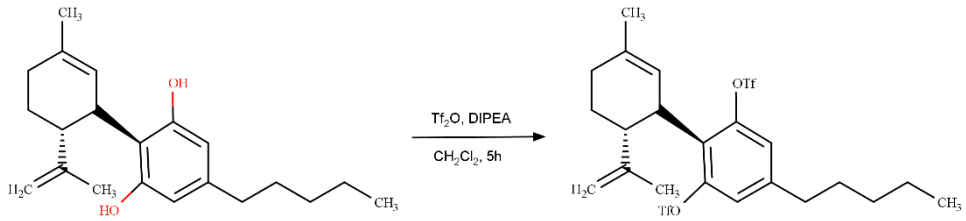

Cannabidiol (1.26 mg, 4.0 mmol) was dissolved in CH_2Cl_2 (16 ml) in a round bottomed flask, and the mixture was cooled at -78°C. DIPEA (1.7 ml, 10.0 mmol) was added, the system was purged with nitrogen atmosphere, and stirred for 10 minutes. Tf_2O (1.7 ml, 10.0 mmol) was then injected with a syringe and the solution was mixed at -78°C for 5 hours (TLC: C.E./EtOAc, 80/20 + vanillin).

The reaction was quenched by adding H_2O (16 ml), then the organic layer was washed with 2 × $NaHCO_3$ 5% solution and 1 × brine, dried on Na_2SO_4, filtered and the solvent was evaporated under reduced pressure, yielding CBD triflate (2.2 g, quantitative yield).

^{1}H-NMR ($CDCl_3$-*d*): 7.09 (s, br, 2H), 5.27 (s, 1H), 4.52 (t, J=3.4, 1H), 4.37 (m, 1H), 3.86 (m, 1H), 2.70-2.59 (m, 3H), 2.30-2.14 (m, 1H) 2.07-1.97 (m, 1H), 1.85-1.75 (m, 2H), 1.72-1.67 (s, 3H), 1.64-1.56 (m, 2H), 1.59 (s, 3H), 1.33-1.26 (m, 4H), 0.91 (t, J=6.7, 3H).

2.3.4.2 SYNTHESIS OF DH-CBD TRIFLATE

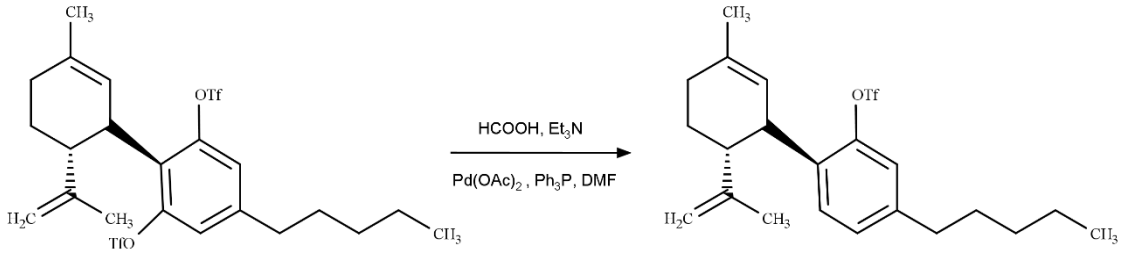

To a solution of CBD triflate (1.7 g, 3.0 mmol) in DMF (9 ml), $Pd(OAc)_2$ (0.03 g, 0.15 mmol) and Ph_3P (0.08 g, 0.3 mmol) were added. The system was kept under nitrogen atmosphere for 15 minutes and heated to 40°C. Et_3N (1.7 ml, 12.0 mmol) and HCOOH (0.3 ml, 9.0 mmol) were consecutively added, and the system was reheated to 60°C for 60 minutes (TLC: Petroleum ether 100% + vanillin).

The mixture was cooled in an ice bath, then the reaction was quenched by addition of H_2O, NH_4Cl and $NaHCO_3$. The product was extracted with 3 × $CHCl_3$, then the organic layers were combined, dried over anhydrous Na_2SO_4 and filtered. The solvent was evaporated under reduced pressure, then re-suspended with 10 ml of diethyl ether. The organic layer was washed with 3 × brine, dried over anhydrous Na_2SO_4, filtered and the solvent was evaporated under reduced pressure, obtaining DH-CBD triflate (0.7 g, yield 50.1%).

^{1}H-NMR ($CDCl_3$-*d*): 7.20 (d, J=8.0, 1H), 7.12-7.09 (dd, 1H), 6.98 (d, J=4.8, 1H), 5.27 (s, 1H), 4.55 (t, J=3.4, 1H), 4.35 (m, 1H), 3.70 (m, 1H), 2.60-2.56 (m, 3H), 2.16-2.00 (m, 3H), 1.70 (s, 3H), 1.59 (s, 3H), 1.58-1.54 (m, 2H), 1.35-1.27 (m, 4H), 0.93-8.67 (m, 3H).

2.3.4.3 SYNTHESIS OF DH-CBD

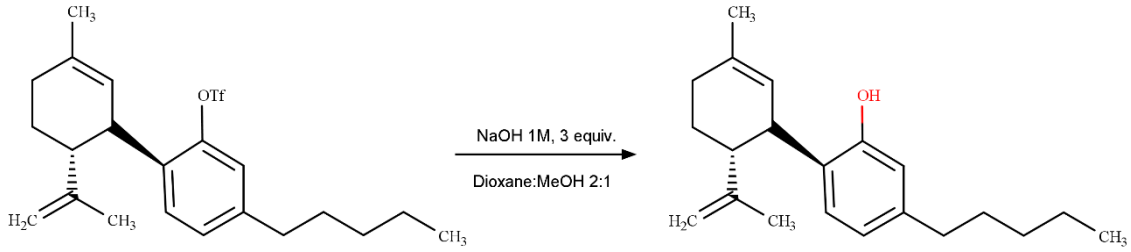

DH-CBD triflate (0.9 g, 2.0 mmol) was dissolved in a mixture of 1,4-dioxane (20 ml) and MeOH (10 ml) using a magnetic stirrer. A solution of NaOH 1M (9 ml, 9.0 mmol) was slowly added at room temperature, and the mixture was left stirring for 3 hours (TLC: Petroleum ether 100% + vanillin).

The reaction was stopped by addition of HCl 1M until neutralization, then the aqueous phase was diluted with a saturated solution of NH_4Cl. The product was extracted with 3 × EtOAc, then the organic layers were combined, dried with anhydrous Na_2SO_4, filtered, and evaporated under reduced pressure. The obtained dark resin was purified in a chromatographic column (eluent: CE/EtOAc, 98/2) to yield desoxy-CBD as a colorless oil (0.5 g, yield 82.0%).

^{1}H-NMR spectrum resulted identical to the peaks reported in Paragraph 2.3.3.4 for the synthesis of DH-CBD.

2.4 CONCLUSIONS

Cannabinoids and the endocannabinoid system have been extensively studied throughout the XX century, and nowadays, the research is still very active. An improvement of the available technologies and analytical techniques empowered the knowledge over the molecular structures of phytocannabinoids (cannabinoids derived from cannabis strains) and their interactions with complex signaling pathways in the human brain not only limited to the so-called cannabinoids receptors, CB1 and CB2. Moreover, the research allowed to better understand the structure-activity relationship of Δ^9-tetrahydrocannabinol, as well as the crystalline structure of the CB1 receptor, available in high quality since 2016 (131). Several synthetic cannabinoids were developed in the last 50 years with the purpose to interact with CB receptors, or to reduce any interaction with the subtype CB1 to avoid psychoactivity. In this framework, this project aimed to develop a model molecule to mimic the solubility behavior of THC but avoiding its effects on the central nervous system, and its benzopyranic structure for requirements coming from Italian narcotic law. The choice was desoxycannabidiol (DH-CBD), a synthetic cannabinoid with a structure amenable to CBD and showing interesting pharmacological properties, as its interactions with glycine receptors make it an enticing candidate to open a new class of drugs to be used in pain therapy.

The preparation of this compound is based on the condensation of two synthons: *p*-mentha-2,8-dien-1-ol and *m*-pentylphenol. DH-CBD and its precursors have limited commercial availability, and for the preparation of the synthons, there is little precedence in the chemical literature. The approach proposed by Wilkinson, Price, and Kassiou was replicated in our laboratories but failed to yield appreciable quantities of DH-CBD. The limiting step of the process in the synthesis of *p*-mentha-2,8-dien-1-ol starting from (+)-limonene was the lack of stereoselectivity. Our studies led to the desired diastereomer by selectively forming a *trans*-bromohydrine and consequently epoxidizing with a strong base. Thus, although using an additional step in the pathway, the total yield was improved, obtaining useful amounts of this fragment for the condensation with *m*-pentylphenol. Including the production of the two synthons, the total reaction yield reached a maximum of 6%.

New possibilities were opened when a considerable amount of pure crystals of cannabidiol (99% purity) became available. The semisynthetic approach had some intrinsic difficulties, as the selective deoxygenation of a single phenol group in the aromatic ring was considered very difficult, as demonstrated with the deoxygenation on THC. In our laboratories, a palladium-catalyzed reaction allowed to selectively reduce one hydroxyl group calibrating the molar ratios of reducing agent and the reaction kinetics. In this way, we obtained DH-CBD with a total yield of 41% and improved the accessibility to this compound for the formulation into vesicular systems for the transdermal delivery of cannabinoids, as described in Chapter 3.

Chapter 3

Pharmaceutical technology development

3.1 SKIN DELIVERY

Skin is the largest organ of the human body. Its primary role is protective from the external environment, both being a first-line defense against harmful microorganisms, chemicals, and UV rays, as well as permeability barrier preventing the loss of fluids and salts. Its structure can vary from different locations on the same body, but generally is about 1.5 mm thick and consists of three main layers (132). The epidermis composes the outermost layer. It consists of viable cells below a 10-20 μm thick matrix of keratinocytes embedded in highly ordered lipid layers, called the stratum corneum (SC) (133). The viable epidermis is usually about 0.06–0.8 mm thick and is located immediately under the SC. This layer is mainly composed of 4–5 layers of dermal fibroblasts and keratinocytes. The whole epidermis is mainly responsible for the primary function of the skin and is the strongest agent preventing drug absorption through the skin. Below the epidermis is located the dermis, a 0.3-5 mm thick connective tissue containing the sweat glands, hair follicles, capillaries, lymphatic vessels, and nerve endings, primarily responsible of the viability of the viable epidermis and the response to injuries. The deeper layer of the skin is the hypodermis, where loose connective tissue contains adipocytes providing cushioning (134, 135).

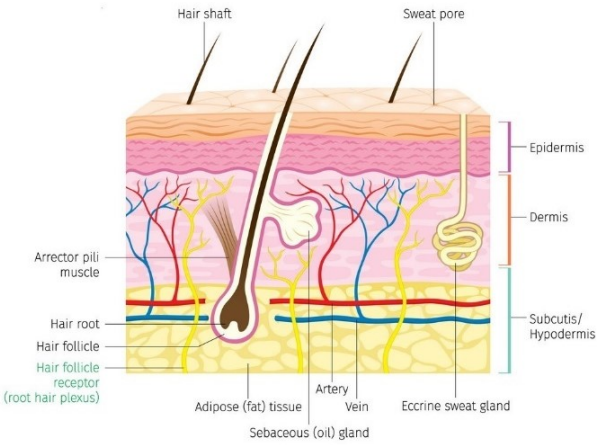

Figure 3.1 – Representation of the skin structure.

Across this barrier, only small molecules with lipophilic nature can penetrate freely through the SC. The efficacy of the topically applied drugs from simple formulations is often far from the required. Many therapeutic agents can exercise their function only when they are able at least

to enter the SC. The main pathway for the penetration of most molecules is believed to be the tortuous intercellular route (136–138), while intracellular and intrafollicular routes are believed to be less exploited by free drugs.

Most therapeutic agents require permeation enhancement in order to be delivered to the deeper skin layers at efficient concentrations. Skin delivery of actives using lipid vesicular carriers as enhancing delivery agents has raised considerable interest in the last decades. Liposomes were one of the first investigated carriers in this field. Despite the ability of classic liposomes to generate significant reservoirs of drugs in the superficial strata of the skin, the delivery to the deeper skin layers was proved to be limited (139, 140). More recently, innovative systems were developed to overcome the SC barrier and facilitate the delivery of active ingredients to these regions (141). Vesicular systems classified as "ultra-deformable vesicles" have been recently developed with the aim of producing soft, deformable systems which can adapt to several environments to overcome barriers, including the stratum corneum, and different drugs, both hydrophilic and lipophilic. As an example, deformable vesicles can be transfersomes, elastic nanovesicles with a similar composition to liposomes, but including edge activators like bile salts or nonionic surfactants. These systems were firstly introduced in 1992 by Cevc (142). A deformable vesicular system composed of phospholipids and ethanol was developed in 1998: the ethosome.

3.2 ETHOSOMES AND VESICULAR SYSTEMS

3.2.1 CHARACTERISTICS OF ETHOSOMES

In 1998 Touitou invented a unique soft vesicular system called 'ethosome' (143, 144). In the last 20 years, several studies have proven the ability of this carrier to enhance the delivery of both hydrophilic and lipophilic drugs to low skin strata and systemic circulation. Ethosomes are vesicles composed of phospholipids and short-chain alcohols (mainly ethanol) at concentrations up to 50%, suspended in an aqueous medium. These carriers are prepared by a simple mixing method: the phospholipid and the drug are dissolved in the short-chain alcohol by mechanical stirring, followed by slow addition of water while continuously mixing. This method has many advantages, as it is considered an environmentally friendly process which involves the use of safe ingredients (144). It is essential to underline that preparation methods involving solvent evaporation and thin layer formation (145, 146) are not recommended by the inventor, since such techniques may alter the properties and consequently the effect of these carriers.

The unique feature of ethosomes is their soft, deformable structure which is imparted by high alcohol concentrations that fluidize the phospholipid bilayers. Touitou extensively investigated the features of these delivery systems. Phosphorous (^{31}P)–NMR studies showed that phosphatidylcholine is organized in bilayers exhibiting a spherically organized fluid line-shape when ethanol is present at concentrations between 20 and 45%. The values of the effective chemical shift anisotropy obtained in these experiments were lower than those obtained with liposomes, confirming the motion of polar phospholipids head groups in the ethosomal systems. In the paramagnetic-ion (Pr^{+3}) NMR spectra, it was shown that these vesicles were packed less tightly and characterized by higher permeability of cations compared to liposomes, where ethanol was not present. At 50% of ethanol, the signal becomes isotropic and narrow, indicating that the phospholipid exists in the form of small, fast-tumbling micelles. This finding was further confirmed by the results of the fluorescent anisotropy measurements of 9-antrivinyl labeled analog of PC (AVPC) where a high degree of fluidity and a lower transition temperature for the phospholipid bilayers in ethosomes, as compared to liposomes, was found (144).

DSC thermograms showed differences of up to 30ºC in the transition temperatures (T_m) between the phospholipids in ethosomes and phospholipids in liposomes containing the same concentration of the main ingredients. Thermograms of empty systems showed that the T_m values were -15.2°C for ethosomes (5% phospholipid, 30% ethanol, and water) and 6.38°C for liposomes, respectively. Ethosomal systems containing 1 and 3% bacitracin exhibited T_m values of -16.1 and -19ºC, respectively. This value was compared to T_m exceeding 14ºC for liposomal systems loaded with an equal drug concentration (147).

Cryo-scanning electron microscopy confirmed the closed spherical shape of ethosomes (144, 148). TEM micrographs showed differences in the lamellarity of these systems: depending on the composition and the type of active ingredients, the multilamellar structure can be evenly spaced to the core, as in the case of testosterone and minoxidil. With more hydrophilic compounds such as trihexyphenidyl hydrochloride, ethosomes have only few (two to three) lamellae (149). Unilamellar vesicles were observed when incorporating erythromycin and buspirone (148, 150). The systems are generally characterized by a narrow and homogenous size distribution. Generally, the mean size distribution of ethosomes can vary from thirty nanometers to microns. DLS data showed a mean size of 150 ± 4 nm for systems containing 2% phospholipid and 30% ethanol. These carriers had a smaller and more homogenous size than that of liposomes obtained by the film-forming method (144).

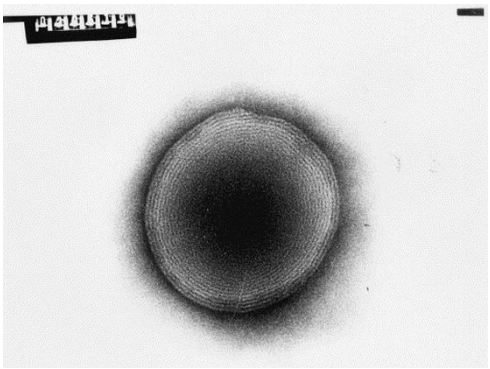

Figure 3.2 – TEM micrograph of an ethosome. The multilamellarity of the structure can be noticed, as well as the soft structure given by an irregular spherical shape. Adapted from (144).

Touitou *et al.* studied the influence of each component on the particle size and system stability. An increase in ethanol concentration from 20 to 45% in a system containing 2% soy lecithin caused a gradual size decrease from 193 to 103 nm (144), and an increase in the surface negative charge to the vesicles. The charge of the systems measured by DLS showed a transition in the zeta potential from 4.6 ± 0.2 mV in liposomes to -4.3 ± 0.2 mV in ethosomal system due to the presence of 30% ethanol. This shift in the vesicles charge from positive to negative is important since such properties may affect the carrier stability and the skin–vesicle interactions (144). The characteristics and concentrations of active ingredients can also affect the vesicular systems. Incorporation of 30 mg/g of buspirone in the system resulted in mean size distribution of vesicles of 194.8 ± 98.6 nm with a polydispersity index (PDI) of 0.75 (148). Likewise, the size distribution of 1% trihexyphenidyl hydrochloride (THP) ethosomes showed one narrow peak, indicating that the vesicles population is relatively homogenous in size (109 ± 2 nm). Also, THP liposomes prepared by the classic method exhibited one narrow peak but had a mean size of 324 ± 9 nm, more than twice that of THP ethosomes (149).

The ability of ethosome to entrap various molecules was also reported. The entrapment capacity of buspirone HCl in these soft vesicles was found to be 75.3 ± 1.5% as measured by

ultracentrifugation combined with HPLC quantification (148). In another work using a similar method, it was shown that the THP entrapment capacity in ethosomes was almost 2-fold higher than that in liposomes, with values of 75 ± 0.8 vs. 36 ± 1.6%, respectively (149). Moreover, lipophilic molecules such as minoxidil and testosterone were highly entrapped in the vesicles reaching capacities of 83 and 90%, respectively (144). Fluorescent probes demonstrated the capability of molecules to be efficiently entrapped in the whole vesicular system. FITC-bacitracin (FITC-Bac) and the labeled phospholipid rhodamine red-dihexadecanoylglycerophosphoethanolamine (RR) filled up the entire volume of the ethosomes. On the opposite, RR in liposomes was visualized only inside the vesicle membrane, and FITC-Bac appeared only in its core. Such observations could be explained by the multilamellarity of ethosomes to the core and the existence of a hydroethanolic environment throughout the vesicles (147).

3.2.1.1 PROPOSED MECHANISM OF ACTION OF ETHOSOMES

Touitou has first shown that drug permeation into and through the skin was enhanced by means of the ethosomal composition and not by any component of the system alone (144, 147, 149). The high fluidity of phospholipid bilayers is the main feature that imparts malleability and softness to ethosomes. In a CLSM study, Godin and Touitou showed that FITC-Bac administrated *in vivo* from ethosomes penetrated the rat skin through the inter-corneocyte pathways, which typically exist among the lipid domain of the SC. On the other hand, significantly lower fluorescence intensity of the intercellular penetration pathway and no inter- or intra-corneocyte fluorescence were observed with FITC-Bac delivered by a hydroethanolic solution and liposomes, respectively (147).

In another work by the same authors, the efficiency of transcellular delivery into Swiss albino mice 3T3 fibroblasts of D-289 fluorescent dye, rhodamine red (RR), calcein, and labeled fluorescent phosphatidylcholine from ethosomes was investigated. CLSM micrographs showed that the soft carrier improved the penetration into the cells of all tested probes. When the molecules were delivered as a hydroethanolic solution or classic liposome, almost no fluorescence was detected. Furthermore, enhanced delivery of a hydrophilic probe, calcein, and a lipophilic one, RR, from the ethosomal carrier was observed in permeation experiments with whole nude mouse skin. Ethosomes improved the skin permeation of calcein to a depth of 160 µm, whereas a hydroethanolic solution and liposomes made the same molecule to reach a skin depth of 80 and 60 µm, respectively. Maximum measured fluorescence intensities for RR delivered from ethosomes were 150 AU compared to 40 and 20 AU from the two control systems (151).

Based on the results obtained and on the characteristics of ethosomes, the mode of action for these vesicles could be delineated. This model assumes that the enhancement is the result of a double action of the soft vesicle and the high ethanol concentration. Ethanol fluidizes the phospholipid bilayers generating malleable and soft vesicles, but also fluidizes and disturbs the stratum corneum lipid bilayers. Consequently, the penetration of the soft ethosomal vesicles through these layers is facilitated resulting in the efficient delivery of molecules to the deeper skin layers, where they fuse with the cell membranes and release the incorporated drug (144). Such a unique effect can only be seen with ethosomes. It was previously reported that the permeation enhancement was negligible from phospholipid vesicular carriers containing low ethanol concentrations (5 and 10%). This lack of effect is supported by the DSC results, which indicate a less fluid state for the vesicles containing 10% ethanol versus ethosomes. In an *in vitro* experiment, Touitou compared the effect of an ethosomal system containing 35% ethanol, and a formulation containing 5% ethanol on the skin permeation of sodium diclofenac. It was found that the ethosomal systems lead to enhanced delivery of the drug through the skin by 8-folds compared with the composition containing only 5% ethanol (309.2 vs. 37.7 µg/cm²) (143).

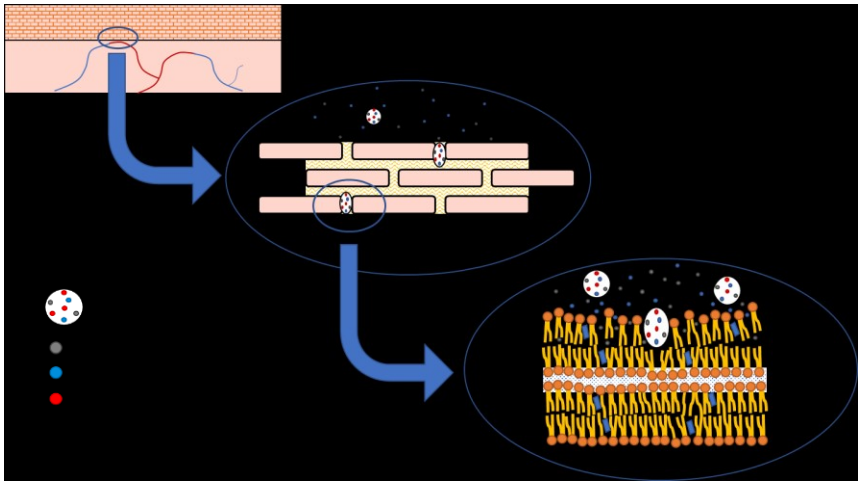

Figure 3.3 – Proposed mechanism of action of ethosomes: ethanol fluidizes both the vesicular and skin lipids, allowing the vesicles to reach the deep skin strata via intercellular pathway.

3.2.1.2 EXPERIMENTS ON ETHOSOMES AND VESICULAR CARRIERS

In this work, experiments were carried on both at The Hebrew University of Jerusalem and the University of Padova. In the first case, under the supervision of Prof. Elka Touitou, the main characteristics of ethosomes and soft vesicular systems were investigated, and the results will be illustrated in the following paragraph. Meanwhile, innovative deformable systems were developed in the laboratory of Prof. Nicola Realdon at the University of Padova. Systems containing high concentrations of propylene glycol were produced and characterized in terms of stability over time and entrapment efficiency of lipophilic drugs. The vesicles were incorporated into hydrogels, and its rheological and release properties were tested. The results are reported in Paragraph 3.3.

3.2.2 MATERIALS AND METHODS

3.2.2.1 MATERIALS

Ethanol absolute (Gadot, Israel)
Fluorescein isothiocyanate, FITC (Sigma Aldrich, Israel)
Lidocaine base (Trima, Israel)
Phospholipon 90G (Lipoid GmbH, Germany)
Propylene glycol (Tamar, Israel)

3.2.2.2 CHARACTERIZATION

Preparation method

The ethosomal dispersions were prepared by a simple mixing method using an overhead Heidolph® stirrer (Heidolph Digital 200 RZR-2000, Schwabach, Germany). Briefly, the phospholipid (Phospholipon 90G, PL) was dissolved in ethanol (EtOH). The active ingredient and propylene glycol (PG), if present, were then dissolved in this solution consecutively. Double distilled water (DDW) was added slowly with continuous mixing at 700 rpm and mixed for further 5 minutes. The formulations were left to rest for 30 min, and when stability tests were run 12 ml of each formulation were stored in a separate vial. The preparations were stored in well-sealed glass vials protected from light. When FITC was used, the preparation was performed in a dark room. The compositions of the prepared formulations are given in Table 3.1.

Table 3.1 – Composition of the prepared formulations. Values are expressed as percentage %w/w.

NAME	PL (%)	EtOH (%)	PG (%)	DDW (%)	Lidocaine base (%)	FITC (%)
E001	2.00	30.00	-	68.00	-	-
E002	2.00	40.00	-	58.00	-	-
E004	2.00	30.00	20.00	48.00	-	-
E014	2.00	30.00	20.00	47.95	-	0.05
E021	2.00	30.00	-	67.00	1.00	-
E024	2.00	30.00	20.00	47.00	1.00	-

pH measurement

The formulations were characterized in terms of pH, viscosity, and particle size. With a Mettler Toledo SevenEasy pH-meter the formulations were analyzed after dilution with DDW at a ratio 1:5 v/v. Two dilutions were performed for each sample.

Viscosity measurement

The viscosity was assessed using Brookfield DV III Rheometer-LV (Brookfield engineering labs, USA), spindle 18, on 9 ml of formulation in a small sample adaptor. The measurement was carried out at a rotation speed of 30 rpm.

Mean vesicles size distribution measurement

Mean vesicles size distribution was analyzed using the DLS apparatus Malvern Zetasizer-nano, ZEN 3600 (Malvern Instruments, Malvern, UK). One hour prior to measurement, the systems were diluted 1:500 with diluent prepared as described below. Three batches of each system were tested. Each batch was analyzed by intensity three times, at 25°C. The duration and the set position of each measurement were fixed automatically by the apparatus.
Diluting solution preparation: for each formulation, an equivalent hydroethanolic or hydro-ethanolic-glycolic mixture was prepared. The mixtures were then vortexed for 30 seconds, filtered with 0.2 µm pore size disposable filter in cellulose acetate (Minisart syringe filter, Sartorius, Israel) and stored in Eppendorf 50 ml tubes. Tubes were sealed with Parafilm® and protected from light. The solutions were prepared 24 hours before the dilution.

3.2.2.3 CLSM EXPERIMENT

Formulations

CLSM experiment was run with FITC-PG formulations using liposomes containing FITC as control group. The liposomes were prepared as following: the PC was suspended in 200 µl of water (around 20% of the total amount), then FITC was added and the remaining amount of DDW was added in portions while mixing by vortex. The formulation was prepared one hour prior to the penetration experiment, kept in well-sealed vessel and protected from light.

Table 3.2 – Composition of liposomes containing FITC.

Ingredients	w/w (%)
FITC	0.05
PC	2.00
DDW	97.95

In vitro skin permeation experimental protocol

The ability of the formulations to deliver FITC into the skin was tested in six Franz static diffusion cells using porcine skin and a 30% hydroethanolic solution as a receiver medium. Twenty-five microliters of each formulation were applied on the epidermal side of the skin under non-occlusive conditions for 30 minutes, in a dark room. An untreated skin sample

handled under the same conditions of the treated groups served as control to rule out the autofluorescence of the skin tissue.
At the end of 30 minutes, the skin was removed from the cell and its surface was carefully washed and wiped three times with 600 µl of DDW and Kimwipes (Kimberly-Clark, Canada). The permeation area was then cut and mounted between two cover slips of 24×60 mm for microscopic examination.

CLSM scanning conditions

The samples were scanned using a confocal laser scanning microscope (Zeiss LSM 710 laser scanning microscopy system, Zeiss, Germany) at 10 µm increments through the z-axis with an air plane × 10 objective lens and 488 nm excitation wavelength.
During the microscopic examination, each skin sample was divided to 5 × 5 tiles and micrographic images were obtained. The fluorescence intensity (arbitrary units) was assessed using the ImageJ software.

3.2.2.4 LIDOCAINE SKIN PERMEATION

Formulations

E024 formulation was used for the evaluation of skin delivery of lidocaine base using liposomes containing lidocaine base at the same concentration as a control. Liposomes were prepared as follows. PC and lidocaine base were grounded finely in two separate mortars. Lidocaine base was then weighted and subsequently added to PC, mixing vigorously with a pestle. After obtaining a homogeneous mixture, 2 ml of DDW were included in the formulation geometrically, while mixing with a pestle. The homogeneous emulsion was transferred in a glass vial, the remaining DDW was added and the system was stirred with an overhead stirrer (Hei-Torque 200, Heidolph, Germany) at 700 rpm for 5 minutes. The formulation was then processed with pulsed ultrasound sonicator (SONIC-650WT-V2, M.R.C. Ltd., Holon, Israel) for 10 minutes, kept in well-sealed vessel and protected from light.

Table 3.3 – Composition of liposomes containing lidocaine base.

Ingredients	w/w (%)
FITC	1.00
PC	2.00
DDW	97.95

In vitro skin permeation experimental protocol

The ability of the ethosomal and liposomal formulations to deliver lidocaine base into and through the skin was tested in six Franz static diffusion cells using porcine skin and a 30%

hydroethanolic solution as a receiver medium. Twenty-five microliters of each formulation were applied on the epidermal side of the skin under non-occlusive conditions for 120 minutes, in a reheated room. Receiver samples of 370 µl were taken at 30 and 120 minutes, and equal amount of receiver was returned.
At the end of 120 minutes, the skin was removed from the cell and its surface was carefully washed two times with 600 µl of DDW and wiped three times with Kimwipes (Kimberly-Clark, Canada). Each skin was then inserted into 15 ml tubes containing 5 ml of extraction solution composed by DDW and ethanol 1:1. The tubes were shaken for 24 hours at room temperature with a Gyrotory® water bath shaker (New Brunswick Scientific, USA) set up to speed 5.5. After the 24 hours treatment, the tubes were mixed by Vortex (Vortex Genie®-2, Scientific Industries, USA) for one minute, the skins were removed, and the tubes were stored at -18°C until the HPLC assay.

HPLC assay conditions

HPLC quantification was performed using Merck Hitachi D-7000 interface equipped with an L-7400 variable UV detector, L-7300 column oven, L-7200 auto sampler, L-7100 pump, and HSM computerized analysis. Separation of Lidocaine base was done using Zobrax eclipse DB-C18 5 µm column, 150×4.6 mm, oven temperature 40°C, flow rate 1.2 ml/min, UV detector 220 nm, mobile phase 35:65 ACN: Buffer phosphate 0.01 M pH 6, RT 6.8 min. The solvent used for lidocaine base standard solutions was 30% hydroethanolic solution. Standards of 20, 10, 4, 1, 0.5, and 0.1 µg/ml were prepared. ANOVA tests on the quantification results were performed with Prism software, version 8 (GraphPad Software, San Diego, CA, USA).

3.2.3 RESULTS AND DISCUSSION

3.2.3.1 CHARACTERIZATION

Appearance

All the empty formulations were white, homogeneous liquids. After 3 months of storage, E002 formulation showed remarkable phase separation with sedimentation. On the opposite, E001 maintained a homogeneous appearance for all the 3 months observation. In E004 minor sedimentation was noticed during the first 6 days, after which a phase separation was noticed. After 3 months, the formulation was homogeneous, semi-transparent liquid.
The two lidocaine base systems were semi-transparent, homogeneous liquids which became completely transparent over three months.

pH measurement

In Table 3.4 the pH values for each dilution performed are given. Loaded formulations (E021 and E024) showed a basic pH due to the presence of lidocaine base.

Table 3.4 – pH values for each for prepared ethosomal systems. Values are expressed as mean pH values ± SD.

Formulation name	Mean pH values
E001	6.05 ± 0.24
E002	6.29 ± 0.40
E021	9.51 ± 0.15
E024	9.41 ± 0.06

After three months, E024 formulation showed no appreciable differences in pH: 9.27 ± 0.11 vs. 9.41 ± 0.06 obtained at zero-time.

Viscosity

The viscosity of the samples was evaluated at a room temperature of 21.5 ± 1.0°C. E001 torque value was 15.9%, while for E002 resulted 12.0%. Formulation E024 showed a mean torque value of 21.3% ± 2.69 at 20.6°C, and after three months there were no apparent differences, as the mean viscosity resulted 20.7 ± 0.85 mPa·s.

Mean vesicles size

DLS measurements revealed vesicles with mean nanometric size and low PdI in most cases. Loaded systems showed a small percentage of larger particles. In E004, unstable, the highest percentage of aggregates was registered. Loaded formulations showed a reduction of the vesicles size compared to the equivalent empty formulations. Moreover, E021 showed a second population of very small particles with a mean size of 19.75 nm in each dilution and measurement. In the following table the mean values for each formulation are reported.

Table 3.5 – Mean values of vesicle size expressed for each analyzed ethosomal formulation, expressed as mean size ± SD.

Sample	Peak 1 (nm)	Z-average (nm)	PdI
E001	293.7 ± 90.2	320.3 ± 63.9	0.349 ± 0.265
E002	145.5 ± 46.2	148.9 ± 31.2	0.312 ± 0.081
E004	162.5 ± 87.8	150.1 ± 36.1	0.683 ± 0.184
E021	257.7 ± 30.0	164.3 ± 14.9	0.545 ± 0.096
E024	149.2 ± 33.7	149.9 ± 35.0	0.435 ± 0.128

After three months, in E024 formulation a decrease (~32%) in the vesicles mean size distribution was registered. The values were maintained in the nanometric size and low PdI. A population of relatively large particles (2500-3000 nm) that was observed on the zero-time characterization was also present after three months (Table 3.6).

Table 3.6 – Mean particle size of ethosomes containing lidocaine base 1% (E024 repeated) and stability over three months. Values are expressed as mean size ± SD.

Sample	Peak 1 (nm)	Z-average (nm)	PdI
Zero-time	176 ± 77.6	221.6 ± 162.6	0.7 ± 0.2
After three months	119.1 ± 39.7	181.4 ± 149.3	0.6 ± 0.3

3.2.3.2 CLSM EXPERIMENT

The obtained micrographs are reported in Appendix section A and showed a greater fluorescence intensity in the case of ethosome treated skin as compared to liposomes. It should be mentioned that sample 2 in the ethosome treatment group showed an irregular surface when observed under the microscope. The fluorescent signal, although low compared to other samples from the same group, was still higher than the liposome treated samples.
The mean values of fluorescence intensity in the skin measured following ethosomes and liposomes treatments are given in Figure 3.4.

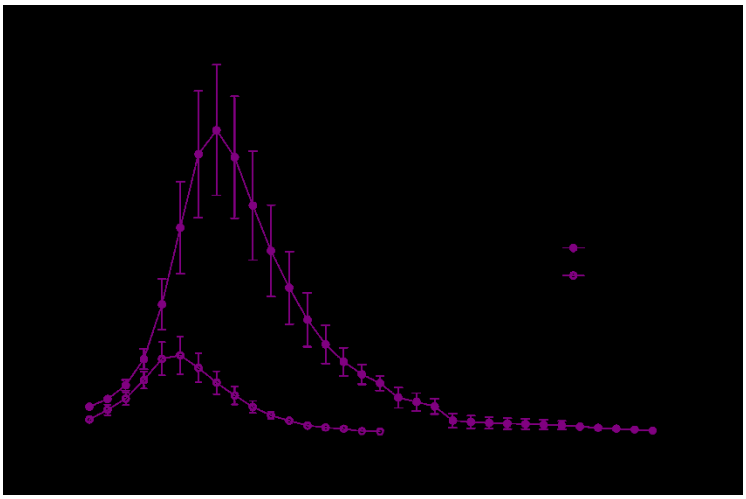

Figure 3.4 – Mean fluorescence intensity of skin micrographs obtained following application of FITC ethosomal and liposomal samples (± SEM).

In the ethosomes group, the skin depth penetration was deeper than in liposomes group: 320 and 170 µm, respectively. At 30 minutes, the maximum fluorescence for the ethosomal system was measured as of 80 µm, while in the liposomes group at only 60 µm.

The area under the curve (AUC) was 9083.815 for ethosomes treated group as compared to 1823.97 of liposomes treated group, meaning an enhanced bioavailability by 5 times with ethosomes.

3.2.3.3 SKIN PENETRATION OF LIDOCAINE BASE EXPERIMENT

Lidocaine permeated amount was calculated according to the obtained calibration curve, having a correlation coefficient (R^2) value of 0.996.

The mean percentages of lidocaine base permeated into or across the skin after 30 and 120 minutes of application of the formulations are given in Table 3.7.

Table 3.7 – Mean percentage of lidocaine permeated amount following 30 or 120 minutes of application, and mean percentage of lidocaine amount delivered into the skin following 120 minutes of application of 1% w/w lidocaine in ethosome vs in liposomes.

Sample	Lidocaine permeated amount after 30 min (%)	Lidocaine permeated amount after 120 min (%)	Lidocaine amount in the skin after 120 min (%)
Ethosomes	0.67 ± 0.34	11.24 ± 2.45	27.84 ± 3.90
Liposomes	1.56 ± 1.24	16.13 ± 7.67	60.22 ± 17.99

The mean percentage values of lidocaine base permeated amount after 30 and 120 minutes of permeation are reported in Figure 3.5. In the same figure is reported the mean percentage of lidocaine base delivered into the skin after 120 minutes of application of the formulations.

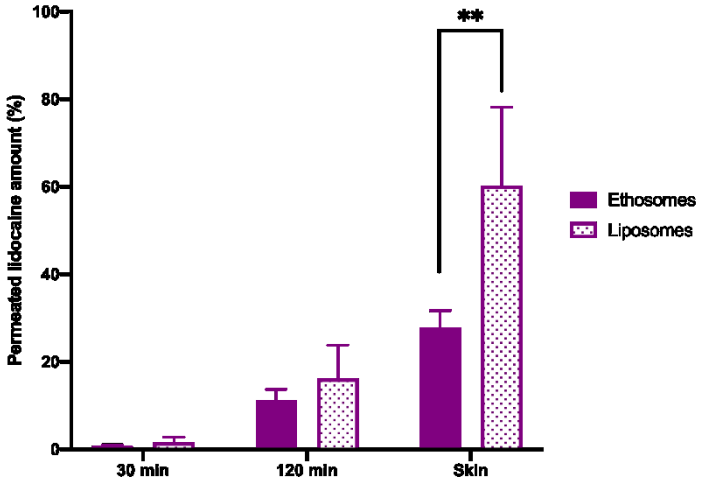

Figure 3.5 – Lidocaine base permeated amount across the skin at 30 and 120 minutes of diffusion, and into the skin at 120 minutes of diffusion. Values are expressed as mean percentage (± SD).

As reported in the previous tables and graphs, higher delivery of lidocaine base into the skin was registered when the liposomal system was applied: the mean percentage amount of drug resulted 60.22 ± 17.99%, while ethosomes lead to 27.84 ± 3.90%.

Receiver samples taken at 30 and 120 minutes did not show statistically significant differences in skin permeability of Lidocaine base between the two groups, but a statistically higher (two-way ANOVA, $p < 0.005$) mean permeation through the skin can be registered with liposomes: phospholipidic dispersion lead to 1.56% ± 1.24% of permeated drug after 30 minutes and 16.13 ± 7.67% after 120 minutes, while ethosomes reached 0.67 ± 0.34% and 11.24 ± 2.45%, respectively.

3.2.4 DISCUSSION

Skin penetration of a fluorescent probe, FITC, was assessed with Franz diffusion cells on porcine skin after 30 minutes of application. Ethosomes improved the bioavailability by 5 times as compared to a liposomal formulation of an equal amount of FITC. This is an indication of the superior properties of ethosomes compared to other rigid vesicular systems. Despite these promising results, the penetration of lidocaine base into and across the skin of the ethosomal formulation resulted less effective than the liposomal formulation. This resulted by HPLC quantification of receiver samples collected after 30 minutes and 120 minutes, with a confirmation by quantification of the drug delivered to the skin. The results indicate that there is no statistical difference between the permeated amount of lidocaine between the ethosomal and the liposomal group (ANOVA test, $p > 0.05$), and the tendency suggests a higher efficacy of the control group. The delivered amount of lidocaine resulted statistically higher ($p < 0.05$) in the control group, indicating a "lower" efficacy of ethosomal systems. These results can be misleading: in fact, many aspects must be taken into account. First, as previously mentioned, the ethosomal system and the control showed a basic pH (around 9.4 in both cases). This pH is not compatible with the cutaneous physiological pH (around 5). The differences in the pH can cause different absorption rates in in vitro tests, while skin irritation could be registered in vivo. This hypothesis is supported from the results obtained in the CLSM study, where the fluorescent probe was not basic, and it was successfully delivered into the skin by ethosomes with an improved bioavailability. Moreover, in the control group lidocaine base was not homogeneously dispersed in the sample. Small crystals of undissolved drug could be seen, and precipitation of drug could occur during the application in the permeation test. The presence of the drug in a different dispersion state can have influenced the skin penetration rate.

3.3 VESICULAR SYSTEMS WITH HIGH CONCENTRATION OF PROPYLENE GLYCOL

3.3.1 MATERIALS AND METHODS

Vesicular systems with low amounts of ethanol and good entrapment efficiency of cannabinoids were developed by evaluating the effect of high concentrations of propylene glycol (PG). As demonstrated in the previous chapter, the introduction of propylene glycol in the system leads to a decrease in particle size, influencing the ethosomal properties of size, entrapment efficiency, permeation, and stability. As the combination of high ethanol concentration and cannabinoids could lead to toxicity in patients, vesicular systems containing a fixed minimum amount of ethanol, *i.e.*, 20% w/w (143, 144), and different PG concentrations higher or equal to ethanol concentrations were prepared and characterized.

3.3.1.1 MATERIALS

Carbopol® Ultrez 10 Polymer (Lubrizol Advanced Materials Europe BVBA, Belgium)
CBD Crystal-99one (kindly provided by Enecta®, The Netherland)
Desoxy-cannabidiol (synthesized as described in Chapter 2)
Ethanol extra pure 96% Pharmpur (Scharlab, Spain)
Lipoid S100 (kindly provided by Lipoid GmbH, Germany)
Phenol Red (J.T.Baker®, Fisher Scientific Italia, Milan, Italy)
Phospholiphon® 90G (kindly provided by Lipoid GmbH, Germany)
Propylene glycol (Fagron, Italy)
Triethanolamine 85% (Fagron, Italy)

3.3.1.2 PREPARATION

Vesicles containing high concentrations of propylene glycol were developed in the laboratories of Pharmaceutical Technology under the supervision of Prof. Nicola Realdon, at the University of Padova. These systems were designed with the aim of reducing the total ethanol amount, which could show some toxicity for the patient when used for the delivery of cannabinoids. This had to be developed while maintaining some of the unique properties of ethosomes, especially small size, deformability and homogenous size distribution of the vesicles.
The production method of these system was similar to the method previously described. Briefly, ethanol and propylene glycol were weighed in a small beaker and mixed for a short time with an overhead mechanical stirrer ALC quiet-sL (Vetrochimica s.r.l., Como, Italy). The phospholipid and the active ingredient, when present, were subsequently added to the beaker and mixed at 200 rpm until complete dissolution (between 15 and 30 minutes). The rotation speed was then increased to 700 rpm and ultrapure milliQ water was slowly added using a

syringe with a needle. After the addition of the total amount of water, the formulation was left stirring for additional 10 minutes, then treated in an ultrasound bath for 30 discontinuous minutes (alternating 5 minutes treatment and 5 minutes rest) to homogenize the size distribution of the vesicles. During all the process, the beaker was carefully closed with Parafilm® to prevent solvent evaporation.

The effect on the stability of the formulation given by the variation of each component was evaluated in unloaded formulations. Ethanol concentration was kept at the minimum concentration for the formation of the vesicular systems, *i.e.*, 20% w/w (143, 144). Propylene glycol concentration ranged between 20 and 50% w/w at every phospholipid concentration. The investigated phospholipid amounts ranged between 2 and 5% w/w, considering two different phospholipid types: Pospholipon® 90G and Lipoid S100. Both phospholipids are composed of minimum 94% w/w of phosphatidylcholine, while the remaining part is given by lysophosphatidylcholine (Pospholipon® 90G) or fatty acids (Lipoid S100) in different ratios. The impact of the active ingredient on the formulation was also considered, comparing the results obtained with cannabidiol (99% CBD, 1% terpenes) with synthetic DH-CBD at the same concentration.

After realization, the samples were transferred in Falcon™ 15 ml conical tubes and stored at different temperatures. Storage under refrigerated conditions (4 ± 1°C) was compared to storage at room temperature (25 ± 5°C), while all the preparations were protected from light by coverage with aluminum foil. Formulations containing DH-CBD or CBD were stored only in refrigerator to prevent oxidation phenomena, which occurred under storage at room temperature. The compositions of the most stable loaded formulations are reported in Table 3.8.

Table 3.8 – Composition of the most stable loaded systems containing variable PG and fixed 20% w/w ethanol.

Sample name	Phospholipid	PC % (w/w)	PG % (w/w)	mQ water % (w/w)
E031	Phospholipon® 90G	5.0	50.0	44.0
E032		4.0	40.0	55.0
E033		3.0	50.0	46.0
E041	Lipoid S100	5.0	40.0	54.0
E042		5.0	30.0	64.0
E045		4.0	40.0	55.0
E046		4.0	30.0	65.0

3.3.1.3 CHARACTERIZATION OF THE FORMULATIONS

Each sample was evaluated under visual analysis and particle size analysis 24 hours after preparation and most formulations underwent three months stability tests.
Dynamic Light Scattering (DLS) analysis were performed using a Zetasizer Nano ZEN 3600 (Malvern, United Kingdom) with a backscattering detector at 173°, equilibration time of 60 seconds and automatic attenuator position. Tests were run at 25°C, with three replications of 12 scans for each sample. Three samples were analyzed for each formulation.
Empty formulations were filtered before analysis with 0.45 μm pore size PTFE syringe filters (Thermo Fischer Scientific, USA) to remove major residues of dust and undissolved phospholipid without interfering with the structure of the vesicular systems. In fact, DLS data of unfiltered formulations were compared to the results obtained after filtration, indicating the presence of vesicles with a maximum size of 350 nm, together with bigger aggregates. The aggregates could be observed under light microscope at the magnification of 40×, confirming the non-homogeneous dispersion of the vesicles.
Stability tests were performed on empty formulations, which allowed to consider the most stable formulation to be loaded with cannabinoids. DLS analysis on empty formulations were performed after two months at the same conditions. Both filtered and unfiltered samples were considered, comparing the results after storage in refrigerator or at room temperature. Loaded formulations were visually observed daily, and DLS measurements were performed on unfiltered samples after three months.

3.3.1.4 EVALUATION OF THE ENTRAPMENT EFFICIENCY

Loaded formulations were evaluated for their capability to efficiently retain cannabinoids in the vesicular systems, *i.e.*, their entrapment efficiency. Briefly, Visking Dialysis Tubing membranes of regenerated cellulose, wall thickness 0.03 mm, diameter 28.6 mm, MWCO 12–14000 Da (Medicell Membranes Ltd, London, United Kingdom) were cut into 5 cm length and hydrated with milliQ water for at least 24 hours. After closure at one end, 1 ml of vesicular dispersion was injected, and the upper end was closed. The system was then immersed in 30 ml of an equivalent hydro-alcoholic-glycolic solution (142, 153) and left stirring for 5 hours. Aliquots of 1 ml were taken from the media at 1, 2, 3, and 5 hours, restoring the total volume by addition of fresh solution. The samples were collected into 1.5 ml Eppendorf Safe-Lock Tubes, closed with Parafilm® and stored at 4°C until UV analysis.
Spectrophotometric analyses with UV-Vis Cary® 50 (Agilent, Varian, The Netherlands) were performed onto the samples without dilution and using an equivalent hydro-alcoholic-glycolic solution for the baseline correction. The quantification of the free drug concentration was performed using a calibration curve previously optimized. Briefly, the samples were obtained by dilution of DH-CBD or CBD from a concentrated ethanolic solution of 1 mg/ml into 10 ml

hydro-alcoholic-glycolic solutions. Standards of 8, 16, 24 and 32 µg/ml for CBD, and 4, 6, 8 and 10 µg/ml for DH-CBD were prepared in triplicate and re-analyzed before each sample analysis. Two different curves were obtained according to the loaded active ingredient: CBD showed a maximum peak at 206 nm, while DH-CBD at 202 nm.
The entrapment efficiency of the vesicular systems was calculated according to this equation:

$$EE\% = \frac{total\ drug\ concentration - free\ drug\ concentration}{total\ drug\ concentration} \times 100$$

The total drug concentration was calculated by dilution of 8 µl of initial formulation to 10 ml with ethanol to disrupt the vesicular systems, and the prepared sample was then analyzed by UV detection. The free drug concentration was calculated from the analysis of the receiver sample collected after 5 hours of diffusion.

3.3.1.5 DEVELOPMENT AND CHARACTERIZATION OF HYDROGELS CONTAINING VESICLES

Loaded vesicles suspensions were incorporated into a semisolid system, a hydrogel. This was performed to enhance vesicles stability and prevent ethanol evaporation; furthermore, the use of a semisolid form is recommended for the *in vivo* application of vesicular systems and favor the correct distribution of the drug onto the skin.
A Carbopol® Ultrez 10 hydrogel was previously formulated. Briefly, the polymer was homogeneously dispersed into the desired amount of ultrapure water with an overhead stirrer. The carbomer was then titrated with triethanolamine, of which 0.7 ml were required to reach pH 7.02 with 1 g of carbomer. Based on the viscosity properties of different carbomer concentrations, the hydrogel containing 0.75% of Carbopol was chosen for the following incorporation 1:1 in weight of vesicular preparations (154). The resulting preparations were then stored at +4°C in well-sealed plastic vials.
The rheologic properties of the loaded formulations were compared to hydrogels containing empty vesicles, and hydrogels containing equivalent hydroethanolic solutions to simulate the complete disruption of the vesicular systems.
The viscosity of hydrogel systems was analyzed with Rotovisco RV20TM (HAAKE™, Berlin, Germany), composed by PK100 and Rheocontroller RC20 units. Tests were run with a cone-plate PK1, a ramp rate of 3 minutes, a shear rate of 30 s^{-1}, and temperature of 20 ± 0.5°C.

3.3.1.6 RELEASE STUDIES ON HYDROGELS CONTAINING VESICLES

The release properties of loaded hydrogels were studied using specifically designed Perspex release cells of 20 mm diameter, 5 mm depth. Samples were loaded into the cavity and covered with a cellulose nitrate membrane of 25 mm diameter and 0.45 µm pore size (Prat Dumas,

France) soaked in mQ water for 24 hours (155). The cells were immerged in 50 ml of receiver composed of reheated mQ water maintained at 32 ± 0.5°C and stirred at 60 rpm with an overhead stirrer. Samples of 1 ml were collected after 15, 30, 45, 60, 90, 120, 150 and 180 minutes, into 1.5 ml Eppendorf Safe-Lock Tubes and stored at +4°C until analysis with UV-vis spectrophotometer. Receivers volumes were restored each time by addition of an equivalent amount of pre-heated mQ water.
A selected formulation (DH-CBD 1%, S100 4%, PG 30%, EtOH 20%) was tested for its release in 72 hours, where samples were collected also hourly for six hours after the 120 min sample, then after 24, 32, 48, 56 and 72 hours. The samples analysis was performed using a calibration curve obtained from water diluted solutions of CBD or DH-CBD at 25, 50, 100 and 200 µg/ml, respectively.

3.3.2 RESULTS

3.3.2.1 CHARACTERIZATION OF THE FORMULATIONS

Physical appearance of empty samples was evaluated at 30 minutes from the completing of the formulation and after 60 days. Phase separation was registered from the beginning in samples containing from 3 to 5% phospholipid and a concentration of PG lower than 30%. On the opposite, phospholipid concentration of 2% led to opaque, homogeneous preparations when PG was added from 20 to 30%, while higher amounts could lead to the formation of transparent solutions. Storage at room temperature or at refrigerated temperature was performed over 60 days and phase separation could be registered in both groups when two main combinations occurred: a) samples with high percentage of phospholipid and low concentration of propylene glycol (*e.g.*, 5% PC and 30% PG), and b) samples with low concentration of phospholipid and the lowest amount of propylene glycol (*e.g.*, 3% PC and 20% PG). Refrigerated storage improved the stability of samples as compared to the same batch stored at room temperature, especially in samples with 5% PC and 40% PG, and in case of intermediate concentration of PG (25-40%) at concentration of phospholipid between 4 and 2%.
After visual analysis of the samples, the vesicular size was evaluated on the most stable preparations. As previously stated in Paragraph 3.3.1.3, DLS measurements were performed on filtered and unfiltered preparations. The filtration process allowed to directly perform the measurement without dilution. Unfiltered, opaque preparations could not be correctly analyzed because of multiple scattering phenomena.

From the results obtained, clear indications on the influence of each component could be observed. The decrease of phospholipid concentration caused an increased instability of the system.

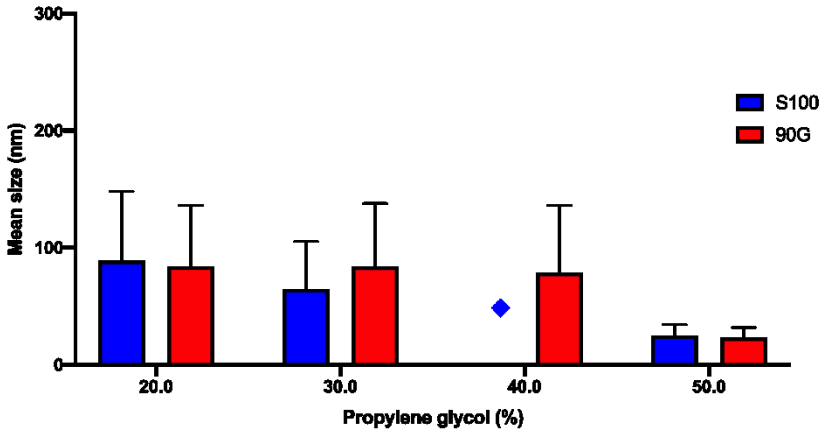

Figure 3.6 – Mean vesicle size of PG formulations with 2% PC. Small structures, polydispersion and micellar structures were registered. Polydisperse samples are indicated with a symbol (♦).

An increase of propylene glycol amount caused a decrease in particle size (Figure 3.6), until at 50% PG concentration micellar structures could be found (Figure 3.7).

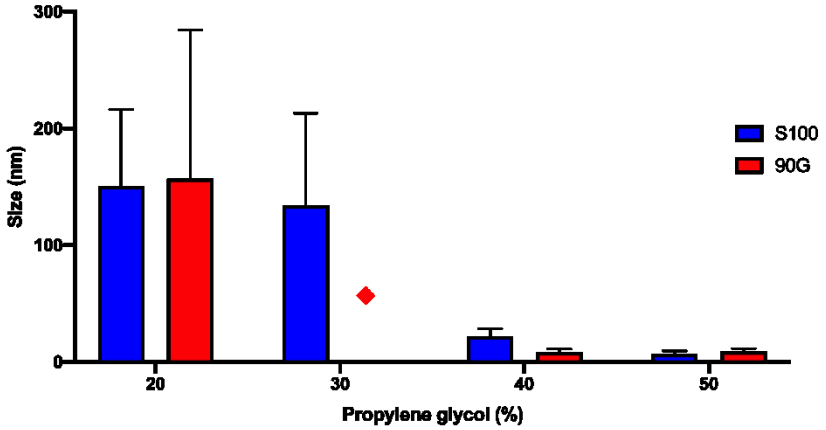

Figure 3.7 – Mean vesicle size (± SD) of PG-containing formulations with 3% PC. An increase of PG concentration leads to micellar systems. Polydisperse samples are indicated with a symbol (♦).

The most stable formulations were then prepared by loading of 1% CBD or DH-CBD. CBD formulations were prepared only with a concentration of 5% PC – 50% PG in order to compare the results with the ethosomal structures of THC developed by Touitou (143). CBD vesicles were prepared both with 90G and S100 phospholipids. Formulations with similar composition containing DH-CBD were prepared and DLS measurement showed clear differences between the mean particle size of the preparations, as reported in Figure 3.8.

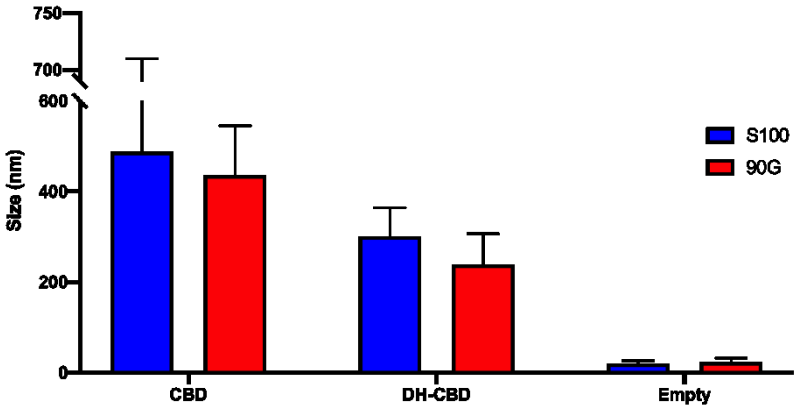

Figure 3.8 – Mean vesicle size (± SD) of samples with 5% PC and 50% PG.

CBD formulations showed vesicles with a mean size generally around 200 nm bigger than DH-CBD formulations with the same composition. Vesicles made of Lipoid S100 phospholipid had a higher mean size than 90G vesicles, and this could be observed especially in the case of CBD-loaded vesicles. Fluctuations of more than 100 nm on vesicular mean size could be registered with CBD-loaded 90G formulations over three months, while DH-CBD vesicles after an initial stabilization of the vesicles showed a mean size between 142.3 and 165.8 nm (Figure 3.9).

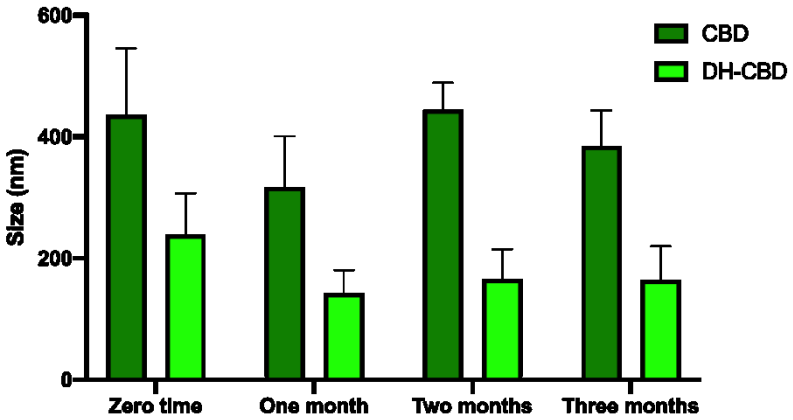

Figure 3.9 – Three months stability of 90G 5% formulations. Vesicles containing DH-CBD showed smaller dimensions. Values are expressed as mean size ± SD.

After comparison between CBD and DH-CBD formulations, the observation of the most stable empty formulations allowed to choose other systems for the loading with 1% DH-CBD.
90G formulations resulted slightly less stable as compared to S100 formulations, so three formulations were loaded with DH-CBD. At the lowest concentration of phospholipid, the sample resulted too polydisperse to be analyzed with DLS, but after one month a mean vesicle size of 105.9 nm could be observed. Recorded mean vesicle sizes over three months of storage at +4°C are shown in Figure 3.10.

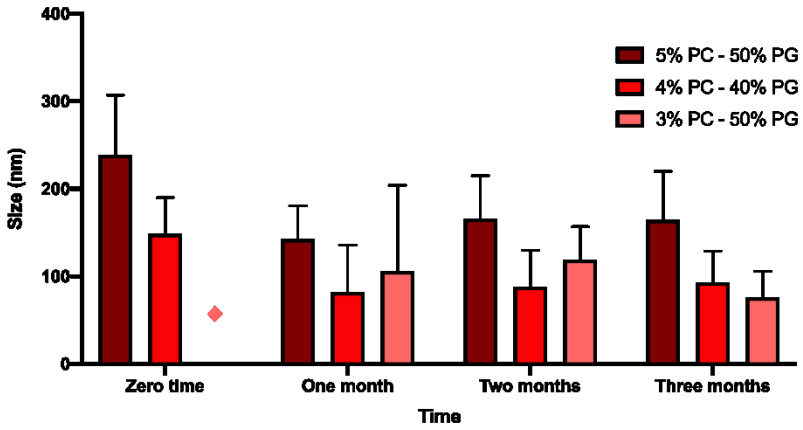

Figure 3.10 – Three months stability of 90G-based systems. Polydisperse samples are indicated with a symbol (♦). Values are expressed as mean size ± SD.

Several fluctuations over time could be seen in three months. In the case of 5% PC formulation, an initial phase expulsion can be observed, then the vesicles were more stable over time. The 4% PC formulation resulted the more stable among the panel, with the narrowest mean vesicle size distribution even after three months. After three months, the formulation with 3% PC showed a smaller mean size distribution, but phase separation phenomena could be visually observed.

Formulations containing S100 phospholipids resulted more stable and semitransparent when the phospholipid concentration was higher (4 and 5%). Among all the tested preparations, which cover from 2 to 5% PC concentrations, the four most stable are reported in Figure 3.11. The DLS results of the missing formulations are reported in Appendix section B.

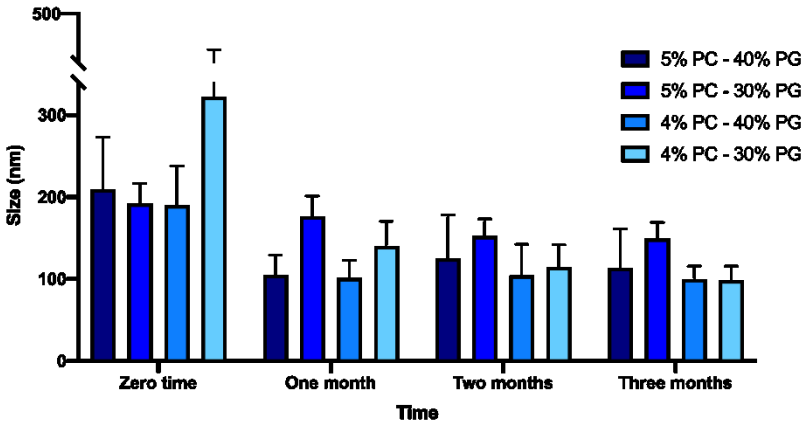

Figure 3.11 – Three months stability of S100-based vesicles containing DH-CBD. Values are expressed as mean size ± SD.

The S100 formulation containing 5% PC and 30% PG resulted the most stable over three months, with a mean particle size between 192.1 and 149.3 nm. Formulation containing 4% PC and 30% PG dramatically decrease its particle size after 30 days from 322.3 nm to 140.2 nm,

becoming 98.5 nm after three months. An increased amount of PG in the 4% formulation (40% PG) improved the stability and reduced the fluctuations in mean size distribution over time.

3.3.2.2 EVALUATION OF THE ENTRAPMENT EFFICIENCY

The entrapment efficiency was evaluated on each loaded formulation. Samples made of 90G phospholipid showed a slightly lower entrapment efficiency as compared to samples made of S100 phospholipid. This behavior was confirmed both for CBD and DH-CBD loaded formulations, as shown in Figure 3.12 a) and b).

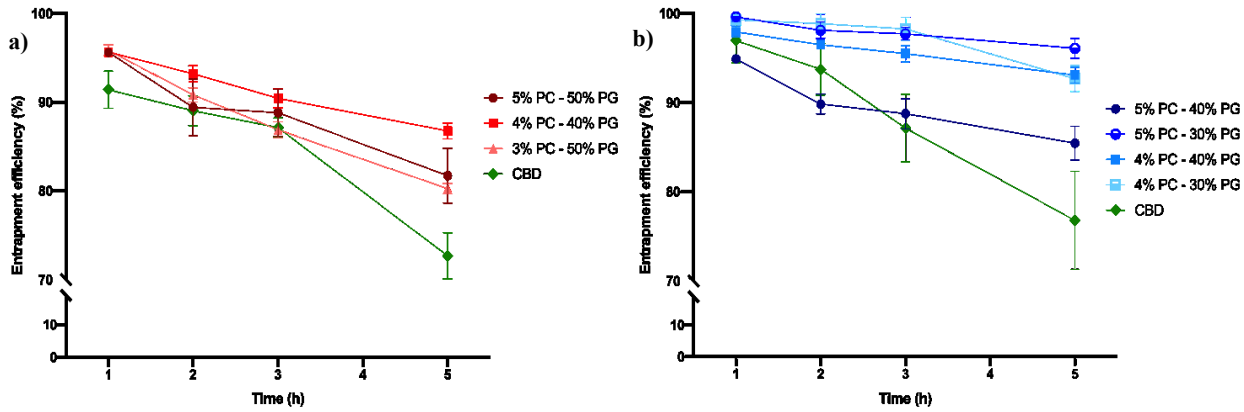

Figure 3.12 – Entrapment efficiency (mean ± SD) of 90G-vesicles (a) and S100-vesicles (b). In both cases a lower entrapment efficiency is shown when CBD was loaded in the system.

Among the samples containing 90G phospholipid, the one at 4% and 40% PG had the highest retained amount of drug, 86.76%. CBD loaded formulations, instead, showed the lowest amount of entrapped drug, *i.e.*, 72.7%.

Preparations containing S100 phospholipid were more efficient in entrapping both CBD and DH-CBD, still showing a decreased efficiency for CBD itself (76.8%). The value obtained with CBD, though, was similar to the result achieved with the equivalent S100 formulation containing DH-CBD (76.7%). Lower amounts of PG, though, led to an increased entrapment efficiency, reaching optimal results with 5% PC – 30% PG and 4% PC – 40% PG (96.1% and 93.10%, respectively), as showed in Appendix section C.

3.3.2.3 DEVELOPMENT AND CHARACTERIZATION OF HYDROGELS CONTAINING VESICLES

Viscosity tests showed that the formulated hydrogels have a plastic behavior with an optimal thixotropy. From the viscosity tests it was enlightened the influence of propylene glycol and phospholipid concentration in loaded formulations containing 90G phospholipid.

As reported in Figure 3.13, higher viscosity was achieved at higher concentration of PC and PG, leading to similar behavior between samples containing 4% PC – 30% PG and 3% PC – 50% PG.

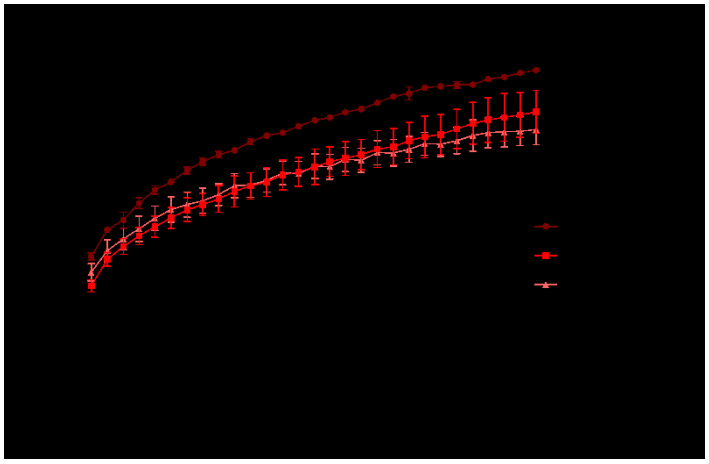

Figure 3.13 – Viscosity shear of hydrogels containing 90G formulations.

Samples made of S100 phospholipid showed an opposite behavior, leading to higher viscosity when lower amounts of PG were used. The main differences between the considered samples could be noticed at lower shear rate values, indicating different yield points. The results are shown in Figure 3.14.

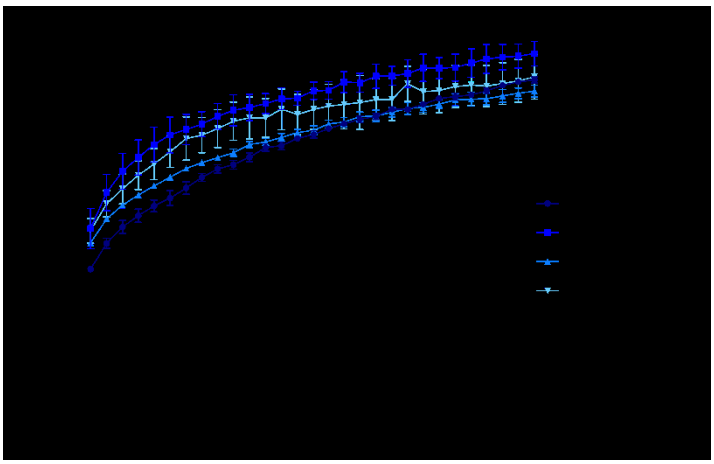

Figure 3.14 – Viscosity shear of hydrogels containing S100 formulations.

By comparison between systems with the same composition, the loaded drug showed a strong impact on the viscosity of the preparations. Samples containing CBD had significantly different shear curves, with lower viscosity in samples containing 90G phospholipid.

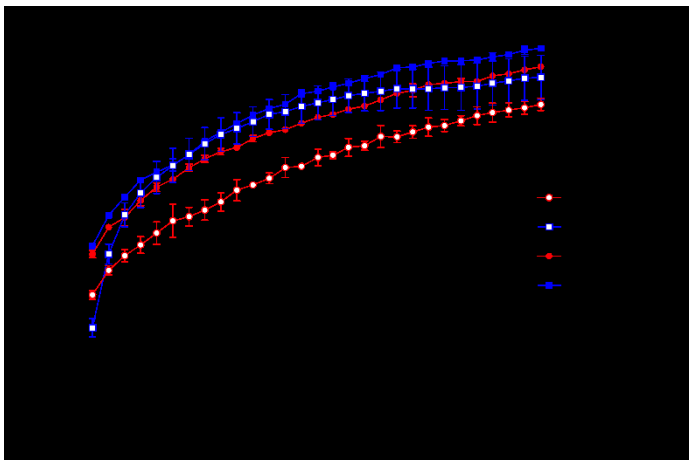

Figure 3.15 – Viscosity shear of hydrogels containing CBD or DH-CBD formulations.

The stability of the vesicles during the incorporation process was confirmed by comparison with the shear curves of the plain Carbopol gel, and of the hydrogel with an equivalent hydroalcoholic solution, as shown in Appendix section D. The differences between samples with or without vesicular systems are so evident that a preliminary indication on the preservation of the loaded sample can be extrapolated.

3.3.2.4 RELEASE STUDIES ON HYDROGELS CONTAINING VESICLES

Release properties of hydrogels containing loaded vesicles were tested and after 180 minutes the formulations with 90G at 5, 4 and 3% revealed a mean release of 87.55 ± 9.92, 81.02 ± 4.47 and 76.67 ± 4.71 $\mu g/cm^2/min^{1/2}$, respectively (Figure 3.16 and Appendix section E).

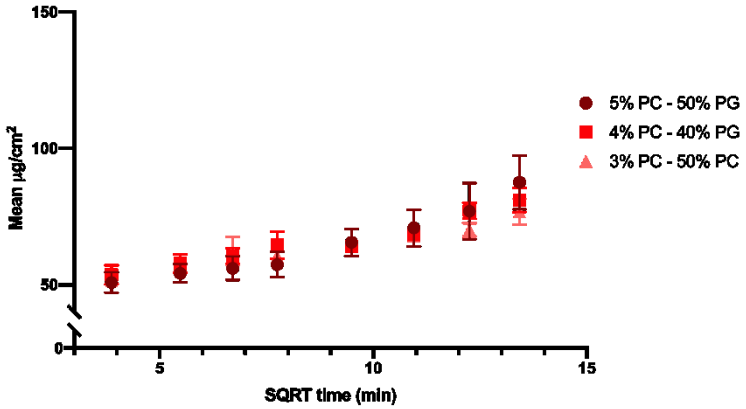

Figure 3.16 – Release profile of 90G-based vesicles. Values are expressed as mean ± SD.

Good linearity in the release profile was obtained with the 5% and 4% PC formulations, while 3% gave discontinuity in the release, probably due to the lower stability of the vesicular systems. Gels containing S100 vesicles, instead, caused a higher release of DH-CBD.

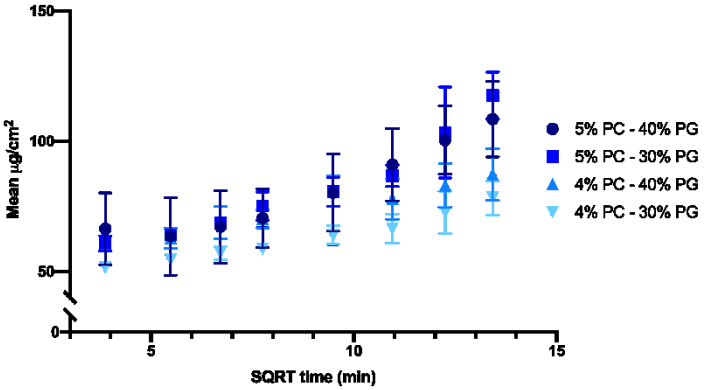

Figure 3.17 – Release profile of S100-based vesicles. Values are expressed as mean ± SD.

In particular, the formulation containing 5% PC – 40% PG reached 108.48 ± 14.50 µg/cm^2/min$^{1/2}$. Similar results could be achieved with 5% PC – 30% PG formulation. The hydrogels containing 4% PC showed slightly lower results but still good linearity (87.23 ± 9.93 and 78.27 ± 6.50 µg/cm^2/min$^{1/2}$ with 40% and 30% PG formulations, respectively).
CBD-loaded formulations showed indeed an enhanced release profile as compared to DH-CBD equivalent formulations, 242.28 ± 30.37 and 266.96 ± 28.22 µg/cm^2/min$^{1/2}$ for S100 and 90G formulations, respectively. Results are reported in Figure 3.18.

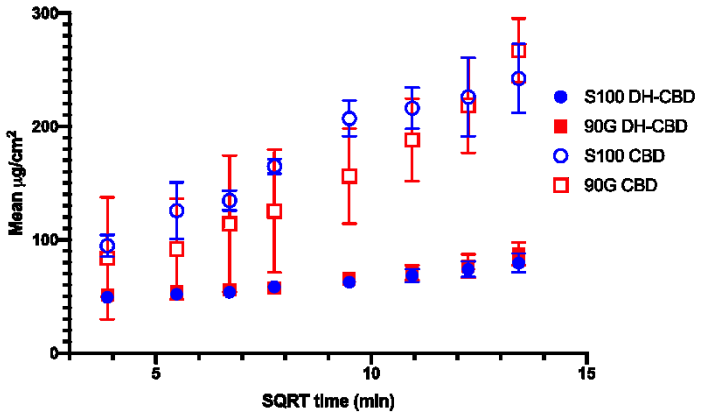

Figure 3.18 – Release profile of hydrogels containing CBD or DH-CBD loaded vesicles. Values are expressed as mean ± SD

The formulation containing 1% DH-CBD, 4% PC – 30% PG was tested for its release over 72 hours (Figure 3.19).

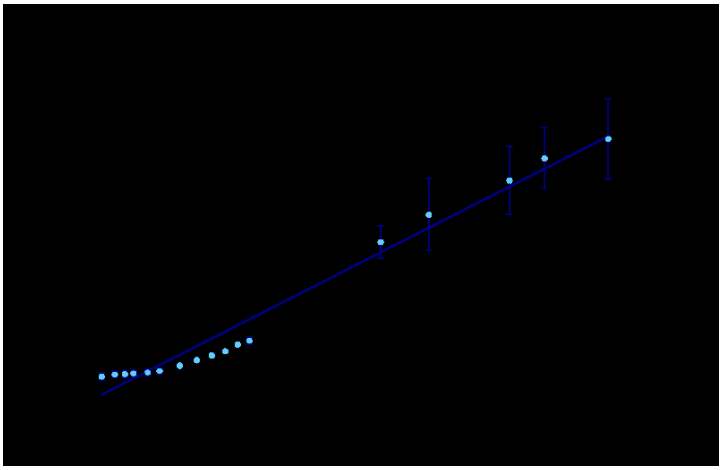

Figure 3.19 – 72 hours release of 90G-based formulation with 4% PC - 30% PG.

In this case, a mean value of 554.98 ± 83.61 $\mu g/cm^2/min^{1/2}$ was achieved at the end of the experiment. The results shown clearly underline the linearity of the prolonged release of the drug.

3.3.3 DISCUSSION

Vesicular systems containing a fixed amount of ethanol (20% in weight) and propylene glycol at high concentrations were developed by gradually evaluating the influence of each component on the stability of the preparation. The main goal of these experiments was the reduction of ethanol amount to reduce the toxicity and the narrowing of the mean particle size to obtain a more efficient transdermal delivery. Results indicate a decreased mean size distribution with a higher concentration of PG, but this caused higher instability with the lowest concentrations of phospholipids. Small structures with a particle size close to micellar systems were detected in formulations with the highest PG concentrations, especially 50% and above 40% at the lowest PC concentration (2% w/w). Stability of the particle size was analyzed over three months, and low concentrations of PC and PG lead to the formation of big aggregates not suitable for the transdermal delivery. The most stable combinations were achieved with S100 phospholipid when PG ranged from 25 to 40%. These observations allowed further investigations using cannabinoids such as CBD and DH-CBD at a concentration of 1%.

CBD-loaded formulations were prepared both with S100 and 90G phospholipids at a concentration of 5% and PG at 50% in weight. Equivalent formulations of DH-CBD were made, and several differences emerged between the four samples, even though similarities in the trend could be observed. CBD-loaded formulations showed a higher mean vesicle size as compared to DH-CBD systems, which persisted over the observation time of three months of storage. Considering the entrapment efficiency of the vesicular systems, the loaded amount of CBD was lower than in the cases of vesicles containing DH-CBD. These findings suggest that DH-CBD could be a more reliable model molecule to mimic the behavior of THC, the major phytocompound of cannabis extracts.

Among the formulations made of S100 and 90G phospholipids, the most stable were chosen for the loading with DH-CBD at 1% w/w. 90G formulations resulted less stable when stored at refrigerated conditions, and this phenomenon allowed the loading of only three preparations: 5% PC – 50% PG, 4% PC – 40% PG and 3% PC – 50% PG. S100 formulations, instead, resulted more stable, and nine formulations were tested. Among these, the most promising had a composition of 5 or 4% PC and a PG concentration of 40% or 30% w/w. Their mean particle size resulted around 200 nm or even lower, which is considered optimal for transdermal drug delivery (139), and it was maintained over three months of storage at +4°C.

High entrapment efficiency of DH-CBD was achieved in all the formulations (always above 75%), with increased efficiency in the formulations containing 30% PG and a maximum concentration of 4% PC. 90G systems had a slightly lower entrapment efficiency as compared to S100 systems, and the 4% PC – 40% PG resulted in the most efficient for entrapping DH-CBD. S100 formulations had very high efficiency, with the best results given by 4 and 5% PC, and 30 or 40% PG. The formulation containing 5% PC and 40% PC, though, showed an entrapment efficiency lower than 90%, so we could assume a higher permeability of these systems when a high concentration of propylene glycol is present.

Hydrogels were prepared to increase the viscosity and stability of the vesicles, which eventually will contribute to improving tolerability for the patient to be treated with cannabinoids. Hydrogels of 0.75% Carbopol® Ultrez 10 were mixed in ratio 1:1 with vesicular systems and their viscosity and release properties were tested. Hydrogels containing vesicles made of S100 phospholipid showed higher viscosity as compared to equivalent 90G formulations. In all cases, the viscosity always resulted higher than in the case of hydrogels mixed in ratio 1:1 with equivalent hydro-alcoholic-glycolic formulations, which could suggest preservation of the vesicular systems during the process of incorporation. Furthermore, the viscosity increased at higher phospholipid concentration, and in the case of the same amounts of PC, viscosity is also influenced by propylene glycol concentrations. Same compositions with different active ingredients (CBD vs. DH-CBD formulations) resulted in very similar values of viscosity and shear stress.

Release tests verified the capability of loaded hydrogels to maintain a prolonged release of CBD or DH-CBD. A high short-term release was achieved with formulations containing high PG concentrations, especially in the case of CBD-loaded systems. A 72-hours test proved the long-term capability of these systems to release the drug with desirable linearity.

Considering all the results on the stability, entrapment efficiency and release properties of vesicular systems containing cannabinoids, the best results were obtained when 4 or 5% PC was employed, and PG ranged between 30 and 40% w/w. These findings were essential as preliminary information for the further development of suitable systems for cannabis extracts, which will be described in Chapter 4.

Chapter 4

Simulation and preparation of cannabis extracts

4.1 CANNABIS EXTRACTS

Cannabis extraction has been performed since ancient times by means of different procedures and solvents. As described in Chapter 1, several advantages come from the use of plant-derived medicines thanks to the so-called "entourage effect" (156, 157), although high variability on the quali-quantitative profile of cannabinoids can be observed. Uncertainties derive from a lack of standardized conditions such as temperature and time of extraction, which may deeply impact in the final concentration of cannabinoids (158–161). Moreover, different treatments could lead to a degradation of THC (along with its acidic form) into cannabinol, CBN, a mildly psychoactive cannabinoids mainly responsible of sedative effects on patients. The impact of cannabis flowers treatment could vary not only the concentration of the major cannabinoids, but also the amount of volatile terpenoids, which contribute to the pharmacological activity of cannabis-based drugs (159, 161). The fluctuations in extraction profiles caused by unique standardized extraction protocols are even more enhanced by the variability in the concentration of cannabinoids in the plant product, although declared by the producers (162). In particular, the most suitable cannabis breed must be carefully chosen for the specific needs of the patients. The most frequently available cannabis varieties show high inter- and intra-variability in terms of major cannabinoids concentrations. As previously described, authorized cannabis products in Italy can be both imported or produced by the SCFM of Florence, being divided in THC-rich strains (Bedrocan, FM1) or mean equal amounts of THC and CBD strains (Bediol, FM2). Peculiar attention should be given to the toxicity profile of THC, which could be mitigated by CBD (42). In a phase 1 randomized controlled trial, THC was administered orally at different concentrations, showing higher rates of adverse events when 6.5 mg vs. 3 mg of active ingredient were administered (163). Despite the difficulties of ensuring good repeatability among chemical profiles of cannabis extractions, standardized cannabis extracts have been approved on the market as an oromucosal spray (Sativex, as described in Chapter 1). However, the daily administration to the patient of this drug can be up to 12 times, leading to lower compliance for the patient (164). Hence the need of finding different administration routes to support the breakthrough episode treatment with a long-lasting administration of the drug.

Formulations of cannabis extracts in transdermal delivery systems could be very beneficial in this direction, ensuring a continuous, controlled release of phytocannabinoids. In the following paragraphs a short overview of the most recent literature on cannabis extractions in olive oil or in ethanol, on which the experimental activities were based, will be illustrated.

4.1.1 EXTRACTION IN OLIVE OIL

The extraction in olive oil has been generally performed by continuously heating and stirring of a mixture composed by oil and flowering tops in ratios of 10 ml for each gram, respectively. The minimum temperature of extraction is 70°C in a water bath (165), while a maximum of 110°C was reported (159, 165). The extraction time varied from 40 minutes (165, 166) to 120 minutes (159–161, 165). Higher concentrations of cannabinoids were reported when Bedrocan variety was used (165, 166), as well as when Bediol and FM2 varieties underwent an extraction at around 100°C (159–161). Prolonged extraction times improved the total concentration of cannabinoids, but attention should be paid in order to prevent the evaporation of the more volatile compounds (159). Preheating cannabis flowers allows the conversion of acidic forms of the major cannabinoids, thus increasing the total concentration of THC and CBD in the extract. This process was performed in static ovens at different temperatures and times. A treatment of minimum 115°C for 40 minutes resulted sufficient for achieving a total conversion of THC (161, 165, 166), while higher temperatures led to a complete conversion of CBD but an increase in CBN concentrations or volatilization of THC (160, 165). A summary of the achieved concentrations of the major cannabinoids is reported in Table 4.1.

Table 4.1 – Reported literature methods for the extraction of cannabis in olive oil.

Variety	Decarboxylation	Solvent	Conditions	Mean THC	Mean CBD	Ref.
Bedrocan	115°C, 40 min	Olive oil, 10 ml/g	100°C, 40 min	1.7 ± 0.3 % p/p	NA	(166)
Bedrocan	115°C, 40 min		70°C, 40 min	1.1 ± 0.4 % p/p	NA	(165)
			100°C, 120 min	1.8 ± 0.3 % p/p		
	145°C, 30 min		70°C, 40 min	2.3 ± 0.2 % p/p		
			100°C, 120 min	1.5 ± 0.1 % p/p		
Bediol	No		110°C, 120 min	2.2 ± 1.0 mg/ml	2.8 mg/ml	(159)
FM2	145°C, 30 min		98°C, 120 min	4.7 ± 0.7 mg/ml	7.3 ± 0.7 mg/ml	(160)
Bedrocan	NA		NA	16.5 ± 2.4 mg/ml	NA	(158)

Bediol				4.3 ± 1.0 mg/ml	7.2 ± 1.4 mg/ml	
FM2				4.7 ± 1.2 mg/ml	8.7 ± 2.1 mg/ml	
Bedrocan	120 - 140°C, 30 min		100°C, 120 min	9.4 ± 7.7 mg/ml	NA	(161)
Bediol				3.3 ± 1.8 mg/ml	3.0 ± 2.8 mg/ml	

4.1.2 EXTRACTION IN ETHANOL

Extractions of cannabis in alcohols were performed according to the higher solubility of cannabinoids in this solvent (167, 168). As reported in the study of Citti (159), the extraction in ethanol resulted more efficient in a short time (60 minutes) as compared to olive oil extraction, while the cannabinoids profiles were similar between the two solvents when the extraction time was fixed at 120 minutes. Different solvent-drug ratios were used, resulting in higher concentrations of cannabinoids when 10 ml per gram were used. Moreover, the extraction efficiency resulted much higher when the system was refluxed than in the case of room temperature extraction processes. Good results and terpene profiles were obtained when using a condenser, both with ethyl alcohol and olive oil extractions. It is worth noting that the results were still relatively high even without a pre-heating of the cannabis flowers, so potentially a pre-treatment could improve the total concentration of both THC and CBD. In Table 4.2 is reported a summary of the characteristics of these ethanol extractions.

Table 4.2 – Reported literature methods for the extraction of cannabis in ethanol.

Variety	Decarbox.	Solvent	Conditions	Mean THC	Mean CBD	Ref.
Bediol	No	EtOH 10 ml/g	Reflux, 120 min	2.5 ± 0.3 mg/ml	4.1 ± 0.2 mg/ml	(159)
		EtOH 40 ml/g	RT, 180 min	1.4 ± 0.1 mg/ml	0.8 ± 0.2 mg/ml	

4.1.3 EXPERIMENTAL ACTIVITY

Considering the methods and the results previously reported, the pre-heating treatment of cannabis flowering tops appear to be more efficient in "activating" the phytocannabinoids, although attention should be payed to prevent an excessive volatilization of terpenes and minor compounds. For this reason, a raw estimate of the concentration of cannabinoids in oil or ethanol with previous decarboxylation was performed by conversion of the values expressed in milligrams per milliliters into percentage on weight. This calculation led to a maximum total concentration of the major cannabinoids of 1% w/w when using olive oil, while an approximated maximum of 2% w/w can be expected in ethanolic extractions.

4.2 VESICULAR SYSTEMS WITH OLEIC ACID AND SIMULATION OF CANNABIS EXTRACTS

4.2.1 VESICLES CONTAINING OLEIC ACID

Oleic acid is a C18 *cis*-9 monounsaturated fatty acid. Due to their key role in the permeability and fusion of cellular membranes, the physicochemical properties of fatty acids in phospholipidic membranes and water environment have been extensively since XIX century (169–171). Aqueous dispersions of oleic acid (OA) and phospholipids can adopt different nanostructures depending on several factors such as concentrations, temperature, ionic strength and pH (170). Several applications of vesicles containing OA were proposed, such as a crucial involvement in the early evolution of cellular life (172, 173). OA is considered not only a penetration enhancer in dermal delivery, but also an interesting agent which influences vesicular structures, enhancing flexibility of the system with its *cis*-double bond structure (174). At room temperature, the main variables influencing the stability of vesicular systems composed of OA and phosphatidylcholine (PC) are the molar ratio between PC and OA, the pH and the ionic strength of the aqueous environment (170, 175). In fact, it is well established that vesicular systems composed of PC can include in their structure up to 60 mol% of long chain fatty acids (176, 177). Moreover, the stability of the systems can be deeply influenced by the ionization of fatty acids. The pK_a value of free carboxylic groups in monomeric fatty acids is known to be 4.8 (178, 179), but equilibrium titration experiments showed the presence of self-association of fatty acids into lamellar structures according to their ionization degree and to the pH of the solution. In these experiments, oleic acid showed an apparent pK_a value of 8.0-8.5, probably due to the formation of a high negative charge density on the surface of lamellar structures, and a lowering of the local dielectric constant, thus elevating the apparent pK_a causing the formation of bilayers and vesicular systems (177). Similarly, fatty acids incorporated into PC membranes have elevated apparent pK_a values, around 7.2-7.5, due to the dielectric effect of the non-polar lipid membrane environment (170, 177). This was confirmed in unilamellar vesicles dispersed in 0.1 M phosphate buffer, registering differences in apparent pK_a between different buffering systems such as sodium carbonate, potassium phosphate and borax buffers (170).

Thus, vesicular systems containing PC and OA in presence of ethanol were studied, considering the influence of phosphate buffer 0.1 M as an aqueous medium. Also, the most stable preparations coming from Paragraph 3.3 and from OA containing systems were considered for the loading with cannabinoid solutions in olive oil and ethanol, to mimic cannabinoid extracts as described in the following paragraph.

4.2.2 MATERIALS

Carbopol® Ultrez 10 Polymer (Lubrizol Advanced Materials Europe BVBA, Belgium)
CBD Crystal-99one (kindly provided by Enecta®, The Netherland)
Desoxy-cannabidiol (synthesized as described in Chapter 2)
Ethanol absolute, Ph. Eur. (Scharlab, Spain)
Lipoid S100 (kindly provided by Lipoid GmbH, Germany)
Monosodium phosphate dihydrate, Ph. Eur. (A.C.E.F., Italy)
Olive refined European Pharmacopeia oil (Olive Oil, Ph.Eur) (A.C.E.F., Italy)
Phospholiphon® 90G (kindly provided by Lipoid GmbH, Germany)
Propylene glycol (Fagron, Italy)
Super Refined™ Oleic Acid NF (kindly provided by Croda, United Kingdom)
Triethanolamine 85% (Fagron, Italy)
TRIS for molecular biology (Panreac AppliChem, Germany)

4.2.3 METHODS

4.2.3.1 PREPARATION OF VESICLES CONTAINING OA AND CANNABINOIDS SOLUTIONS IN OLIVE OIL OR ETHANOL

The preparation of vesicles containing oleic acid was performed with a simple mixing method. Ethanol was weighed in a vessel and the phospholipid was dissolved. Oleic acid was added to the formulation and the system was mixed with a magnetic stirrer for two minutes. When present, the active ingredient was subsequently added, and the rotation speed was set up at 1000 rpm. The aqueous phase was gradually injected, and the system was stirred for additional five minutes. After 30 minutes, the preparations were stored at room temperature in well-sealed glass vessels, protected from light. Loaded formulations were stored at 4°C for 24 hours in a glass vial, then transferred into well-sealed 15 ml plastic tubes, protected from light, and stored at +4°C.

PC and OA were used in two different ratios, above and below the critical molar ratio OA:PC of 0.67 (170): 0.87 and 0.54, respectively. These combinations were tested at PC concentrations of 2, 3 or 4% w/w. Different concentrations of ethanol were tested in a range from 20 to 50% w/w, showing better stability at a concentration of 30% in most cases.
As to improve the stability of the formulations, a pH 8 TRIS buffer 10 mM was used to evaluate the influence of a buffering system on vesicular systems containing oleic acid. The compositions of the most stable systems are reported in Table 4.3.

Table 4.3 – Composition of the most stable preparations containing OA. Formulations E067-E075 had a concentration of OA of 54 mol% as compared to PC mol, while E081 had a concentration of 0.87 mol%. Values are expressed as % w/w.

Sample name	PC	OA	EtOH	H_2O mQ	TRIS buffer
E067	4.0	0.8	30.0	65.2	-
E149	4.0	0.8		-	65.2
E055	3.0	0.6		66.4	-
E075	2.0	0.4		67.6	-
E081	2.0	0.6	40.0	57.3	-

From the concentrations available from literature, as described in Paragraph 4.1, simulated olive oil or ethanol extracts were prepared with solutions of CBD or DH-CBD. The solutions were then formulated into the most stable vesicular systems, which were then characterized and tested for their release when incorporated in hydrogels. These operations were fundamental to anticipate the formulation of actual cannabis extracts. The formulations with the best stability profile, as well as entrapment efficiency of cannabinoids, were chosen among PG containing preparations of Paragraph 3.3. The simulated extracts were prepared by dissolving CBD or DH-CBD in olive oil or in ethanol absolute, in a concentration of 1% w/w in oil and 2% w/w in ethanol, as described in Paragraph 4.1.

Vesicles containing PG were prepared with a simple mixing method. Ethanol was weighed in a vessel and the phospholipid was dissolved. PG and the cannabinoid solution were subsequently added, and the system was mixed with a magnetic stirrer for two minutes. The rotation speed was then set up at 1000 rpm, the aqueous phase was gradually added, and the system was stirred for additional five minutes. The preparations were then stored at +4°C in well-sealed glass vessels, protected from light. After 24 hours the preparations were transferred into well-sealed 15 ml plastic tubes, protected from light, and stored at +4°C.

Vesicles containing OA were prepared as previously described, by addition of the cannabinoid solution after mixing the phospholipid and OA. The storage was performed under the same condition of vesicles containing PG. As the TRIS buffer led to improved characteristics of empty vesicles, a 0.1 M phosphate buffer was used for the preparation of all the loaded preparations (170).

The composition of each formulation containing cannabinoid solutions is reported in Table 4.4-4.7.

Table 4.4 – Composition of vesicles containing PG loaded with CBD solutions in olive oil (CBD in OO) or absolute ethanol (CBD in EtOH). Values are expressed as percentage on the total weight of the formulation.

Sample name	PC	PG	CBD in OO	CBD in EtOH	EtOH	H_2O mQ
E235	4	40	5	-	20	31
E237	4	40	5	-	20	31
E241	4	40	-	5	15	36
E243	4	40	-	5	15	36

Table 4.5 – Composition of vesicles containing PG loaded with DH-CBD solutions in olive oil (DH-CBD in OO) or absolute ethanol (DH-CBD in EtOH). Values are expressed as percentage on the total weight of the preparation.

Sample name	PC	PG	DH-CBD in OO	DH-CBD in EtOH	EtOH	H_2O mQ
E247	4	40	5	-	20	31
E249	4	40	5	-	20	31
E253	4	40	-	5	15	36
E255	4	40	-	5	15	36

Table 4.6 – Composition of vesicles containing OA loaded with CBD solution in olive oil (CBD in OO) or absolute ethanol (CBD in EtOH). Values are expressed as percentage on the total weight of the formulation.

Sample name	PC	OA	CBD in OO	CBD in EtOH	EtOH	Buffer phosph.
E239	4.0	0.8	5.0	-	30.0	60.2
E245	4.0	0.8	-	5.0	25.0	65.2

Table 4.7 – Composition of vesicles containing OA loaded with DH-CBD solution in olive oil (DH-CBD in OO) or absolute ethanol (DH-CBD in EtOH). Values are expressed as percentage on the total weight of the formulation.

Sample name	PC	OA	DH-CBD in OO	DH-CBD in EtOH	EtOH	Buffer phosph.
E251	4.0	0.8	5.0	-	30.0	60.2
E257	4.0	0.8	-	5.0	25.0	65.2

4.2.3.2 CHARACTERIZATION OF THE PREPARATIONS

Visual observation

Stored formulations were observed 30 minutes after the reparation and daily during the storage. When phase separation was registered, the formulations were transferred in an Eppendorf 1.5 ml tube, well-sealed and protected from light. Visual observation was further performed on preparations containing olive oil with a light microscope Leitz HM-LUX 3 (Ernst Leitz Wetzlar Gmbh, Portugal). A droplet of the selected suspension was mounted between two cover slips of 24 × 60 mm and observed under 40× magnification.

pH measurement

With a 744 pH Meter (Metrohm, Switzerland), the formulations containing OA were analyzed after dilution with milliQ water at a ratio of 1:5 v/v. Two dilutions were performed for each sample.

DLS measurement

Each sample was tested with a Zetasizer Nano ZEN3600 (Malvern, United Kingdom) 24 hours after preparation. Thirty minutes prior to measurement, the systems were diluted 1:500 v/v with an equivalent hydroalcoholic mixture previously filtered with a 0.45 µm pore size PTFE disposable syringe filter (ThermoFisher Scientific, USA). DLS analyses were performed using a backscattering detector at 173°. Tests were run at 25°C, with three replications of 12 scans for each sample. The duration and the set position of each measurement were fixed automatically by the apparatus. Two-way ANOVA tests were performed with Prism software, version 8 (GraphPad Software, San Diego, CA, USA).

4.2.3.3 EVALUATION OF THE ENTRAPMENT EFFICIENCY

Loaded formulations were evaluated for their capability to efficiently retain cannabinoids in the vesicular systems, *i.e.*, their entrapment efficiency. BioDesignDalysis Tubing™, with 15.5 mm wet diameter and 1.91 ml/cm volume, 14000 Da MWCO (BioDesign Inc., ThermoFisher Scientific, New York, USA), was cut into 5 cm length pieces and hydrated with mQ water for at least 24 hours. After closure at one end, 1 ml of vesicular dispersion was injected, and the upper end was closed. The system was then immersed in 30 ml of an equivalent hydroethanolic (or hydro-glycolic-ethanolic) solution (142, 153) and left stirring for 5 hours. Aliquots of 1 ml were taken from the media at 1, 2, 3, and 5 hours, restoring the total volume by addition of fresh solution. The samples were collected into 1.5 ml Eppendorf Safe-Lock Tubes, closed with Parafilm® and stored at +4°C until UV analysis.

Spectrophotometric analyses with UV-Vis Cary® 50 (Agilent, Varian, The Netherlands) were performed onto the samples without dilution and using an equivalent hydroethanolic solution for the baseline correction. The quantification of the free drug concentration was performed using a calibration curve previously optimized. Briefly, the samples were obtained by dilution of DH-CBD or CBD from a concentrated ethanolic solution of 1 mg/ml into 10 ml hydroalcoholic or hydro-glycolic-ethanolic solutions. Standards were prepared in triplicate and re-analyzed before each sample analysis. Two different curves were obtained according to the absorption peaks of CBD and DH-CBD, 206 and 202 nm, respectively. Standards were prepared at different concentrations according to the different receivers' composition. Samples of 1, 1.5, 2, 2.5 µg/ml were prepared for CBD in ethanolic solution, 1, 2, 3 and 4 µg/ml for CBD in glycolic solution, and 2, 3, 4 and 5 µg/ml for DH-CBD both for ethanolic and glycolic solution.

The entrapment efficiency of the vesicular systems was calculated according to this equation:

$$EE\% = \frac{total\ drug\ concentration - free\ drug\ concentration}{total\ drug\ concentration} \times 100$$

The total drug concentration was calculated by dilution of 40 or 20 µl of the initial formulation to 10 ml with absolute ethanol, according to the estimated concentration of the cannabinoid, and analyzed by UV detection. The free drug concentration was calculated from the analysis of the receiver collected after 5 hours of diffusion.

4.2.3.4 DEVELOPMENT AND CHARACTERIZATION OF HYDROGELS CONTAINING VESICLES

DH-CBD loaded vesicles were incorporated into a semisolid system, a hydrogel. This was performed to enhance vesicles stability and prevent ethanol evaporation; furthermore, the use of a semisolid form is recommended for the *in vivo* application of vesicular systems and favor the correct distribution of the drug onto the skin.

A Carbopol® Ultrez 10 hydrogel was previously formulated. Briefly, the polymer was homogeneously dispersed into the desired amount of ultrapure water with an overhead stirrer. The carbomer was then titrated with triethanolamine, of which 0.7 ml were required to reach pH 7.02 with 1.0 g of carbomer in 100 ml of mQ water. Based on the viscosity properties of different carbomer concentrations, the hydrogel containing 1.0% of Carbopol was chosen for the following incorporation 1:1 in weight of the vesicular preparations (154). The resulting preparations were then stored at +4°C in well-sealed plastic vials.

The rheological properties of hydrogels were analyzed with MCR 92 Rheometer (Anton Paar Srl, Rivoli, Italy). Tests of strain and frequency sweep were run with a cone-plate CP20-2 (19.977 mm diam., 2.014° angle). Strain sweep tests were performed in a 0.1-100% range of shear strain and fixed 1 Hz frequency. Frequency sweep tests were performed with a shear strain

of 1% or 5% according to the strength of the hydrogels, within a 0.1-20 Hz range of frequencies. Samples were analyzed at a controlled temperature of 20 ± 0.02°C.

4.2.4 RESULTS

4.2.4.1 CHARACTERIZATION OF THE PREPARATIONS

pH measurement

Stable vesicular dispersions containing oleic acid showed initially a mean pH value between 7.5 and 8.3. This can be considered close to the value of apparent pK_a of PC-OA vesicular systems. When a pH higher than 8.3 was registered, phase separation occurred more frequently, as in the case of sample E081, which showed a pH of 8.84 ± 0.05 and resulted in phase separations after three weeks of observation. The results are shown in Table 4.8.

Table 4.8 – pH values of empty formulations containing OA. Values are expressed as mean pH values ± SD.

Formulation name	pH measurements	
	Zero-time	Three months
E067	8.30 ± 0.08	5.89 ± 0.01
E149	7.53 ± 0.20	6.55 ± 0.11
E055	7.58 ± 0.18	6.28 ± 0.06
E075	8.25 ± 0.21	6.60 ± 0.20

While the pH was tendentially basic at zero-time, over three months the values decreased to slightly acidic pH, which is closer to the physiological skin pH of 5.5. This could indicate higher compatibility with human skin. Considering the composition of the formulations, lower pH values were reached at higher OA total concentrations. The presence of a buffering systems led to lower differences between pH values from zero-time to three months, around one pH point. Unstable samples showed higher pH values: with E081 the zero-time value was 8.84 ± 0.05.

Loaded formulations were analyzed and their pH, reported in Table 4.9, resulted very close to the equilibrium, as expected from the apparent pK_a value of PC-OA systems.

Table 4.9 – pH values of CBD and DH-CBD formulations containing OA. Values are expressed as mean pH values ± SD.

Formulation name	pH measurements
E239	7.83 ± 0.04
E245	7.74 ± 0.01
E251	7.70 ± 0.02
E257	7.71 ± 0.02

DLS measurement

DLS measurement of vesicles containing OA showed populations of acceptable particle size and good PdI for all the most stable empty formulations All the formulations showed an overall good PdI, with a maximum of 0.548 ± 0.160 and a minimum of 0.254 ± 0.195. The formulation with the best particle size was prepared using buffer phosphate 0.1 M, showing a mean particle size of 210.1 ± 87.2 nm (Figure 3.20).

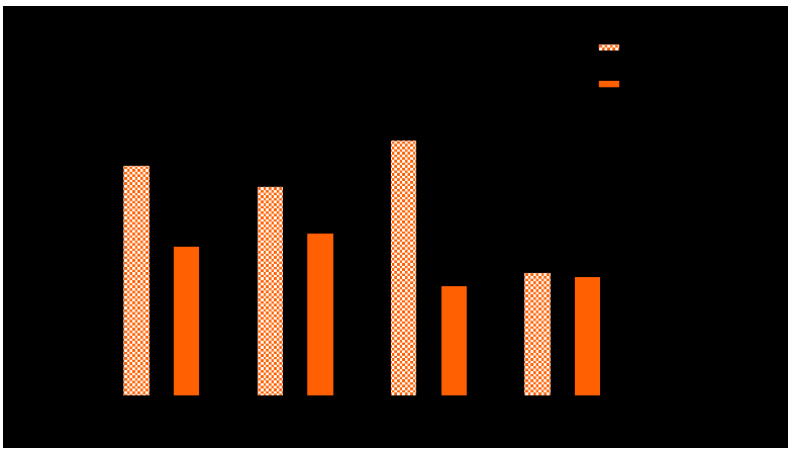

Figure 4.1 – Three months stability of vesicular systems containing OA. Values are expressed as means size ± SD.

After three months, the mean size of the vesicular systems was generally lower than at zero-time, with a statistically significant difference (two-way ANOVA test, $p < 0.001$) in the case of S100-based vesicles. Great stability was registered when buffer phosphate 0.1 M was used, underlying the influence of the ionic strength on the systems.

The mean particle size of loaded formulations was evaluated at zero-time. The use of olive oil solutions led to the formations of major structures with micrometric size. Only in the case of vesicles containing OA and olive oil solution of DH-CBD a population of nanometric size (299.3 ± 130.1 nm) could be registered together with micrometric structures. These observations are consistent with optical microscopy observations of the preparations, which showed spherical structures of very different sizes. Vesicular systems with ethanolic solutions of cannabinoids showed an overall good size, with low polydispersity (PdI values from 0.184 ± 0.068 to 0.342 ± 0.174), and nanometric size suitable for optimal transdermal delivery of drugs (between 93.0 ± 5.5 and 277.8 ± 35.0 nm). Results are shown in Figure 4.2.

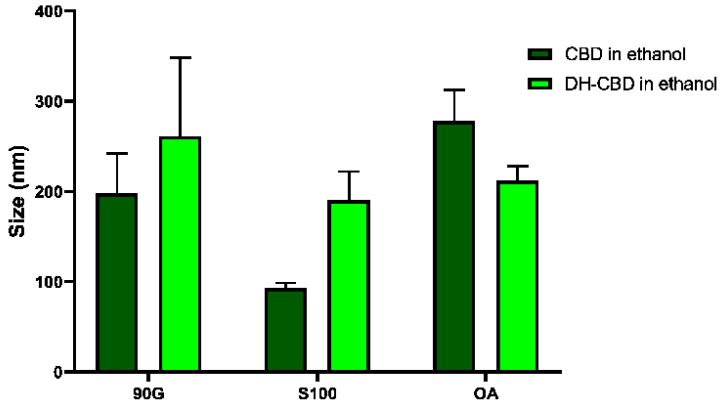

Figure 4.2 – Mean particle size (± SD) of vesicles containing ethanolic solutions of CBD or DH-CBD.

In this figure, the differences between systems containing CBD and DH-CBD can be appreciated. In the case of PG-containing vesicles, the preparations showed an increase in particle size when DH-CBD was loaded, while systems containing OA showed a decrease in particle size in presence of the same drug.

4.2.4.2 EVALUATION OF THE ENTRAPMENT EFFICIENCY

All the loaded formulations showed good entrapment efficiency with values ranging from 86.0 ± 3.0 to 89.9 ± 1.5 % in the case of CBD, and from 82.3 ± 3.6 to 92.8 ± 0.9 % for DH-CBD. The results are given in Figure 4.3 a)-d).

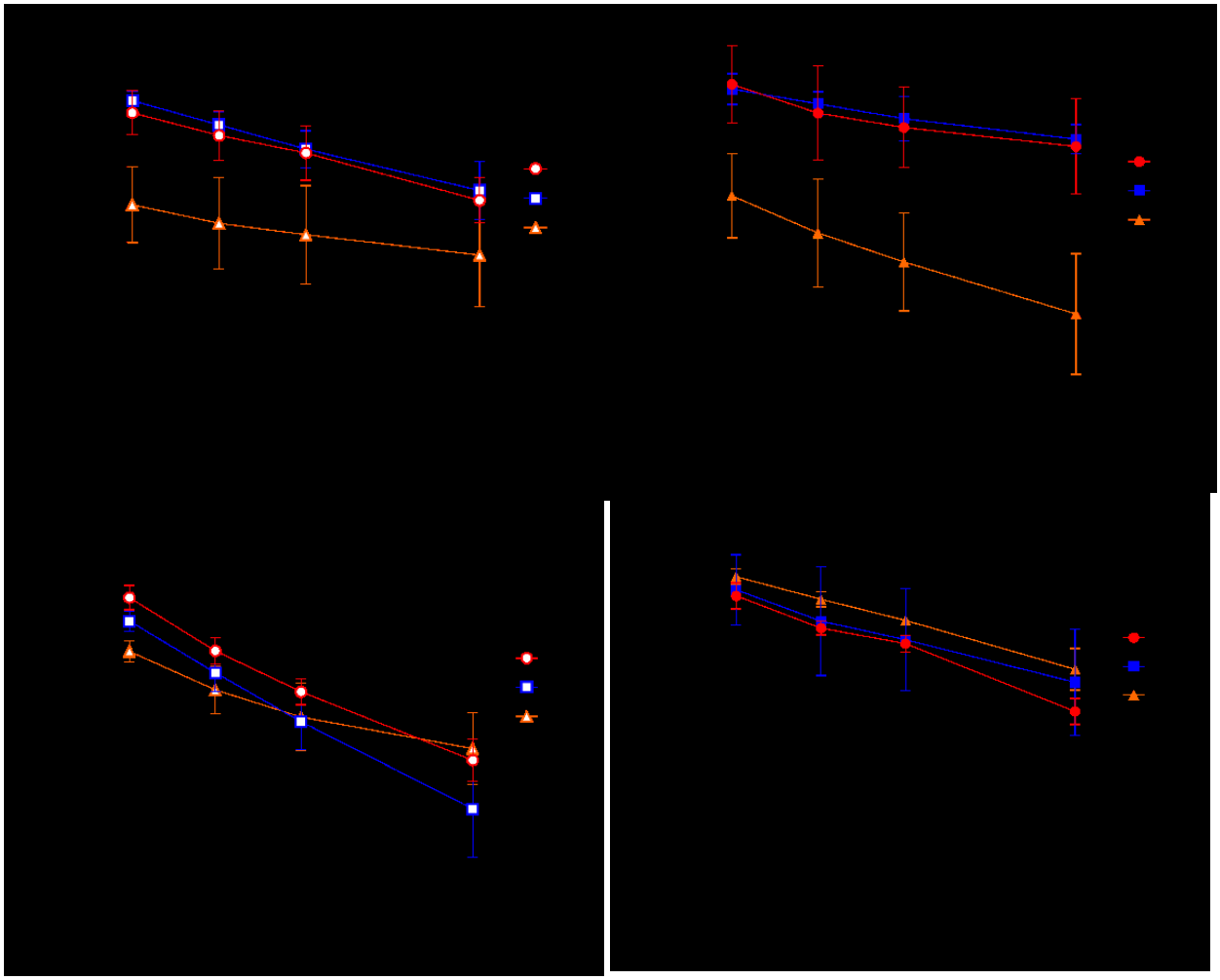

Figure 4.3 – Entrapment efficiency of systems containing CBD (○, □, △) or DH-CBD (■, ●, ▲) in olive oil solutions (a, b) or in ethanol (c, d). Values are expressed as mean percentage ± SD.

Although with narrow differences between samples, the general trend indicates a slightly higher entrapment efficiency of DH-CBD than CBD, except in the case of vesicles containing OA and olive oil solution. Systems containing PG showed very similar values of entrapment efficiency between olive oil or ethanol solutions, both with CBD and DH-CBD.

4.2.4.3 DEVELOPMENT AND CHARACTERIZATION OF HYDROGELS CONTAINING VESICLES

Strain sweep tests confirmed the presence of well-structured hydrogels. The conservative modulus (G') always resulted greater than the values of the loss modulus (G"). The yield points and the flow points of the four hydrogels revealed evident differences between their strength.

Hydrogels loaded with vesicles containing oleic acid showed an interesting profile. The obtained values are reported in Table 4.10 and shown in Figure 4.4.

Table 4.10 – Yield points and flow points obtained by strain sweep measurements of the four selected hydrogels.

Samples	Yield points		Flow points	
	Shear Strain (%)	Storage G' (Pa)	Shear Strain (%)	Storage G' (Pa)
E263	0.982	101.18	73.4	19.773
E265	6.560	368.3	64.1	125.08
E267	8.41	404.82	67.3	129.84
E269	0.751	766.51	12.6	262.09

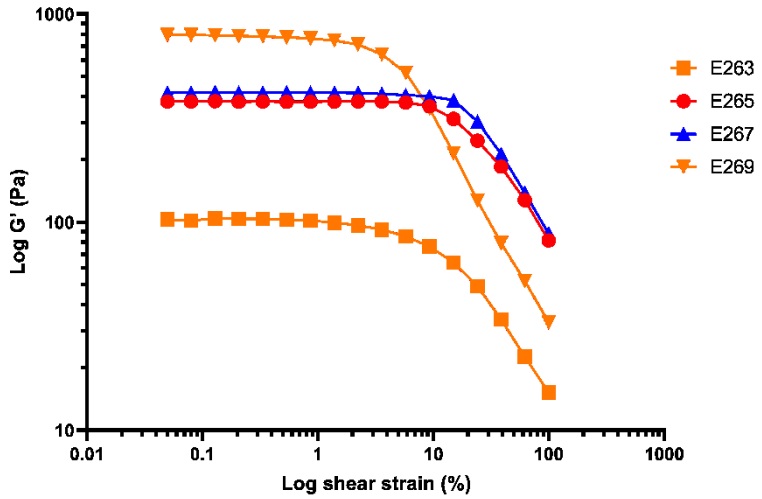

Figure 4.4 – Storage moduli values (G') obtained in strain sweep pivotal tests.

Frequency sweep tests showed good linearity at low frequencies with all the analyzed hydrogels. Very similar profiles were registered between the two hydrogels loaded with vesicular systems containing propylene glycol, while the most evident discrepancies were obtained in hydrogels loaded with OA-containing vesicles. The results are shown in Figure 4.5.

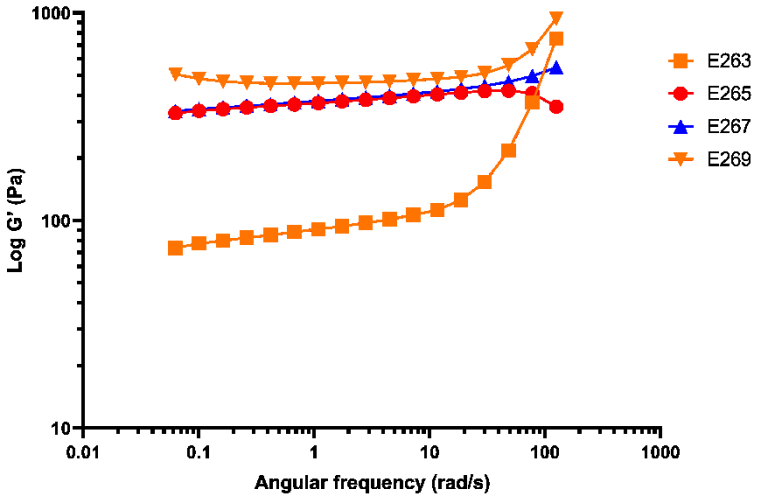

Figure 4.5 – Storage moduli values (G') of frequency sweep pivotal tests.

The formulation containing vesicles loaded with olive oil solution of DH-CBD resulted the least stable at high frequencies, while the opposite was registered with similar vesicles containing an ethanolic solution. These observations were confirmed by both the strain sweep test and the frequency sweep test.

The complete strain sweep and frequency sweep profiles of the four hydrogels are reported in Appendix F.

4.2.5 DISCUSSION

The influence of oleic acid in vesicular systems containing phosphatidylcholine and ethanol was investigated by considering two different molar ratios between OA and PC. The most stable preparations were composed by an OA:PC ratio of 0.54, *i.e.*, below the critical ratio of 0.67 reported in the literature, at a concentration of ethanol equal to 30% on the total weight of the preparation. The use of these parameters resulted in the formation of semi-transparent, homogeneous dispersions which appeared stable over at least three months. The concentration of the phospholipid, at equivalent OA:PC ratios, did not affect the appearance of the preparations, but differences were registered in terms of particle sizes. Higher phospholipid concentrations led to greater stability over time in terms of mean particle size, showing narrower fluctuations in vesicular size. This phenomenon was furthermore improved when a TRIS buffer was used in the preparations. The obtained results are in accordance with literature indications on the effects of concentrations of PC, OA, and pH on the preparations. Ethanol could further influence the behavior of fatty acids in PC vesicular systems, as the alcohol intercalates between the phospholipidic bilayers changing the hydrophobic environment where OA should be located. As the hydrophobicity of the environment highly influences the apparent pK_a of OA, a change in the pH of the formulations was expected to occur. The phenomenon of a pH shifting from slightly basic to slightly acidic seemed correlated to the total concentration of OA in the

preparations, leading to lower pH at the highest concentration of the fatty acid. This change was observed in preparations both with and without using buffering systems, although a lower ΔpH was observed in the presence of TRIS buffer. Worth noting that the millimoles of buffering systems were more than three times lower as compared to OA millimoles (0.065 vs. approximately 0.2). This fact could be the explanation of a reduced pH change, and not a complete buffering action. Nonetheless, a good improvement in pH fluctuations was achieved, leading to loaded formulations containing 0.1 M buffer phosphate.

Although a change in the pH values was registered after three months of observation, the mean particle size of empty systems was not equally affected. Whereas samples containing lower concentrations of PC showed greater differences in mean particle size, little differences could be noticed in systems containing 4% PC, and even no differences at all when TRIS buffer was included in the system. This could be correlated to the formation of a negative charge density on the surface of the vesicles, partially induced both by oleic acid and by the presence of ethanol, as demonstrated by Touitou. The charge density could lead to higher stability of the systems when a buffer is used, both in terms of particle size and pH changes. Further investigations over the influence of buffering systems and pH changes over time, as well as transition temperature studies and *z*-potential analyses on these systems, could be performed in order to investigate deeply the mechanisms underlying these phenomena.

Loaded samples containing olive oil solutions of cannabinoids appeared as white, homogeneous dispersions, although high polydispersity was noticed. Spherical formations of micrometric sizes were registered, as confirmed by visual observation under a light microscope. Only in the case of systems containing an olive oil solution of DH-CBD and OA, a population with an average size of 300 nm was observed. Systems containing ethanolic solutions, though, were semi-transparent and homogeneous, showing good stability by visual observation. Their mean particle sizes resulted between 90 and 300 nm, which are suitable for good transdermal drug delivery. The pH values of loaded systems containing OA generally resulted between 7.70 and 7.85, which is slightly higher than the zero–time value of empty preparations with buffer phosphate. This could be explained by the presence of a highly lipophilic drug in the systems, which could increase the hydrophobicity of the environment surrounding OA molecules. The consequence is an increase of apparent pK_a of OA, thus leading to a pH value of the preparation of 7.70-7.80, instead of maximum 7.5. Loaded systems showed differences in their mean particle size among CBD or DH-CBD equivalent formulations. PG-containing vesicles showed narrower with CBD, while OA-containing vesicles were smaller with DH-CBD. Very high entrapment efficiencies were observed, always above 80%, even though slight differences could be recorded among CBD and DH-CBD containing systems. In particular, almost all the preparations showed higher entrapment efficiency when DH-CBD was incorporated, except in the case of OA-containing systems loaded with olive oil solutions. In conclusion, all the loaded formulations had good properties in terms of particle size, entrapment efficiency, and pH when

considered, but systems containing PG and loaded with olive oil solutions showed phase separations after two weeks of storage, so that they were excluded from the loading with cannabis oil extract. On the other hand, the good features of vesicular systems containing ethanolic solutions of cannabinoids made them promising candidates for the loading with ethanolic cannabis extracts, which were preliminary performed and characterized.

4.3 CANNABIS EXTRACTS AND FORMULATION INTO VESICULAR SYSTEMS

4.3.1 MATERIALS

Ethanol absolute, Ph. Eur. (Scharlab, Spain)
Lipoid S100 (kindly provided by Lipoid GmbH, Germany)
Monosodium phosphate dihydrate, Ph. Eur. (A.C.E.F., Italy)
Olive refined European Pharmacopeia oil (Olive Oil, Ph.Eur) (A.C.E.F., Italy)
Phospholiphon® 90G (kindly provided by Lipoid GmbH, Germany)
Propylene glycol (Fagron, Italy)
Super Refined™ Oleic Acid NF (kindly provided by Croda, United Kingdom)

4.3.2 METHODS

4.3.2.1 CANNABIS EXTRACTION

Decarboxylation of acidic cannabinoids

The extractions were performed on previously reheated cannabis flowers to activate the acidic forms of cannabinoids. The heating of a thin layer of flowering tops was performed in a static oven. Briefly, cannabis flowering tops were finely ground and placed in maximum 1 cm layer into a closed glass box. The system was treated in static oven at 115 ± 1°C for 40 min then cooled down for 10 minutes before opening and proceeding with the samples preparation (165, 166). The impact of the preheating treatment was assessed by changing the duration. The 40 minutes treatment was compared with an overnight treatment (at least 12 hours) at 121 ± 1°C, then cooled down for 10 minutes and extracted in different solvents as following described.

Extraction with olive oil

For the preparation of cannabis oil extract, 500 mg of preheated cannabis flowering tops were placed in 5 ml of olive oil and heated in a water bath (100°C) for 120 min (160). The extraction was carried out in a closed beaker with continuous mixing. After two hours, the system was cooled down at room temperature, then the mixture was transferred in a 15 ml well-sealed centrifuge tube and centrifuged with Universal 320R (Hettich, Tuttlingen, Germany) centrifuge at 5000 rpm for 20 minutes. The supernatant was collected and transferred in 2 ml Eppendorf Safe-Lock tubes. The extract was then stored at 4°C, tightly closed and protected from light. The extraction was performed in six replicates, while extracts from overnight preheated cannabis were performed in four replicates.

Extraction with ethanol

Extraction with ethanol was performed on 1000 mg pre-heated cannabis flowering tops. Finely powdered cannabis was placed in a round bottomed flask with 10 ml absolute ethanol and a condenser. The extraction was performed by reflux over 120 minutes with continuous magnetic stirring (159). The system was then cooled down to room temperature, then transferred in a 15 ml centrifuge tube and centrifuged with Universal 320R (Hettich, Tuttlingen, Germany) centrifuge at 5000 rpm for 20 minutes. The supernatant was then transferred in a new 10 ml plastic tube and stored at +4°C, well-sealed and protected from light. The extraction was performed in six replicates, while extracts from overnight preheated cannabis were performed in four replicates.

The resume of the performed extractions is reported in Table 4.11.

Table 4.11 – Operative conditions of the performed cannabis extracts in olive oil or ethanol.

SOLVENT	PREHEATING	EXTRACTION
Olive oil 10 ml per g	115 ± 1°C, 40 min 120 ± 1°C, overnight	100°C, 120 min
Ethanol abs. 10 ml per g	115°C, 40 min 120 ± 1°C, overnight	Reflux, 120 min

Quantification of the major cannabinoids in the extracts

The quantification of cannabinoids in the obtained samples was performed in collaboration with Prof. Dall'Acqua at the University of Padova, with different methods. For the quantitative analysis of the first extracts, diluted samples were compared to an ethanolic extract of 100 mg of dried flowering tops of FM2 in 50 ml of ethanol with 15 minutes ultrasound treatment. Each extract was diluted 1:25 with the same solvent, either olive oil or ethanol, for the analysis with HPLC-DAD. Analyses were performed with an HPLC system Agilent 1260 (600Bar), using a Kinetek C-18 (4.6 x 150mm) column, and a mobile phase composed by ACCN and water 1% formic acid. The elution gradient started with 65% ACCN, reaching 80% ACCN in 30 minutes. The flux was kept at 1 ml/min and the UV spectra were detected in a range of 200-400 nm, using the 280 nm trace for the quantification. Peak assignation was made by comparison from elution order and UV-vis absorption available from the literature (180), and reference compounds available in the laboratory.

The chromatogram with the elution order of cannabinoids and their acidic forms, and their UV-vis spectra, are reported in Appendix F.

For the analysis via HPLC-DAD, a solution of CBD and a solution of THC were used as a standard, as in this case a single standard reference cannot be used for the quantification of cannabinoids. The two obtained calibration curves resulted y = 2.2233x – 0.3798 and y = 1.7774x + 0.3451 for THC and CBD, respectively.

Extracts performed on cannabis preheated overnight were analysed via GC-MS as indicated in Paragraph 4.3.2.4.

4.3.2.2 PREPARATION AND CHARACTERIZATION OF VESICLES CONTAINING CANNABIS EXTRACTS

Four formulations were selected for the loading of cannabis extracts: one with olive oil, and three with ethanolic extracts. Olive oil was used from extraction E273, while the used ethanol extract was E275. Formulations with the same compositions were prepared by loading extracts derived from overnight preheating, thus obtaining formulations E297, E299, E301 and E303. The formulations were prepared with a simple mixing method. Briefly, the formulations were prepared by dissolving the phospholipid in ethanol, then PG or OA and 500 mg of extracts were added. The formation of the vesicles was achieved by vigorous mixing, then stored at +4°C well protected from light.

The compositions of the performed formulations are reported in Table 4.12 and 4.13.

Table 4.12 – Composition of the vesicles containing propylene glycol, Phospholipon 90G (90G) or Lipoid S100 (S100) phospholipids, and cannabis ethanolic extract. Values are expressed as percentage on the total weight of the preparation.

Sample name	PC	PG	EtOH extract	EtOH	H_2O mQ
E279, E297	4.0 (90G)	40.0	5.0	15.0	36.0
E281, E299	4.0 (S100)	40.0	5.0	15.0	36.0

Table 4.13 – Composition of the vesicular systems containing oleic acid and olive oil (OO) or ethanolic (EtOH) cannabis extracts. Values are expressed as percentage on the total weight of the preparation.

Sample name	PC	OA	OO extract	EtOH extract	EtOH	Buffer phosph.
E277, E303	4.0	0.8	5.0	-	30.0	60.2
E283, E301	4.0	0.8	-	5.0	25.0	65.2

Visual observation

Stored formulations were observed 30 minutes after the reparation and daily during the storage. When phase separation was registered, the formulations were transferred in an Eppendorf 1.5 ml tube, well-sealed and protected from light. Visual observation was further performed on preparations containing olive oil with a light microscope Leitz HM-LUX 3 (Ernst Leitz Wetzlar Gmbh, Portugal). A droplet of the selected suspension was mounted between two cover slips of 24 × 60 mm and observed under 40× magnification.

pH measurement

With a 744 pH Meter (Metrohm, Switzerland), the formulations containing OA were analyzed after dilution with milliQ water at a ratio of 1:5 v/v. Two dilutions were performed for each sample.

DLS measurement

Each sample was tested with a Zetasizer Nano ZEN3600 (Malvern, United Kingdom) 24 hours after preparation. Thirty minutes prior to measurement, the systems were diluted 1:500 v/v with an equivalent hydroalcoholic mixture previously filtered with a 0.45 µm pore size PTFE disposable syringe filter (ThermoFisher Scientific, USA). DLS analyses were performed using a backscattering detector at 173°. Tests were run at 25°C, with three replications of 12 scans for each sample. The duration and the set position of each measurement were fixed automatically by the apparatus. Multiple *t*-tests were performed with Prism software, version 8 (GraphPad Software, San Diego, CA, USA).

4.3.2.3 EVALUATION OF THE ENTRAPMENT EFFICIENCY

Loaded formulations E297-E303 were evaluated for their capability to efficiently retain cannabinoids in the vesicular systems, *i.e.*, their entrapment efficiency. BioDesignDalysis Tubing™, with 15.5 mm wet diameter and 1.91 ml/cm volume, 14000 Da MWCO (BioDesign Inc., ThermoFisher Scientific, New York, USA), was cut into 5 cm length pieces and hydrated with mQ water for at least 24 hours. After closure at one end, 1 ml of vesicular dispersion was injected, and the upper end was closed. The system was then immersed in 30 ml of an equivalent hydroethanolic (or hydro-glycolic-ethanolic) solution (142, 153) and left stirring for 5 hours. Aliquots of 1 ml were taken from the media at 1, 2, 3, and 5 hours, restoring the total volume by addition of fresh solution. The samples were collected into 2 ml Eppendorf Safe-Lock Tubes, closed with Parafilm® and stored at -18°C until UV analysis.

Spectrophotometric analyses with UV-Vis Cary® 50 (Agilent, Varian, The Netherlands) were performed onto the samples without dilution and using an equivalent hydroethanolic solution

for the baseline correction. The quantification of the free drug concentration was performed as compared to a diluted solution of each formulation, previously disrupting the vesicles by dilution 1:1 with ethanol absolute, then diluting 1:250 with an equivalent hydroethanolic (or glycolic) solution.

4.3.2.4 EVALUATION OF SKIN PERMEATION OF CANNABIS EXTRACTS

Formulations

Formulations E297, E299, E301 and E303 were used for the evaluation of skin delivery of cannabinoids using liposomes containing cannabis extracts at the same concentrations as control groups.
Liposomes were prepared as follows. In a mortar, PC and cannabis extract were subsequently ground and mixed vigorously with a pestle. After obtaining a homogeneous mixture, 1.5 ml of mQ water were included in the formulation geometrically, while mixing with a pestle. The homogeneous emulsion was transferred quantitatively in a glass vial, by washing the mortar with 3×0.75 ml of mQ water. The remaining mQ water was added and the system was stirred with magnetic stirring at 1500 rpm for 5 minutes. The dispersion was then transferred in a plastic vial and stored at +4°C.

The compositions of the control formulations are reported in Table 4.14.

Table 4.14 – Composition of liposomes containing olive oil (OO) or ethanolic (EtOH) extracts of cannabis. Values are expressed as percentage on the total weight of the preparation.

Sample name	PC	OO extract	EtOH extract	mQ water
E305	4.0	-	5.0	91.0
E307	4.0	5.0	-	91.0

In vitro skin permeation experimental protocol

The ability of the deformable vesicles and liposomal formulations to deliver cannabis extracts into and through the skin was tested in the laboratories of Dr. Casiraghi at the University of Milan. The four formulations and two control groups were tested in 24 Franz static diffusion cells using full thickness porcine skin and a 30% hydroethanolic solution as a receiver medium. Two hundred and fifty microliters of each formulation were applied on the epidermal side of the skin under non-occlusive conditions for 180 minutes. Receiver samples of 200 µl were taken at 30, 60, 120 and 180 minutes, and equal amount of receiver was returned.

At the end of 180 minutes, the skin was removed from the cell and its surface was carefully washed two times with 600 µl of ultrapure water. Each skin was then inserted into 15 ml tubes

containing 5 ml of extraction solution composed by mQ water and ethanol 1:1. The tubes were shaken for 24 hours at room temperature. After the 24 hours treatment, the tubes were mixed by Vortex (Vortex Genie®-2, Scientific Industries, USA) for 30 seconds, the skins were removed, and the tubes were stored at -18°C until analysis.

GC-MS assay conditions

Samples were analyzed with GC-MS system composed by a chromatograph Varian 3900 and an ion trap mass spectrometer Varian Saturn 2100T. The injector was set to 225°C and the heating ramp was set from 110° to 290°C in 28 minutes. EI spectra were collected between 50-350Da, while the identification of the compounds was performed by Kovatz index calculation, injection of a standard compound and library NIST 2017. Two calibration curves were prepared with two THC and CBD standards.

4.3.3 RESULTS

4.3.3.1 CANNABIS EXTRACTION AND FORMULATION

Preheating and extraction of cannabinoids

The mean concentrations of the cannabinoids and their acidic forms obtained by olive oil or ethanol extracts are reported in Table 4.15.

Table 4.15 – Mean concentrations of the major cannabinoids obtained by extractions in olive oil (E273 and E287) or ethanol (E275 or E289). Values are expressed as mg/ml ± SD.

Extraction	THC	THCA	CBD	CBDA	CBN
E273	0.605 ± 0.095	0.602 ± 0.170	0.644 ± 0.104	3.142 ± 0.567	0.909 ± 0.147
E275	0.450 ± 0.066	0.484 ± 0.016	0.499 ± 0.034	2.729 ± 0.111	0.690 ± 0.045
E287	0.691 ± 0.237	2.630 ± 0.947	0.659 ± 0.216	7.080 ± 2.462	1.023 ± 0.340
E289	0.388 ± 0.026	1.542 ± 0.022	0.356 ± 0.020	4.187 ± 0.013	0.518 ± 0.028

From these results, several observations can be remarked. First, two different batches of preheated cannabis were used for the performed extractions: the first batch was used for E273 (oil) and E275 (ethanol) extractions, which were performed in triplicate. The second batch was used for E287 (oil) and E289 (ethanol), both performed in triplicate too. As clearly shown in the table, with the second batch the total concentration of THCA and CBDA are much higher than in the previous case. This could be explained with a lower efficiency of the preheating

treatment, even though the same conditions of temperature and time were maintained between the two batches.

On the opposite, overnight preheating led to higher extraction efficiency when ethanol was used as a solvent. Results are reported in Table 4.16.

Table 4.16 – Concentration of CBD and THC in cannabis extracts in olive oil (OO) or ethanol (EtOH) after an overnight preheating, analyzed via GC-MS method. Values are expressed as mg/ml ± SD.

Extraction	THC	CBD
E296 – OO	0.51 ± 0.17	1.50 ± 0.07
E296 – EtOH	2.69 ± 0.63	7.59 ± 0.11

As compared to the 40 min preheating, overnight treatment confirmed a higher extraction efficiency on the total amount of CBD, while THC was extracted less efficiently. Lower variability was achieved with ethanolic extractions, where THC levels were maintained. Further examinations on the carboxylated and decarboxylated forms will be performed to evaluate the efficacy of the preheating treatment.

4.3.3.2 CHARACTERIZATION OF THE FORMULATIONS

Vesicular systems containing oleic acid, loaded with olive oil or ethanolic cannabis extracts, were analyzed for their pH. The results are reported in Table 4.17.

Table 4.17 – Mean pH values (± SD) of vesicular systems containing OA and cannabis olive oil (E277, E303) or ethanol (E283, 301) extracts.

Formulation name	pH measurements
E277	7.66 ± 0.03
E283	7.64 ± 0.05
E301	7.70 ± 0.01
E303	7.74 ± 0.01

All the systems showed pH values around 7.7, as expected from the presence of phosphate buffer in the aqueous phase. A slight increase in the mean values was registered in E301 and 303, where most likely extracts with lower concentrations of acidic cannabinoids were incorporated. Further investigations on the three months stability will be made to evaluate changes in the pH, or the lack thereof.

DLS measurements on the four vesicular systems obtained from the first cannabis olive oil (E277) or ethanolic (E279 – E283) extracts showed a mean particle size of nanometric range in all the formulations. As expected from previous analyses on CBD and DH-CBD formulations, the formulation containing olive oil extract showed two main populations in the micrometric and nanometric range, respectively, as confirmed by the Z-Average value. The main results obtained from DLS analysis are reported in Table 4.18.

Table 4.18 – Mean particle size of the formulations containing olive oil extract (E277) or ethanol extract (E279, E281, E283).

Sample name	Peak 1		Z-Average		PDI	
	nm	SD	nm	SD		SD
E277	356.7	173.4	1263.0	366.6	0.799	0.255
E279	210.5	55.9	227.7	23.5	0.330	0.167
E281	173.3	46.7	225.0	29.2	0.642	0.328
E283	298.0	43.1	232.5	13.4	0.273	0.066

The results were then compared to the mean particle size of the formulations containing CBD or DH-CBD formulations. Statistically significant differences (multiple t-tests, $p<0.05$) were registered between vesicles with CBD and vesicles with extracts in all cases, except from the formulations containing ethanolic extracts, 90G phospholipid and PG. Values are reported in Figure 4.6.

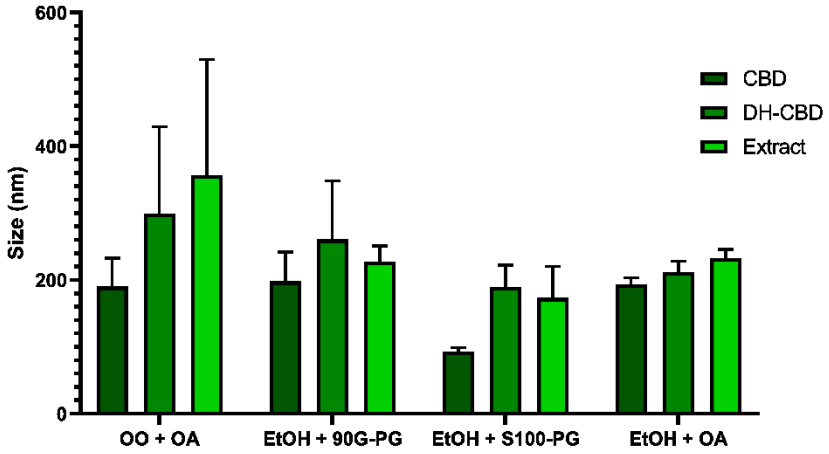

Figure 4.6 – Mean particle size of the formulations containing CBD, DH-CBD or extracts in olive oil (OO) or ethanol (EtOH), according to the different composition of the performed formulations. Values are expressed as mean ± SD.

From this graph, differences in terms of particle size can be appreciated, even though the trend is almost similar in all cases. The most evident difference is given by the formulations containing S100 phospholipid, as the mean particle size always results the lowest, but still around 200 nm both with DH-CBD and the extract. These results must be considered according to the composition of the extract, which resulted rich in CBDA, as previously reported.

Formulations containing extracts obtained from overnight preheating did not show significant differences as compared to formulations loaded with 40 minutes preheating extracts, in the case of PG-containing vesicles. On the opposite, vesicles containing OA showed lower mean particle size, underlying a higher sensitivity to the loaded active ingredient. The mean size registered for each formulation is reported in Table 4.19 and Figure 4.7.

Table 4.19 – Mean particle size of the formulations containing ethanolic extracts obtained after overnight preheating.

Sample name	Peak 1		Z-Average		PDI	
	nm	SD	nm	SD		SD
E297	174.0	25.0	226.6	32.9	0.338	0.276
E299	193.9	17.4	171.9	18.5	0.173	0.085
E301	185.5	21.6	179.1	30.6	0.323	0.076

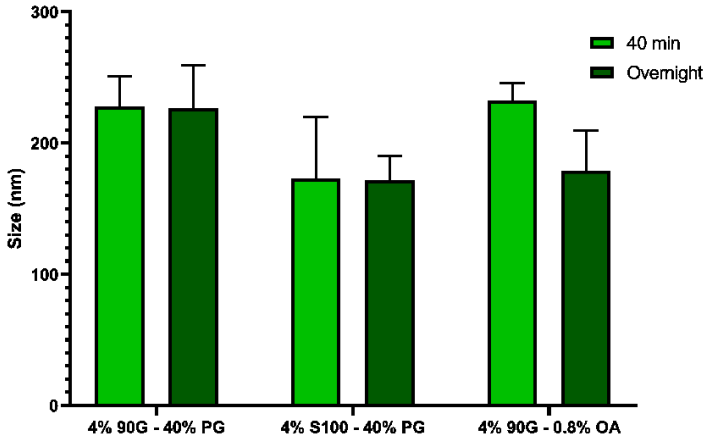

Figure 4.7 – Mean particle size (+ SD) of vesicles containing cannabis extracts in ethanol with different preheating times: 40 minutes and overnight.

Systems loaded with olive oil extracts showed a double population composed by micrometric particles and nanometric structures. However, the bigger population showed a smaller size (around 1500 nm), while the second population was slightly bigger than in the cases of CBD and DH-CBD loaded vesicles (around 600 nm).

4.3.3.3 EVALUATION OF THE ENTRAPMENT EFFICIENCY

The entrapment efficiency of the systems loaded with cannabis extracts resulted very high in all the formulations, always above 90%. The best results were obtained with vesicles containing OA, indicated in Figure 4.8 in orange and golden-yellow, respectively.

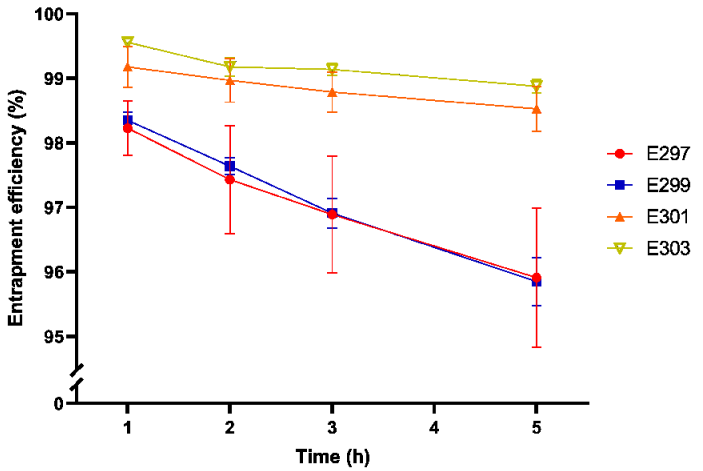

Figure 4.8 – Entrapment efficiency of vesicular systems containing extracts in ethanol (E297, E299, E301) or olive oil (E303). Values are expressed as mean ±SD.

These findings furtherly confirm the high encapsulation efficiency of these systems, as expected from CBD and DH-CBD loaded vesicles.

4.3.3.4 EVALUATION OF THE SKIN PERMEATION OF CANNABINOIDS

Samples collected from the receiver up to three hours of observation did not show permeation through the skin. Considering the permeated amount into the skin, though, a high increase in skin permeation was registered when soft vesicular systems were applied. The percentage of the permeated cannabinoids into the skins are reported in Figure 4.9 and 4.10.

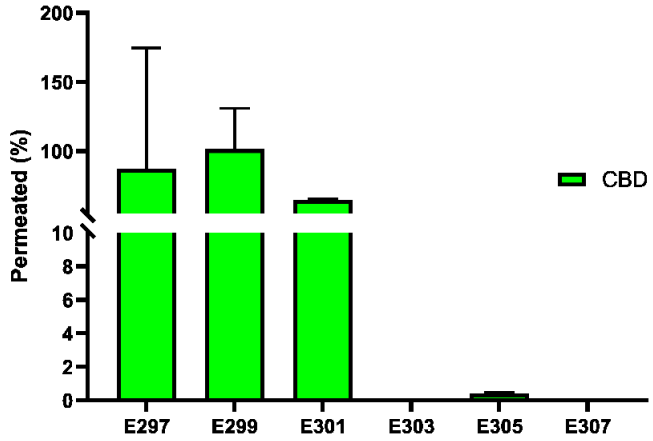

Figure 4.9 – Skin penetration of CBD after 3 hours of treatment with formulations containing ethanolic extracts (E297, E299, E301) or olive oil extracts (E303) and their controls (E305, E307, respectively). Values are expressed as mean ± SEM.

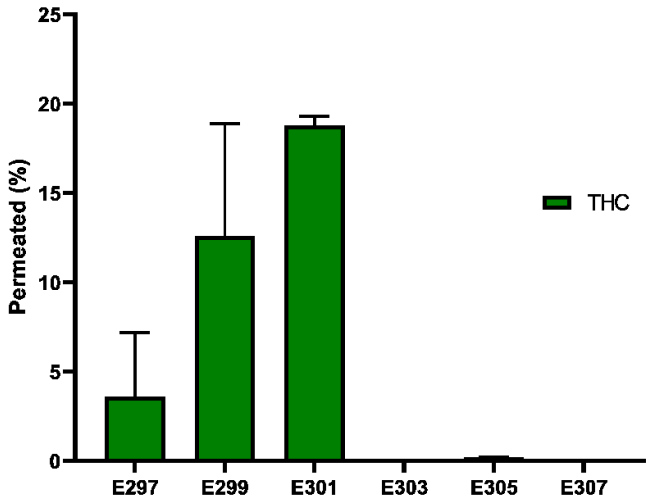

Figure 4.10 – Skin penetration of THC after 3 hours of treatment with formulations containing ethanolic extracts (E297, E299, E301) or olive oil extracts (E303) and their controls (E305, E307, respectively). Values are expressed as mean ± SEM.

CBD permeation resulted very high, especially in the case of PG-containing vesicles loaded with ethanolic extracts (E287, E299), where a maximum of 100% was obtained. The highest THC permeation was achieved with the formulation composed of OA vesicles containing ethanolic extracts, giving a maximum peak of 20%. All the formulations containing olive oil extracts did not show skin penetration of cannabinoids, both in the developed vesicles and in the control group. On the opposite, the control group loaded with ethanolic extract showed minimal permeation of THC (0.2 ± 0.01 %) and CBD (0.4 ± 0.1 %). Thus, the developed vesicular systems increased CBD penetration up to 250 times more than liposomes, and THC penetration up to 100 times higher than liposomes.

4.3.4 DISCUSSION

The first cannabis extracts revealed good cannabinoids profiles, although rich in their acidic forms. When considering the extractions performed in the same batch of preheated cannabis, higher concentrations of cannabinoids were registered at first when olive oil was used as a solvent. Despite the higher efficiency, the extraction in olive oil was more variable. The extraction in ethanol was less efficient, but with the highest reproducibility within the same preheated batch. In fact, very low standard deviations were obtained among ethanolic extracts. The ratios between decarboxylated cannabinoids concentrations were maintained independently from the solvent used, within the same preheated batch of cannabis. Cannabinol resulted more concentrated in olive oil extracts than in ethanol extracts, but its concentration did not vary in accordance with a diminished amount of THCA. This behavior could be connected to the extraction process alone, rather than the preheating process. Very high reproducibility of cannabinoids extractions in ethanol was registered among the same batch of

preheated cannabis. Similar results were obtained among extracts obtained after overnight preheating of a cannabis batch, but not among olive oil extracts, where cannabinoids were found to be much less concentrated. These factors make them very promising for the normalization of the administered dose of cannabinoids to the patient, so these extracts are excellent candidates for the loading into vesicular systems.

The preliminary results on the formulations containing cannabis extracts were encouraging. Mean particle size analysis showed vesicles with diameters ranging from 170 to 360 nm, with better results when an ethanolic extract was loaded, as compared to olive oil extracts. Moreover, no significant differences were registered between PG vesicles laded with extracts obtained after 40 minutes or overnight preheating of the vegetable material. Smaller particles were formed when OA vesicles were prepared with ethanolic extract after overnight preheating of cannabis. Entrapment efficiency studies confirmed an excellent cannabinoids retention, reaching amounts above 90% in all the formulations. Almost no leakage of cannabinoids was registered when OA-containing vesicles were loaded, both with ethanolic and olive oil extracts.

Skin permeation studies revealed very engaging results, as the permeation across the skin was not observed over the treatment time (three hours), but very high skin penetration was achieved with formulations containing ethanolic extracts. CBD permeation into the skin resulted in up to 100% of the administered dose, especially in the case of PG-containing vesicles. THC permeation was highly enhanced when OA-containing vesicles were applied. Further studies can be performed to assess the skin permeation of CBD and THC across the skin by testing the formulation over 24 or 48 hours.

Conclusions

Cannabis and its properties have been extensively studied over the last decades, but many drawbacks on using it for medical purposes are yet to be overcome. The great variability coming from a vegetable source, enhanced by the production of phytocannabinoids depending on cannabis strain, age, and position on the plant of female inflorescences, leads to a poorly define administered dose to the patient. Moreover, the high lipophilicity of the major cannabinoids and the massive first-pass effect when administered orally, cause very different concentrations of cannabinoids in the bloodstream, thus achieving poor management of the diseases when administered to a patient. In addition, poorly designed clinical studies, or the lack of separation between the effects of plant-derived or synthetic cannabinoids, the administration routes, and the previous use of cannabis from the observed patients, did not allow to establish the real dose-response effects of cannabinoids, and the possibility to draw guidelines to help patients and healthcare professionals in choosing to use cannabis or not, in a safe and effective way. Transdermal delivery could be an efficient strategy to grant a good release profile by keeping constant blood levels of cannabinoids for a prolonged time, thus improving the compliance for the patient and the efficacy of the treatment. The transdermal delivery of cannabinoids, though, cannot be easily achieved, because their lipophilicity makes them accumulate in the stratum corneum without reaching the systemic circulation. Thus, the aim of this project was to develop innovative vesicular systems to enhance the dermal and transdermal delivery of cannabinoids.

The formulation of cannabinoids from a natural source is not easy to pursue, as the product is classified among psychotropic drugs and its supply and detention are regulated by the restrictions of narcotic laws. In order to allow the development of transdermal delivery systems, a model molecule with similar solubility behavior of THC but without psychotropic effects was chosen: desoxycannabidiol (DH-CBD). This molecule was synthesized by improving literature synthetic pathways, in particular by introducing of an additional step in the production of *p*-mentha-2,8-dien-1-ol synthon to enhance the stereoselectivity: a bromohydrine was formed from the double bond in the cyclohexene ring of R-(+)-limonene, then epoxidized in the *trans*-form to further proceed with a Cope elimination. The condensation of this synthon with *m*-pentylphenol, obtained from 3-methoxybenzylbromide *via* Gilman reagent, led to the formation of DH-CBD, which was further purified with flash-chromatography allowing to start the development of pharmaceutical forms. The overall yield resulted in 6%. During the third year of this project, another semisynthetic pathway was pursued by reductive dehydroxylation of CBD, similar in structure to DH-CBD. This improved the total yield to 50% and dramatically reduced the production times, allowing to ultimate the pharmaceutical technology development.

The dermal delivery of highly lipophilic drugs was extensively studied by using different systems, especially vesicular structures capable of cross the outmost layer of the skin, the stratum corneum, to reach the systemic blood circulation. Soft, deformable vesicles made of phospholipids are the most promising vesicular systems developed in the last three decades. Vesicles containing high concentrations of ethanol, named "ethosomes", achieved very good results in the delivery of both hydrophilic and lipophilic drugs due to a double action of the ethanol, as extensively demonstrated by their inventor, Prof. Elka Touitou. During the secondment of this PhD project, ethosomes were prepared and tested in the laboratory of Prof. Touitou at The Hebrew University of Jerusalem (Israel), showing the improved permeability of these systems via CLSM experiments. Similar results were expected when lidocaine base was incorporated in ethosomes, but the dispersion state of the drug and the strongly basic pH of the formulations resulted in poorly repeatable results when using liposomes as a control.

In this project, soft vesicular systems were developed by addition of propylene glycol or oleic acid to vesicles composed of phospholipid multilayers and a hydroethanolic core. These compounds deeply influenced the stability and permeability of the vesicular systems. Propylene glycol reduced the particle size of the systems, but high concentrations of this compound caused higher instability with the lowest concentrations of phospholipids. During the three months of observation, low concentrations of PC and PG led to the formation of big aggregates not suitable for the transdermal delivery. The most stable combinations were achieved with 4% phospholipid when PG ranged from 40% to 30%. Loaded formulations with this composition showed good nanometric structures and an entrapment efficiency above 80%. These vesicles were then incorporate into hydrogels to enhance their stability and ease of application to the patients. Their rheological properties showed good profiles, and they were further tested for the release of cannabinoids. Systems loaded with CBD were compared to DH-CBD loaded vesicles and hydrogels, showing great differences in terms of particle size, stability, and release profile. Vesicles containing oleic acid were then developed by carefully evaluating the PC:OA molar ratio, as well as ethanol concentration in the systems. The most stable systems were composed by a PC:OA ratio of 0.54 at any investigated PC concentration, an ethanolic concentration of 30% w/w, and the presence of a buffer phosphate 0.1 M to control the pH of the formulation, which deeply influences the stability of the systems.

PG- and OA-containing vesicles were then loaded with a simulation of cannabinoids extracts, as extrapolated from literature data before using cannabis extracts. Vesicles containing 4% PC, then 30% ethanol and 0.8% OA, or 20% ethanol and 40% PG, were loaded with CBD or DH-CBD solutions in olive oil or ethanol. The results indicated lower stability of the systems when olive oil was loaded, except in the case of OA-containing vesicles, which showed two main populations of nanometric and micrometric size, respectively. Hydrogels containing these systems were then prepared and analyzed with oscillatory tests, showing good strength and stability of these systems, especially when the ethanolic solution was used.

Pivotal studies on the extraction of cannabis in olive oil and ethanol and their formulation into vesicular systems were performed. The inflorescences were previously heated in a static oven for 40 minutes, then extracted in olive oil or ethanol for 120 minutes. HPLC-DAD analyses revealed high concentrations of acidic forms of CBD and THC (CBDA and THCA), which come from a small activation of these compounds in the preheating process. Olive oil showed higher amounts of both acidic and activated cannabinoids, as compared to ethanol, within the same preheated cannabis batch. An extended preheating treatment was then performed, leaving the inflorescence in an oven for at least 12 hours. THC and CBD concentrations were analyzed by GC-MS method, revealing higher performances in the extraction from ethanol rather than in olive oil, thus reversing the preliminary findings. Further investigation via LC-DAD-ESI-MS analysis will be performed to quantify the acidic and activated forms of THC and CBD in the latest extracts. Although more exploited for clinical applications, the olive oil extracts showed very high variability, also within the same cannabis batch, while ethanol extracts had excellent reproducibility. The very low variability on the total amount of THC and CBD in ethanolic extracts, which was not dependent on a short- or long-term preheating, makes the extraction in ethanol an enticing candidate for the formulation into transdermal delivery systems. This element is fundamental for guaranteeing a defined dose to the patient, which is one of the main aims of this project.

The extracts were then formulated into vesicular systems, which showed good nanometric particle size and almost neutral pH in the case of OA-containing vesicles. The differences in particle size between CBD and extracts-containing formulations underlined the importance of having DH-CBD as a model molecule for the development of these vesicular systems. Very high entrapment efficiency was registered in all the loaded systems, above 90% when cannabis extracts were formulated. Skin permeation experiments revealed higher skin penetration of cannabinoids into porcine skin model when ethanolic extracts were formulated into the developed soft vesicular systems. As compared to liposomes, the skin penetration of CBD and THC after three hours of treatment was enhanced up to 250 times and 100 times, respectively.

In conclusion, DH-CBD was successfully synthesized and formulated to anticipate the behavior of cannabis extracts in vesicular systems for the delivery of cannabinoids. Interesting vesicular systems containing PG or OA were developed and characterized in terms of stability over time, entrapment efficiency, and stability and release profiles when incorporated into hydrogels. These results led to the preliminary studies on the formulation of cannabis extracts, newly obtaining desirable particle size, stability, and very high entrapment efficiency of the vesicular dispersions. Preliminary studies on skin penetration highlighted the superior capability of soft vesicular systems to deliver into the skin cannabinoids coming from ethanolic extracts, and further studies will be performed to test the permeability across the skin over 24 hours of treatment.

Appendix

In this section are given supplementary information on the CLSM micrographs and the formulations indicated in Chapter 3.
In section A are reported the CLSM micrographs obtained from the analysis of porcine skin after 120 minutes of contact with FITC-ethosomes or FITC-liposomes, as reported in Paragraph 3.2.3.2. The visual observation of the micrographs suggests an increased amount of permeated fluorescent probe when delivered by ethosomes.

In section B are reported the mean particle size and the stability of the missing formulations containing DH-CBD described in Paragraph 3.3.2.1. Formulations containing lower concentrations of phospholipids showed greater instability with important fluctuations in the mean size over three months, and even too high polydispersity in the case of the formulation containing 2% 90G.

Section C contains the entrapment efficiency values of the excluded formulations (Paragraph 3.3.2.2), although showing greater entrapment efficiency when lower amounts of PC are used. This could be partially explained by the presence of bigger particles and lower amounts of propylene glycol, which tendentially increases the permeability of phospholipidic layers.

Section D shows the viscosity properties of hydrogels containing the less stable formulations (Paragraph 3.3.2.3), and the hydrogel-hydroalcoholic-formulation shear curves. The differences between the viscosity profiles between loaded formulations and a hydrogel containing an equivalent hydroethanolic-glycolic solution could be an indicator of stability of the vesicular systems in the gelled system.

In section E are gathered the release profiles of the hydrogels analyzed in section D and mentioned in Paragraph 3.3.2.4. Higher linearity and good release profiles were obtained with vesicles containing higher concentrations of phosphatidylcholine, while higher variability was obtained at lower concentrations of phospholipids. The formulation containing 90G phospholipid showed high variability, in particular one of the reported values (at 6.71 $min^{-1/2}$) was extrapolated from the data.

In section F are reported the complete strain sweep and frequency sweep profiles of the four hydrogels containing vesicles with DH-CBD solutions.

Section G contains the HPLC-DAD chromatogram of cannabis extracts, together with the UV-vis spectra of the major cannabinoids and their acidic forms.

A CLSM MICROGRAPHS

Table A - CLSM micrograph of the skin samples treated with loaded ethosomes (FITC-Ethosomes) or liposomes (FITC-liposomes) for 120 minutes.

FORMULATION	SAMPLE 1	SAMPLE 2	SAMPLE 3
FITC- Ethosomes	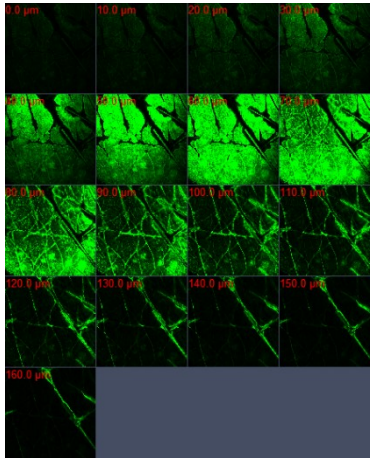	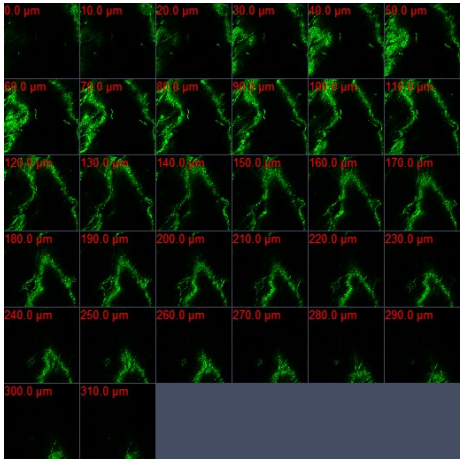	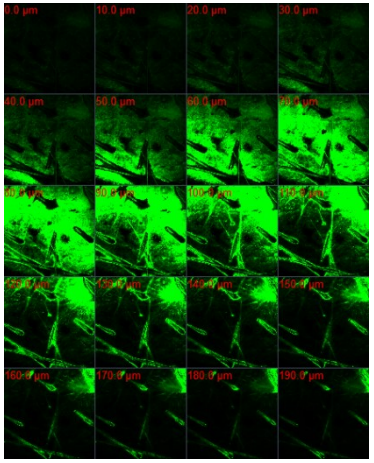
FITC- Liposomes	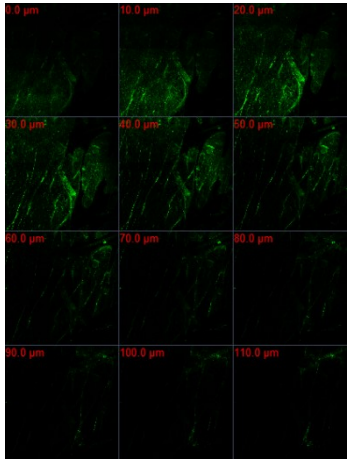	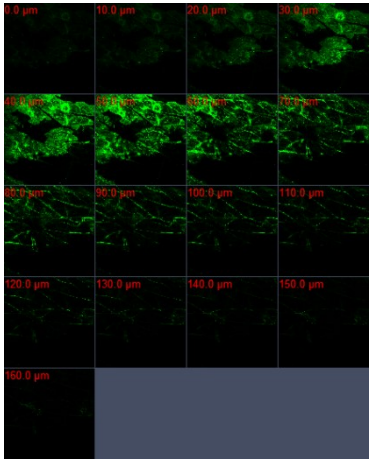	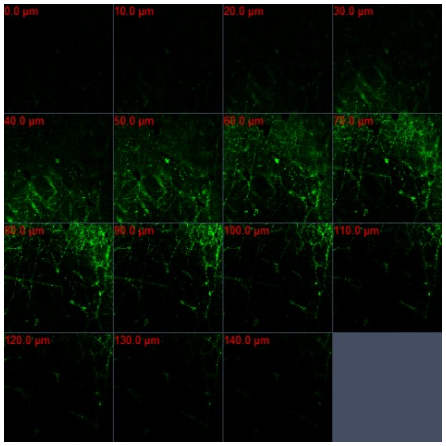

B THREE MONTHS STABILITY OF LOADED FORMULATIONS CONTAINING PROPYLENE GLYCOL

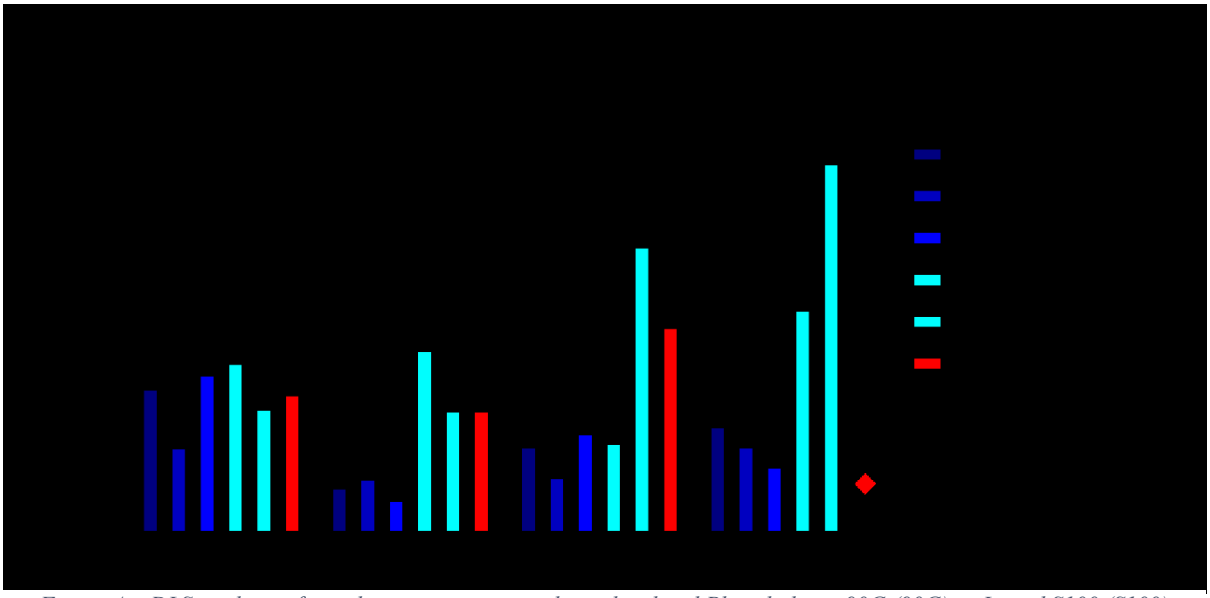

Figure A – DLS analysis of vesicles containing propylene glycol and Phospholipon 90G (90G) or Lipoid S100 (S100) phospholipids, at different concentrations. Values are expressed as mean particle size ± SD. Polydisperse samples are indicated with a symbol (♦).

C ENTRAPMENT EFFICIENCY OF DH-CBD LOADED FORMULATIONS WITH PROPYLENE GLYCOL

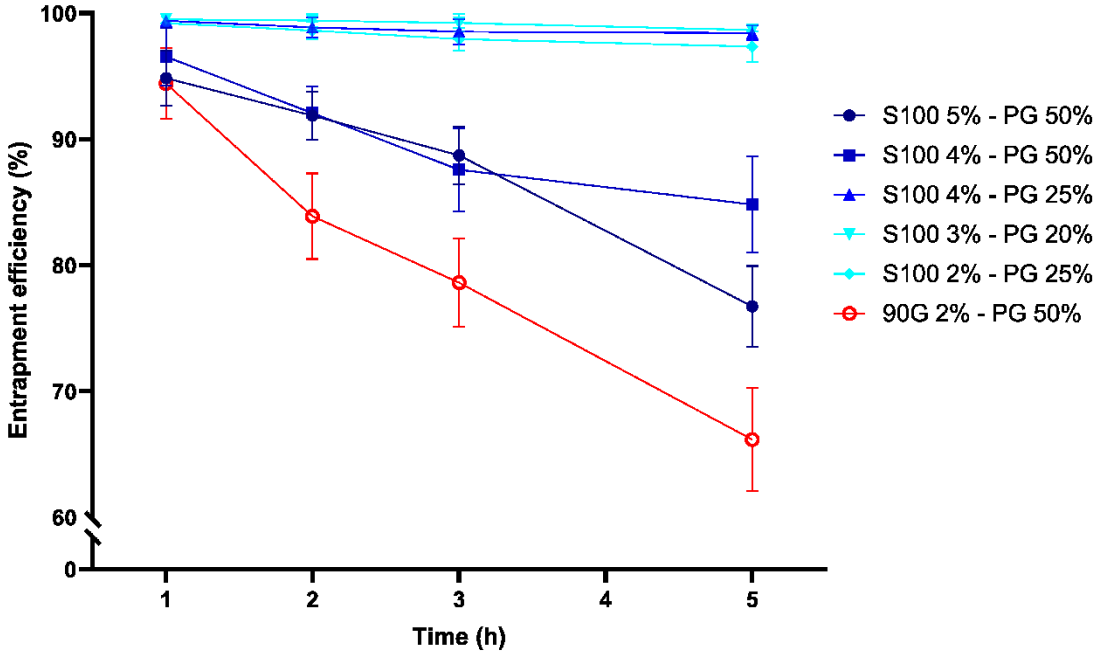

Figure A – Entrapment efficiency of the less stable vesicular dispersions containing Phospholipon 90G or Lipoid S100 and propylene glycol at different concentrations. Values are expressed as mean percentage of retained drug ± SD.

D VISCOSITY SHEAR CURVES OF HYDROGELS CONTAINING DH-CBD VESICLES WITH PROPYLENE GLYCOL

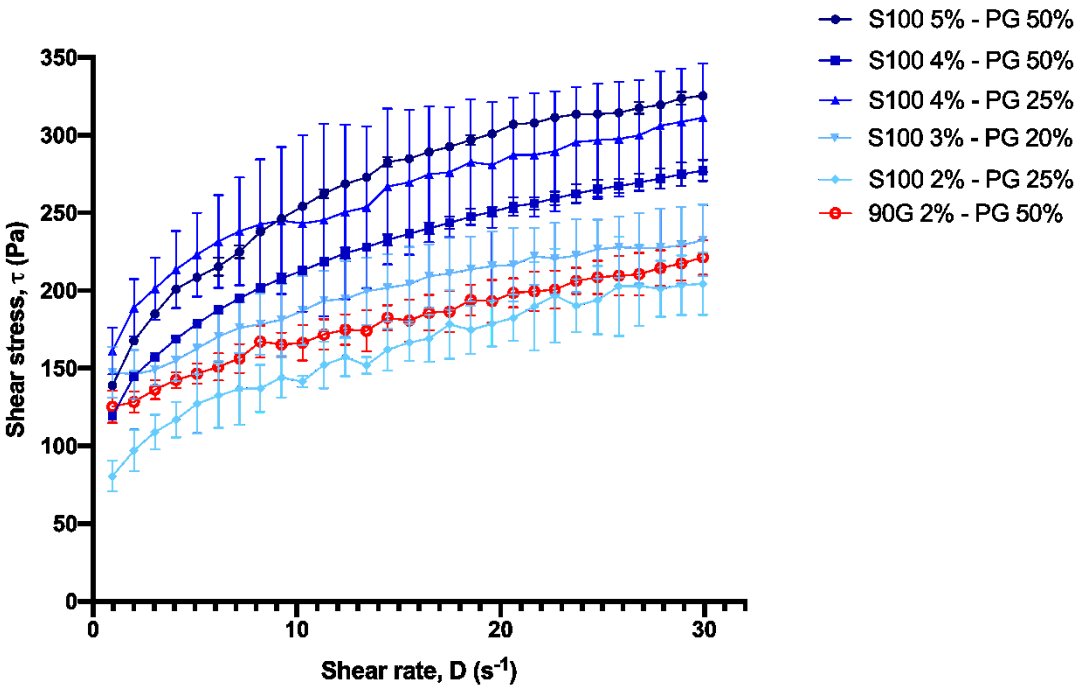

Figure D1 – Viscosity shear of hydrogels containing loaded vesicles at different propylene glycol (PG) and phospholipid (S100 or 90G) concentrations. Values are expressed as mean ± SD.

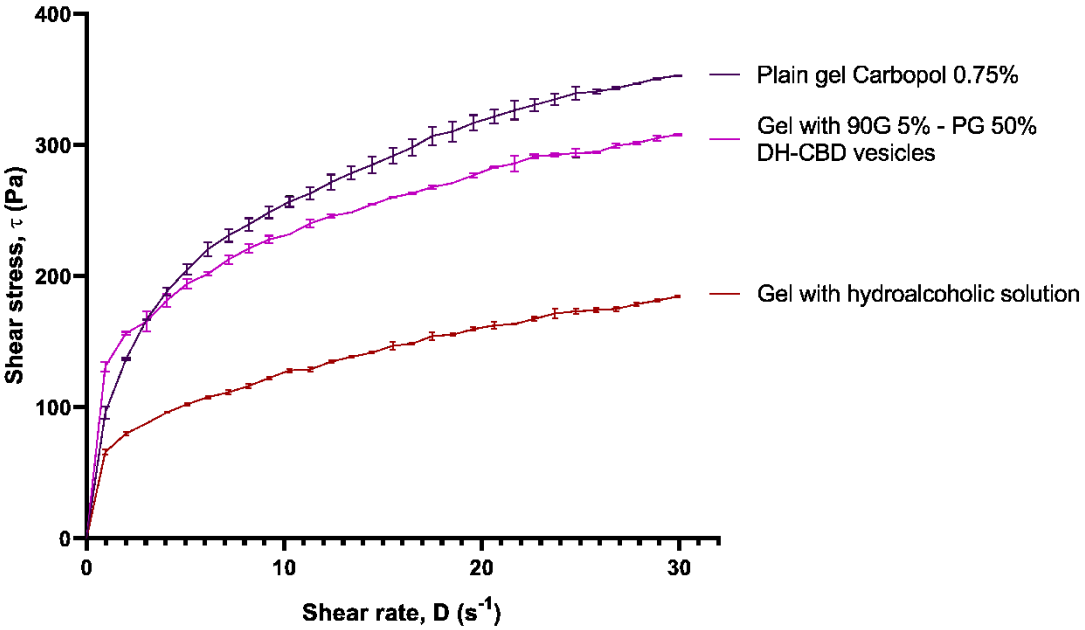

Figure D2 – Viscosity shear of pure Carbopol 0.75% hydrogel vs. viscosity shear of hydrogels containing a hydroalcoholic mixture or a loaded formulation at a 1:1 ratio in weight. Values are expressed as mean ± SD.

E RELEASE PROFILES OF HYDROGELS CONTAINING DH-CBD VESICLES WITH PROPYLENE GLYCOL

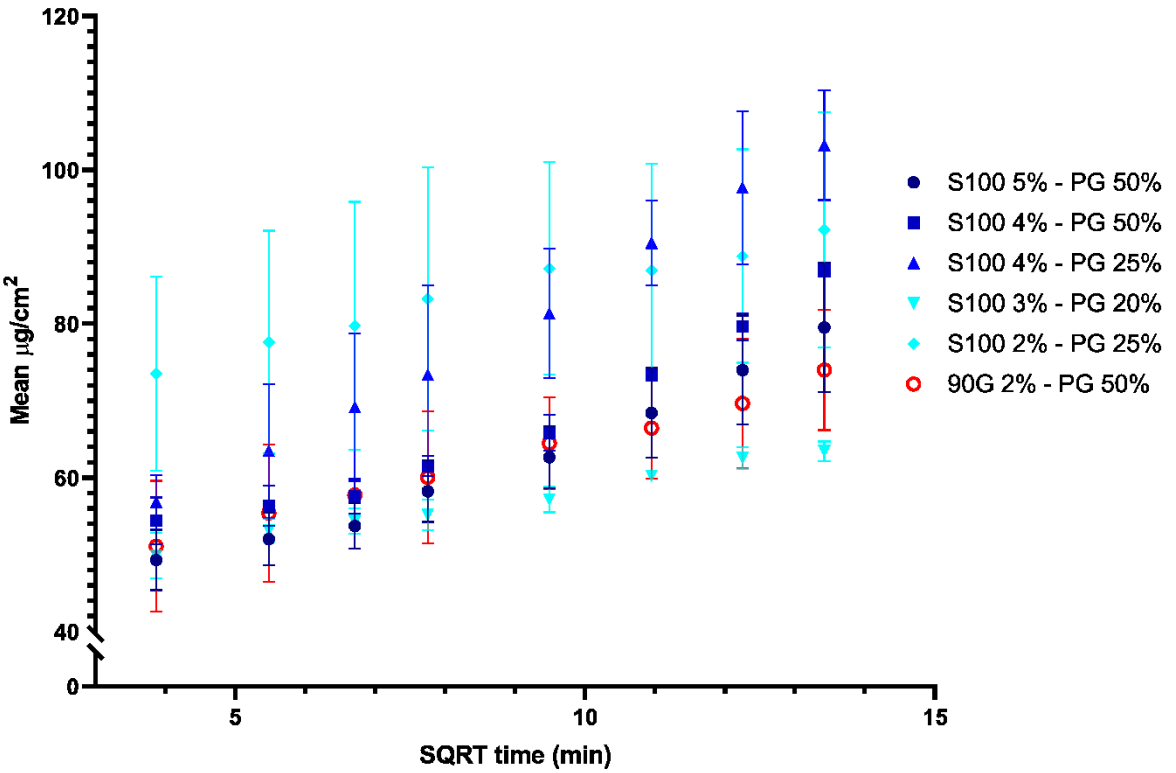

Figure A – Release profiles of hydrogels containing loaded vesicular systems containing DH-CBD. Values are expressed as mean released amount in terms of micrograms per square centimeter, as a function of the square root of time.

F VISCOELASTIC BEHAVIOR OF HYDROGELS LOADED WITH DH-CBD VESICULAR FORMULATIONS

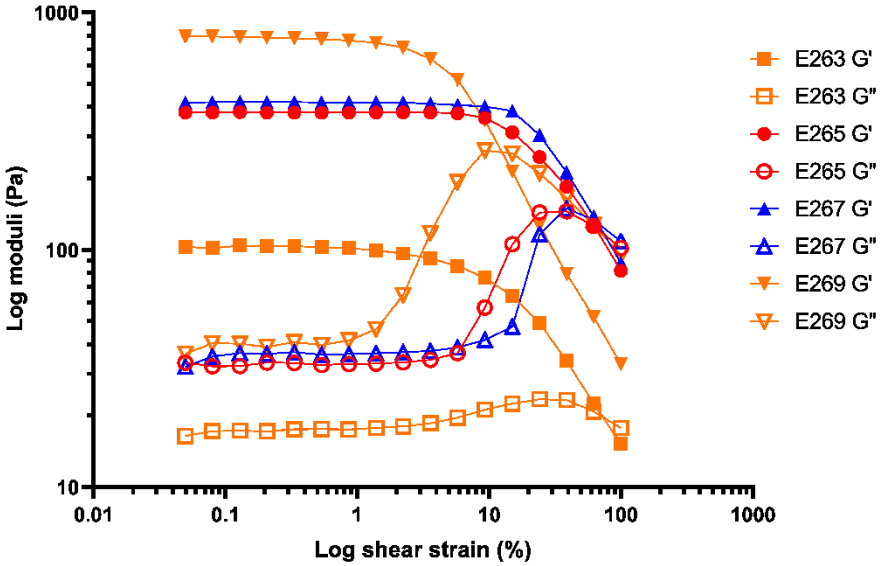

Figure G1 – Strain sweep results of hydrogels loaded with vesicles containing DH-CBD solutions.

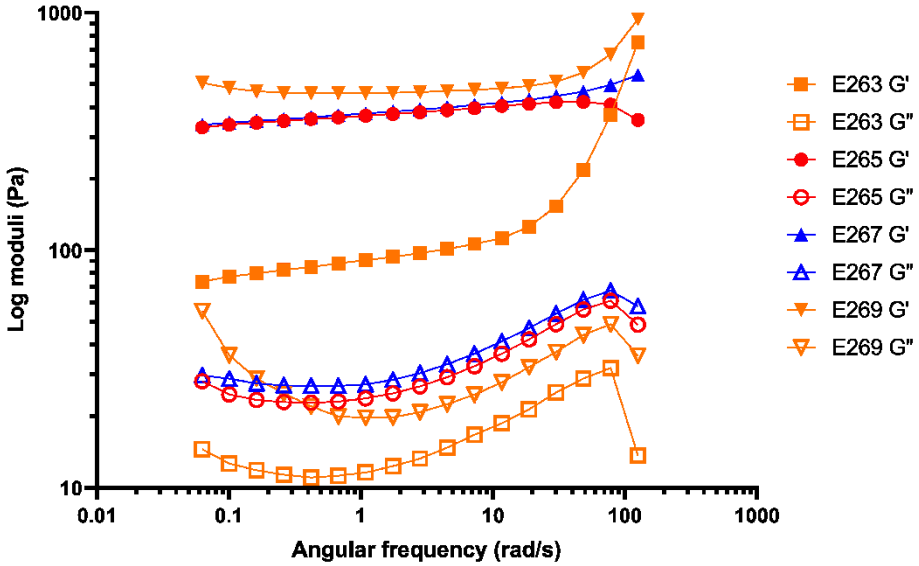

Figure G2 – Frequency sweep results of hydrogels loaded with vesicles containing DH-CBD solutions.

G CHROMATOGRAM OF CANNABINOIDS IN HPLC-DAD AND DETECTED UV-vis SPECTRA

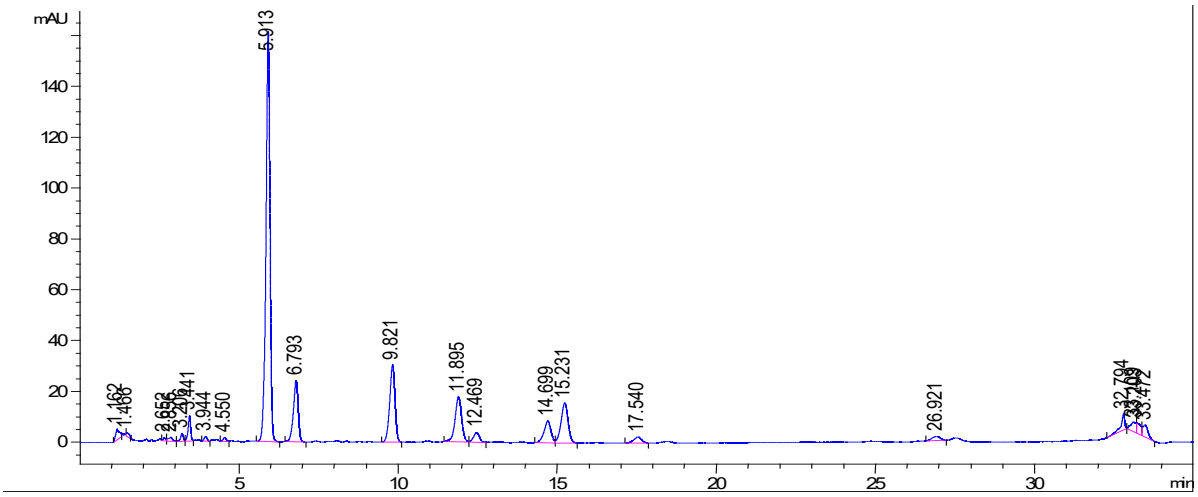

Figure F1 – HPLC-DAD chromatogram of cannabis extract registered at 280 nm.

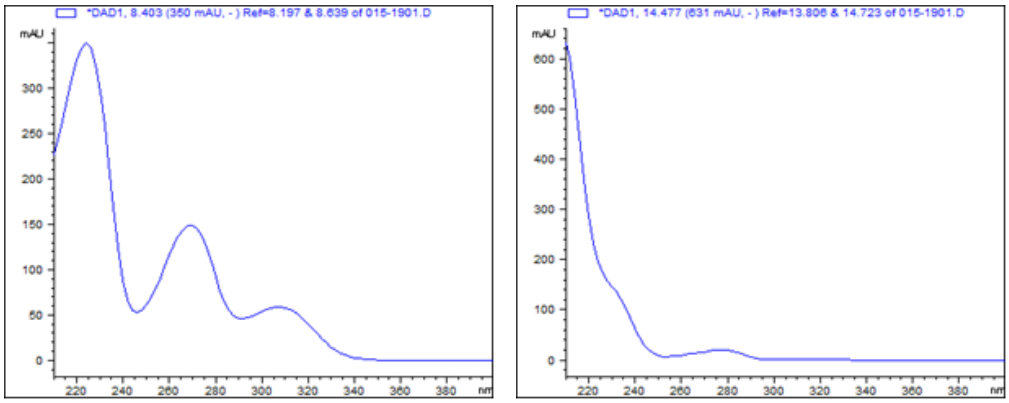

Figure F2 – UV spectra of acidic cannabinoids (left) and decarboxylated cannabinoids (right).

References

1. Russo EB. History of cannabis and its preparations in saga, science, and sobriquet. Chem Biodivers [Internet]. 2007;4:1614–48. Available from: http://doi.wiley.com/10.1002/cbdv.200790144
2. The National Academies of Science, Engineering and Medicine. The health effects of cannabis and cannabinoids: the current state of evidence and recommendations for research [Internet]. Washington, DC: The National Academies Press; 2017. Available from: https://www.nap.edu/catalog/24625
3. Long T, Wagner M, Demske D, Leipe C, Tarasov PE. Cannabis in Eurasia: origin of human use and Bronze Age trans-continental connections. Veg Hist Archaeobot [Internet]. 2017 Mar;26(2):245–58. Available from: https://doi.org/10.1007/s00334-016-0579-6
4. Curran HV, Freeman TP, Mokrysz C, Lewis DA, Morgan CJA, Parsons LH. Keep off the grass? Cannabis, cognition and addiction. Nat Rev Neurosci [Internet]. 2016;17(5):293–306. Available from: http://www.nature.com/doifinder/10.1038/nrn.2016.28
5. Nunn JF. Ancient Egyptian medicine. Norman: University of Oklahoma Press; 1996.
6. Pliny E. Natural History. 1950th ed. Rackman H, editor. Harvard University Press; Volume V, Book XIX, Chapter XXII, p. 461.
7. Pliny E. Natural History. 1950th ed. Rackman H, editor. Harvard University Press; Volume V, Book XIX, Chapter LVI, pp.531–533.
8. Pliny E. Natural History. 1950th ed. Rackman H, editor. Harvard University Press; Volume V, Book XX, Chapter XCVII, p. 153.
9. David T Brown. Cannabis: The Genus Cannabis. Brown DT, editor. Vol. 1. Harwood academic publishers; 2003. 284 p.
10. O'Shaughnessy WB. New remedy for tetanus and other convulsive disorders. Bost Med Surg J [Internet]. 1840;23(10):153–5. Available from: https://doi.org/10.1056/NEJM184010140231001
11. Moreau JJ. Hashish and mental illness. New York: Raven Press; 1845.
12. Hanuš LO, Meyer SM, Muñoz E, Taglialatela-Scafati O, Appendino G. Phytocannabinoids: a unified critical inventory. Nat Prod Rep. 2016;33(12):1357–92.

13. Mariotti K de C, Marcelo MCA, Ortiz RS, Borille BT, dos Reis M, Fett MS, et al. Seized cannabis seeds cultivated in greenhouse: a chemical study by gas chromatography-mass spectrometry and chemometric analysis. Sci Justice [Internet]. 2016;56(1):35–41. Available from: http://dx.doi.org/10.1016/j.scijus.2015.09.002

14. Turner CE, Elsohly MA, Boeren EG. Constituents of Cannabis sativa L. XVII. A review of the natural constituents. J Nat Prod [Internet]. 1980;43(2):169–234. Available from: https://doi.org/10.1021/np50008a001

15. Adams R, Hunt M, Clark JH. Structure of cannabidiol, a product isolated from the marihuana extract of minnesota wild hemp. I. J Am Chem Soc [Internet]. 1940;62(1):196–200. Available from: https://doi.org/10.1021/ja01858a058

16. Adams R, Pease DC, Cain CK, Baker BR, Clark JH, Wolff H, et al. Conversion of cannabidiol to a product with marihuana activity. A type reaction for synthesis of analogous substances. Conversion of cannabidiol to cannabinol. J Am Chem Soc [Internet]. 1940;62(8):2245–6. Available from: https://doi.org/10.1021/ja01865a508

17. Mechoulam R, Burstein SH. Marijuana; chemistry, pharmacology, metabolism and clinical effects. New York: Academic Press; 1973.

18. Razdan RK. Recent advances in the chemistry of cannabinoids. Prog Org Chem. 1973;8:78–101.

19. Wollner HJ, Matchett JR, Levine J, Loewe S. Isolation of a physiologically active tetrahydrocannabinol from cannabis sativa resin. J Am Chem Soc [Internet]. 1942;64(1):26–9. Available from: https://doi.org/10.1021/ja01253a008

20. Gaoni Y, Mechoulam R. Isolation, structure, and partial synthesis of an active constituent of hashish. J Am Chem Soc. 1964;86(8):1646–7.

21. Howlett AC, Johnson MR, Melvin LS, Milne GM. Nonclassical cannabinoid analgetics inhibit adenylate cyclase: development of a cannabinoid receptor model. Mol Pharmacol. 1988 Mar;33(3):297–302.

22. Devane WA, Hanus L, Breuer A, Pertwee RG, Stevenson LA, Griffin G, et al. Isolation and structure of a brain constituent that binds to the cannabinoid receptor. Science. 1992 Dec;258(5090):1946–9.

23. Baron EP. Comprehensive review of medicinal marijuana, cannabinoids, and therapeutic implications in medicine and headache: What a long strange trip it's been ... Headache. 2015;55(6):885–916.

24. Pertwee RG. The diverse CB 1 and CB 2 receptor pharmacology of three plant cannabinoids: Δ^9-tetrahydrocannabinol, cannabidiol and Δ^9-tetrahydrocannabivarin. Br

J Pharmacol. 2008;153(2):199–215.

25. Matsuda LA, Lolait SJ, Brownstein MJ, Young AC, Bonner TI. Structure of a cannabinoid receptor and functional expression of the cloned cDNA. Nature. 1990 Aug;346(6284):561–4.

26. Howlett AC, Barth F, Bonner TI, Cabral G, Casellas P, Devane WA, et al. International Union of Pharmacology. XXVII. Classification of cannabinoid receptors. Pharmacol Rev. 2002 Jun;54(2):161–202.

27. Mechoulam R, Parker LA. The endocannabinoid system and the brain. Annu Rev Psychol. 2013;64(1):21–47.

28. Maccarrone M, Gasperi V, Catani MV, Diep TA, Dainese E, Hansen HS, et al. The endocannabinoid system and its relevance for nutrition. Annu Rev Nutr. 2010 Aug;30:423–40.

29. Battista N, Di Tommaso M, Bari M, Maccarrone M. The endocannabinoid system: an overview. Front Behav Neurosci [Internet]. 2012 Mar 14;6:9. Available from: https://www.ncbi.nlm.nih.gov/pubmed/22457644

30. Walter L, Stella N. Cannabinoids and neuroinflammation. Br J Pharmacol. 2004 Mar;141(5):775–85.

31. Cabral GA, Staab A. Effects on the immune system. Handb Exp Pharmacol. 2005;(168):385–423.

32. Pertwee RG. Pharmacological actions of cannabinoids. Handb Exp Pharmacol. 2005;(168):1–51.

33. Fimiani C, Liberty T, Aquirre AJ, Amin I, Ali N, Stefano GB. Opiate, cannabinoid, and eicosanoid signaling converges on common intracellular pathways nitric oxide coupling. Prostaglandins Other Lipid Mediat. 1999 Jan;57(1):23–34.

34. Mechoulam R, Ben-Shabat S, Hanus L, Ligumsky M, Kaminski NE, Schatz AR, et al. Identification of an endogenous 2-monoglyceride, present in canine gut, that binds to cannabinoid receptors. Biochem Pharmacol. 1995 Jun;50(1):83–90.

35. Baron EP. Medicinal properties of cannabinoids, terpenes, and flavonoids in cannabis, and benefits in migraine, headache, and pain: an update on current evidence and cannabis science. Headache. 2018;58(7):1139–86.

36. Serrano A, Parsons LH. Endocannabinoid influence in drug reinforcement, dependence and addiction-related behaviors. Pharmacol Ther. 2011 Dec;132(3):215–41.

37. Rouzer CA, Marnett LJ. Endocannabinoid oxygenation by cyclooxygenases,

lipoxygenases, and cytochromes P450: cross-talk between the eicosanoid and endocannabinoid signaling pathways. Chem Rev. 2011 Oct;111(10):5899–921.

38. Fu J, Bottegoni G, Sasso O, Bertorelli R, Rocchia W, Masetti M, et al. A catalytically silent FAAH-1 variant drives anandamide transport in neurons. Nat Neurosci. 2011 Nov;15(1):64–9.

39. Gaetani S, Dipasquale P, Romano A, Righetti L, Cassano T, Piomelli D, et al. The endocannabinoid system as a target for novel anxiolytic and antidepressant drugs. Int Rev Neurobiol. 2009;85:57–72.

40. Fan P. Cannabinoid agonists inhibit the activation of 5-HT3 receptors in rat nodose ganglion neurons. J Neurophysiol. 1995 Feb;73(2):907–10.

41. Pertwee RG. The pharmacology and therapeutic potential of cannabidiol. Di Marzo V, editor. Cannabinoids. Kluwer Academic/Plenum Publishers; 2004. 32–83 p.

42. Thomas A, Baillie GL, Phillips AM, Razdan RK, Ross RA, Pertwee RG. Cannabidiol displays unexpectedly high potency as an antagonist of CB1 and CB2 receptor agonists in vitro. Br J Pharmacol. 2007 Mar;150(5):613–23.

43. Kreitzer AC. Neurotransmission: emerging roles of endocannabinoids. Curr Biol. 2005 Jul;15(14):R549-51.

44. Vaughan CW, Christie MJ. Retrograde signalling by endocannabinoids. Handb Exp Pharmacol. 2005;(168):367–83.

45. Pertwee RG, Ross RA. Cannabinoid receptors and their ligands. Prostaglandins Leukot Essent Fatty Acids. 2002;66(2–3):101–21.

46. Pistis M, Ferraro L, Pira L, Flore G, Tanganelli S, Gessa GL, et al. Delta(9)-tetrahydrocannabinol decreases extracellular GABA and increases extracellular glutamate and dopamine levels in the rat prefrontal cortex: an in vivo microdialysis study. Brain Res. 2002 Sep;948(1–2):155–8.

47. Gardner EL. Endocannabinoid signaling system and brain reward: emphasis on dopamine. Pharmacol Biochem Behav. 2005 Jun;81(2):263–84.

48. Nagai H, Egashira N, Sano K, Ogata A, Mizuki A, Mishima K, et al. Antipsychotics improve Δ^9-tetrahydrocannabinol-induced impairment of the prepulse inhibition of the startle reflex in mice. Pharmacol Biochem Behav. 2006 Jun;84(2):330–6.

49. Walter L, Franklin A, Witting A, Wade C, Xie Y, Kunos G, et al. Nonpsychotropic cannabinoid receptors regulate microglial cell migration. J Neurosci. 2003 Feb;23(4):1398–405.

50. Sacerdote P, Martucci C, Vaccani A, Bariselli F, Panerai AE, Colombo A, et al. The nonpsychoactive component of marijuana cannabidiol modulates chemotaxis and IL-10 and IL-12 production of murine macrophages both in vivo and in vitro. J Neuroimmunol. 2005 Feb;159(1–2):97–105.

51. McHugh D, Tanner C, Mechoulam R, Pertwee RG, Ross RA. Inhibition of human neutrophil chemotaxis by endogenous cannabinoids and phytocannabinoids: evidence for a site distinct from CB1 and CB2. Mol Pharmacol. 2008 Feb;73(2):441–50.

52. Capasso R, Borrelli F, Aviello G, Romano B, Scalisi C, Capasso F, et al. Cannabidiol, extracted from Cannabis sativa, selectively inhibits inflammatory hypermotility in mice. Br J Pharmacol. 2008 Jul;154(5):1001–8.

53. Iannotti FA, Hill CL, Leo A, Alhusaini A, Soubrane C, Mazzarella E, et al. Nonpsychotropic plant cannabinoids, cannabidivarin (CBDV) and cannabidiol (CBD), activate and desensitize transient receptor potential vanilloid 1 (TRPV1) channels in vitro: potential for the treatment of neuronal hyperexcitability. ACS Chem Neurosci. 2014 Nov;5(11):1131–41.

54. Russo EB, Burnett A, Hall B, Parker KK. Agonistic properties of cannabidiol at 5-HT1a receptors. Neurochem Res. 2005 Aug;30(8):1037–43.

55. Reddy DS, Golub VM. The pharmacological basis of cannabis therapy for epilepsy. J Pharmacol Exp Ther. 2016;357(1):45–55.

56. Agrawal A, Madden PAF, Bucholz KK, Heath AC, Lynskey MT. Initial reactions to tobacco and cannabis smoking: a twin study. Addiction. 2014 Apr;109(4):663–71.

57. Li R-F, Lu G-T, Li L, Su H-Z, Feng G, Chen Y, et al. Identification of a putative cognate sensor kinase for the two-component response regulator HrpG, a key regulator controlling the expression of the hrp genes in Xanthomonas campestris pv. campestris. Environ Microbiol. 2014 Jul;16(7):2053–71.

58. Gonzalez S, Cebeira M, Fernandez-Ruiz J. Cannabinoid tolerance and dependence: a review of studies in laboratory animals. Pharmacol Biochem Behav. 2005 Jun;81(2):300–18.

59. Hirvonen J, Goodwin RS, Li C-T, Terry GE, Zoghbi SS, Morse C, et al. Reversible and regionally selective downregulation of brain cannabinoid CB1 receptors in chronic daily cannabis smokers. Mol Psychiatry. 2012 Jun;17(6):642–9.

60. Huestis MA. Human cannabinoid pharmacokinetics. Chem Biodivers. 2007 Aug;4(8):1770–804.

61. Carter GT, Weydt P, Kyashna-Tocha M, Abrams DI. Medicinal cannabis: rational

guidelines for dosing. IDrugs. 2004 May;7(5):464–70.

62. Hazekamp A, Ruhaak R, Zuurman L, van Gerven J, Verpoorte R. Evaluation of a vaporizing device (Volcano) for the pulmonary administration of tetrahydrocannabinol. J Pharm Sci. 2006 Jun;95(6):1308–17.

63. Zuurman L, Roy C, Schoemaker RC, Hazekamp A, den Hartigh J, Bender JCME, et al. Effect of intrapulmonary tetrahydrocannabinol administration in humans. J Psychopharmacol. 2008 Sep;22(7):707–16.

64. Wachtel SR, ElSohly MA, Ross SA, Ambre J, de Wit H. Comparison of the subjective effects of Delta(9)-tetrahydrocannabinol and marijuana in humans. Psychopharmacology (Berl). 2002 Jun;161(4):331–9.

65. Agurell S, Halldin M, Lindgren JE, Ohlsson A, Widman M, Gillespie H, et al. Pharmacokinetics and metabolism of delta 1-tetrahydrocannabinol and other cannabinoids with emphasis on man. Pharmacol Rev. 1986 Mar;38(1):21–43.

66. Brunet B, Doucet C, Venisse N, Hauet T, Hébrard W, Papet Y, et al. Validation of Large White Pig as an animal model for the study of cannabinoids metabolism: Application to the study of THC distribution in tissues. Forensic Sci Int. 2006;161(2–3):169–74.

67. Karschner EL, Darwin WD, Goodwin RS, Wright S, Huestis MA. Plasma cannabinoid pharmacokinetics following controlled oral Δ^9-tetrahydrocannabinol and oromucosal cannabis extract administration. Clin Chem. 2011 Jan;57(1):66–75.

68. Perlin E, Smith CG, Nichols AI, Almirez R, Flora KP, Cradock JC, et al. Disposition and bioavailability of various formulations of tetrahydrocannabinol in the rhesus monkey. J Pharm Sci. 1985 Feb;74(2):171–4.

69. Stinchcomb AL, Valiveti S, Hammell DC, Ramsey DR. Human skin permeation of Δ^8-tetrahydrocannabinol, cannabidiol and cannabinol. J Pharm Pharmacol. 2004 Mar;56(3):291–7.

70. Mattes RD, Shaw LM, Edling-Owens J, Engelman K, Elsohly MA. Bypassing the first-pass effect for the therapeutic use of cannabinoids. Pharmacol Biochem Behav. 1993 Mar;44(3):745–7.

71. Pertwee RG. Cannabinoid pharmacology: the first 66 years. Br J Pharmacol. 2006 Jan;147 Suppl:S163-71.

72. Cameron C, Watson D, Robinson J. Use of a synthetic cannabinoid in a correctional population for posttraumatic stress disorder-related insomnia and nightmares, chronic pain, harm reduction, and other indications: a retrospective evaluation. J Clin Psychopharmacol. 2014 Oct;34(5):559–64.

73. GW Pharmaceutocal website - News section [Internet]. [Visited on 2019-08-30]. Available from: https://www.gwpharm.com/about/news/gw-pharmaceuticals-announces-european-medicines-agency-ema-accepts-epidiolexr

74. GW Pharmaceuticals - Sativex [Internet]. [Visited on 2019-05-11]. Available from: https://www.gwpharm.com/healthcare-professionals/sativex

75. Englund A, Morrison PD, Nottage J, Hague D, Kane F, Bonaccorso S, et al. Cannabidiol inhibits THC-elicited paranoid symptoms and hippocampal-dependent memory impairment. J Psychopharmacol. 2013 Jan;27(1):19–27.

76. Bornheim LM, Grillo MP. Characterization of cytochrome P450 3A inactivation by cannabidiol: possible involvement of cannabidiol-hydroxyquinone as a P450 inactivator. Chem Res Toxicol. 1998 Oct;11(10):1209–16.

77. Malfait AM, Gallily R, Sumariwalla PF, Malik AS, Andreakos E, Mechoulam R, et al. The nonpsychoactive cannabis constituent cannabidiol is an oral anti-arthritic therapeutic in murine collagen-induced arthritis. Proc Natl Acad Sci U S A. 2000 Aug;97(17):9561–6.

78. Carlini EA, Karniol IG, Renault PF, Schuster CR. Effects of marihuana in laboratory animals and in man. Br J Pharmacol. 1974 Feb;50(2):299–309.

79. Russo E, Guy GW. A tale of two cannabinoids: the therapeutic rationale for combining tetrahydrocannabinol and cannabidiol. Med Hypotheses. 2006;66(2):234–46.

80. Aurora Europe Gmbh website [Internet]. [Visited on 2019-05-11]. Available from: https://www.auroramedicine.com/

81. U.S. Pharmacopoeial Convention. Pharmacopoeia of the Unites States. Philadelphia, P.A.: P. Blakiston's Son & Company; 1916.

82. U.S. Pharmacopoeial Convention. U.S. Pharmacopoeia - 1926 (10th Ed). Philadelphia, P.A.; 1926.

83. Institute of Medicine. Marijuana and medicine: assessing the science base [Internet]. Joy JE, Stanley J. Watson J, John A. Benson J, editors. Washington, DC: The National Academies Press; 1999. Available from: https://www.nap.edu/catalog/6376/ marijuana-and-medicine-assessing-the-science-base

84. U.S Congress. Public Law: The comprehensive drug abuse prevention and control act of 1970.

85. Food and Drug Administration. FDA Website [Internet]. [Visited on 2019-04-04]. Available from: https://www.fda.gov/NewsEvents/PublicHealthFocus /ucm421163.htm

86. Food and Drug Administration. Marinol® (Dronabinol) Approval [Internet]. 2004. Available from: https://www.fda.gov/ohrms/dockets/dockets/05n0469/05N-0469-emc0004-04.pdf; 2004

87. Food and Drug Administration. Syndros® (Dronabinol) Approval. 2016;

88. Food and Drug Administration. Cesamet® (Nabilone) Approval. 2006.

89. Klieger SB, Gutman A, Allen L, Pacula RL, Ibrahim JK, Burris S. Mapping medical marijuana: state laws regulating patients, product safety, supply chains and dispensaries, 2017. Addiction. 2017 Dec;112(12):2206–16.

90. National Conference of State Legislatures. State Medical Marijuana Laws [Internet]. 2019 [cited 2019 Aug 30]. Available from: http://www.ncsl.org/research/health/state-medical-marijuana-laws.aspx

91. ProCon.org. 33 Legal Medical Marijuana States and DC [Internet]. 2019 [Visited on 2019-09-16]. Available from: https://medicalmarijuana.procon.org/view.resource.php?resourceID=000881

92. Department of Justice. Health Canada Website - Medical use of cannabis [Internet]. [Visited on 2019-09-22]. Available from: https://www.canada.ca/en/health-canada/topics/cannabis-for-medical-purposes.html

93. Government of Canada. Cannabis Regulations Règlement sur le cannabis [Internet]. Canada: Minister of Justice; 2018 p. 232. Available from: https://laws-lois.justice.gc.ca/PDF/SOR-2018-144.pdf

94. Health Canada. Sativex Fact Sheet [Internet]. [Visited on 2019-02-22]. Available from: https://www.canada.ca/en/health-canada/services/drugs-health-products/drug-products/notice-compliance/conditions/fact-sheet-sativex.html

95. Health Canada. Information for Health Care Professionals: Cannabis (marihuana, marijuana) and the cannabinoids.

96. Ablin J, Ste-Marie PA, Schäfer M, Häuser W, Fitzcharles MA. Medical use of cannabis products - Lessons to be learned from Israel and Canada Introduction. Schmerz. 2016;30(1):3–13.

97. Ministry of Health. Israel Ministry of Health website - Cannabis [Internet]. [Visited on 2019-05-25]. Available from: https://www.health.gov.il/English/MinistryUnits/HealthDivision/cannabis/Pages/default2.aspx

98. Schwartz Y. The Holy Land of Medical Marijuana [Internet]. 2017 [Visited on 2019-09-16]. Available from: https://www.usnews.com/news/best-countries/articles/2017-04-11/israel-is-a-global-leader-in-marijuana-research

99. Florida RL, Martin Prosperity Institute. C, Canadian Electronic Library K. Creativity and prosperity : the global creativity index [Internet]. 2012. Available from: https://tspace.library.utoronto.ca/handle/1807/80125

100. European Monitoring Centre for Drugs and Drug Addiction (EMDDA). Cannabis legislation in Europe [Internet]. Luxembourg: Publications Office of the European Union; 2017. 1–30 p. Available from: http://www.emcdda.europa.eu/system/files/publications/4135/TD0217210ENN.pdf

101. Ministero della Salute. Testo unico delle leggi in materia di disciplina degli stupefacenti e sostanze psicotrope, prevenzione, cura e riabilitazione dei relativi stati di tossicodipendenza. Decreto del Presidente della Repubblica 09 ottobre, n. 309; Italy; 1990 p. 1–12.

102. Ministero della Salute. Funzioni di Organismo statale per la cannabis previsto dagli articoli 23 e 28 della convenzione unica sugli stupefacenti del 1961, come modificata nel 1972. Allegato rettificato dal Comunicato 07 gennaio 2016. Decreto 09 novembre 2015; Italy; 2015 p. 1–12.

103. Ministero della Salute. Website [Internet]. [Visited on 2019-05-27]. Available from: http://www.salute.gov.it/portale/temi/p2_6.jsp?lingua=italiano&id=4588&area=sostanzeStupefacenti&menu=organismo

104. The National Academies of Sciences Engineering and Medicine. Website [Internet]. [Visited on 2019-09-16]. Available from: http://nationalacademies.org/about/whoweare/index.html

105. U.S. Department of Justice - Drug Enforcement Administration. Title 21 Code of Federal Regulations [Internet]. [Visited on 2019-09-16]. Available from: https://www.deadiversion.usdoj.gov/21cfr/cfr/2108cfrt.htm

106. Gertsch J, Pertwee RG, Di Marzo V. Phytocannabinoids beyond the Cannabis plant - do they exist? Br J Pharmacol. 2010 Jun;160(3):523–9.

107. Di Marzo V. Cannabinoids. Chichester, West Sussex, United Kingdom: Wiley Blackwell; 2014. 310 p.

108. Appendino G, Taglialatela-Scafati O. Cannabinoids: chemistry and medicine. Nat Prod Phytochem Bot Metab Alkaloids, Phenolics Terpenes. 2013;(1):3415–35.

109. Flemming T, Muntendam R, Steup C, Kayser O. Chemistry and biological activity of tetrahydrocannabinol and its derivatives. Top Heterocycl Chem. 2007;10:1–42.

110. PubChem Dronabinol [Internet]. Available from: https://pubchem.ncbi.nlm.nih.gov/compound/16078#section=Top

111. Izzo AA, Borrelli F, Capasso R, Di Marzo V, Mechoulam R. Non-psychotropic plant cannabinoids: new therapeutic opportunities from an ancient herb. Trends Pharmacol Sci. 2009 Oct;30(10):515–27.

112. PubChem Cannabidiol [Internet]. Available from: https://pubchem.ncbi.nlm.nih.gov/compound/644019

113. Thomas BF, Adams IB, Mascarella SW, Martin BR, Razdan RK. Structure-activity analysis of anandamide analogs: relationship to a cannabinoid pharmacophore. J Med Chem. 1996;39(2):471–9.

114. Appendino G, Chianese G, Taglialatela-Scafati O. Cannabinoids: occurrence and medicinal chemistry. Curr Med Chem. 2011;18(7):1085–99.

115. PubChem Desoxy-CBD [Internet]. Available from: https://pubchem.ncbi.nlm.nih.gov/compounds/50919314#section=Top

116. Xiong W, Cheng K, Cui T, Godlewski G, Rice KC, Xu Y, et al. Cannabinoid potentiation of glycine receptors contributes to cannabis-induced analgesia. Nat Chem Biol [Internet]. 2011;7(5):296–303. Available from: http://dx.doi.org/10.1038/nchembio.552

117. Foster E, Wildner H, Zeilhofer HU, Tudeau L, Haueter S, Ralvenius WT, et al. Targeted ablation , silencing , and activation establish glycinergic dorsal horn neurons as key components of a spinal gate for pain and itch. Neuron. 2015;85:1289–304.

118. Imlach WL. New approaches to target glycinergic neurotransmission for the treatment of chronic pain. Pharmacol Res [Internet]. 2017;116:93–9. Available from: http://dx.doi.org/10.1016/j.phrs.2016.12.019

119. Lynch JW. Molecular structure and function of the glycine receptor chloride channel. Physiol Rev. 2004 Oct;84(4):1051–95.

120. Hejazi N, Zhou C, Oz M, Sun H, Ye JH, Zhang L. Delta9-tetrahydrocannabinol and endogenous cannabinoid anandamide directly potentiate the function of glycine receptors. Mol Pharmacol. 2006 Mar;69(3):991–7.

121. Ahrens J, Demir R, Leuwer M, De La Roche J, Krampfl K, Foadi N, et al. The nonpsychotropic cannabinoid cannabidiol modulates and directly activates α1 and α1-β glycine receptor function. Pharmacology. 2009;83(4):217–22.

122. Xiong W, Wu X, Lovinger DM, Zhang L. A Common molecular basis for exogenous and endogenous cannabinoid potentiation of glycine receptors. J Neurosci. 2012;32(15):5200–8.

123. Xiong W, Cui T, Cheng K, Yang F, Chen SR, Willenbring D, et al. Cannabinoids suppress inflammatory and neuropathic pain by targeting α3 glycine receptors. J Exp

Med. 2012;209(6):1121–34.

124. Reggio PH, Bramblett RD, Yuknavich H, Seltzman HH, Fleming DN, Fernando SR, et al. The design, synthesis and testing of desoxy-CBD: further evidence for a region of steric interference at the cannabinoid receptor. Life Sci. 1995;56(23–24):2025–32.

125. Petrzilka, T, Haefliger, W, Sikemeier C. Synthese von Haschisch-Inhaltsstoffen. Helv Chim Acta. 1969;52(4):1102–34.

126. Wilkinson SM, Price J, Kassiou M. Improved accessibility to the desoxy analogues of Δ^9-tetrahydrocannabinol and cannabidiol. Tetrahedron Lett [Internet]. 2013;54(1):52–4. Available from: http://dx.doi.org/10.1016/j.tetlet.2012.10.080

127. Autoxydation Z, Schenck VG, Ohloff G, Schroeter S. Zur Autoxydation des (+)-Limonens. 1965;1(1957):26–39.

128. Rickards RW, Watson WP. Conversion of (+)-(R)-Limonene into (+)-(1S,4R)-p-mentha-2,8-dien-1-ol, an intermediate in the synthesis of tetrahydrocannabinoids. Aust J Chem [Internet]. 1980;33(2):451–4. Available from: https://doi.org/10.1071/CH9800451

129. Steiner D, Ivison L, Goralski CT, Appell RB, Gojkovic R. A facile and efficient method for the kinetic separation of commercially available cis - and trans -limonene epoxide. 2002;13:2359–63.

130. Hauenstein O, Reiter M, Agarwal S, Rieger B, Greiner A. Bio-based polycarbonate from limonene oxide and CO2 with high molecular weight, excellent thermal resistance, hardness and transparency. Green Chem. 2016;1:760–70.

131. Shao Z, Yin J, Chapman K, Grzemska M, Clark L, Wang J, et al. High-resolution crystal structure of the human CB1 cannabinoid receptor. Nature [Internet]. 2016;540(7634):602–6. Available from: http://dx.doi.org/10.1038/nature20613

132. Prost-Squarcioni C. Histology of skin and hair follicle. Med Sci (Paris). 2006 Feb;22(2):131–7.

133. Bouwstra JA, Honeywell-Nguyen PL, Gooris GS, Ponec M. Structure of the skin barrier and its modulation by vesicular formulations. Prog Lipid Res [Internet]. 2003;42(1):1–36. Available from: http://www.sciencedirect.com/science/article/pii/S0163782702000280

134. Bhandari KH, Lee DX, Newa M, Yoon SII, Kim JS, Kim DD, et al. Evaluation of skin permeation and accumulation profiles of a highly lipophilic fatty ester. Arch Pharm Res [Internet]. 2008 Feb;31(2):242–9. Available from: https://doi.org/10.1007/s12272-001-1148-8

135. Goyal R, Macri LK, Kaplan HM, Kohn J. Nanoparticles and nanofibers for topical drug

delivery. J Control Release. 2016;240:77–92.

136. Schaefer H, Redelmeier TE. Skin barrier : principles of percutaneous absorption. Basel; New York: Karger; 1996.

137. Barry BW. Dermatological formulations: percutaneous absorption. J Pharm Sci [Internet]. 1984;73(4):573. Available from: https://onlinelibrary.wiley.com/doi/abs/10.1002/jps.2600730442

138. Touitou E. Drug delivery across the skin. Expert Opin Biol Ther [Internet]. 2002;2(7):723–33. Available from: http://www.tandfonline.com/doi/full/10.1517/14712598.2.7.723

139. Parnham MJ. Liposome dermatics. In: Braun-Falco O, Korting HC, Maibach HI, editors. Drug News and Perspectives. 1991. p. 567–70.

140. Korting HC, Zienicke H, Schäfer-Korting M, Braun-Falco O. Liposome encapsulation improves efficacy of betamethasone dipropionate in atopic eczema but not in psoriasis vulgaris. Eur J Clin Pharmacol [Internet]. 1990 Oct;39(4):349–51. Available from: https://doi.org/10.1007/BF00315408

141. Natsheh H, Vettorato E, Touitou E. Ethosomes for dermal administration of natural active molecules. Curr Pharm Des. 2019;25:1–11.

142. Cevc G. Transfersomes, liposomes and other lipid suspensions on the skin: permeation enhancement, vesicle penetration, and transdermal drug delivery. Crit Rev Ther Drug Carrier Syst. 1996;13(3–4):257–388.

143. Touitou E. Composition for applying substances to or through the skin. United States Patent; 5,716,638, 1998.

144. Touitou E, Dayan N, Bergelson L, Godin B, Eliaz M. Ethosomes - Novel vesicular carriers for enhanced delivery: characterization and skin penetration properties. J Control Release. 2000;65(3):403–18.

145. Chang LW, Hou ML, Tsai TH. Silymarin in liposomes and ethosomes: Pharmacokinetics and tissue distribution in free-moving rats by high-performance liquid chromatography-tandem mass spectrometry. J Agric Food Chem. 2014;62(48):11657–65.

146. Ramadon D, Wirarti GA, Anwar E. Novel transdermal ethosomal gel containing green tea (Camellia sinensis L. Kuntze) leaves extract: Formulation and in vitro penetration study. J Young Pharm. 2017;9(3):336–40.

147. Godin B, Touitou E. Mechanism of bacitracin permeation enhancement through the skin and cellular membranes from an ethosomal carrier. J Control Release. 2004;94(2–3):365–79.

148. Shumilov M, Touitou E. Buspirone transdermal administration for menopausal syndromes, in vitro and in animal model studies. Int J Pharm [Internet]. 2010;387(1–2):26–33. Available from: http://dx.doi.org/10.1016/j.ijpharm.2009.11.029

149. Dayan N, Touitou E. Carriers for skin delivery of trihexyphenidyl HCl-ethosomes vs liposomes. Biomaterials. 2000;21:1879–85.

150. Godin B, Touitou E. Erythromycin ethosomal systems: physicochemical characterization and enhanced antibacterial activity. CurrDrug Deliv. 2005;2(1567-2018 (Print)):269–75.

151. Touitou E, Godin B, Dayan N, Weiss C, Piliponsky A, Levi-Schaffer F. Intracellular delivery mediated by an ethosomal carrier. Biomaterials. 2001;22(22):3053–9.

152. Shen L-N, Zhang Y-T, Wang Q, Xu L, Feng N-P. Enhanced in vitro and in vivo skin deposition of apigenin delivered using ethosomes. Int J Pharm [Internet]. 2014;460:280–8. Available from: http://dx.doi.org/10.1016/j.ijpharm.2013.11.017

153. Zhang Y, Ng W, Feng X, Cao F, Xu H. Lipid vesicular nanocarrier: Quick encapsulation efficiency determination and transcutaneous application. Int J Pharm [Internet]. 2017;516(1–2):225–30. Available from: http://dx.doi.org/10.1016/j.ijpharm.2016.11.011

154. Jain S, Patel N, Madan P, Lin S. Formulation and rheological evaluation of ethosome-loaded carbopol hydrogel for transdermal application. Drug Dev Ind Pharm. 2016;42(8):1315–24.

155. Ng S-F, Rouse J, Sanderson D, Eccleston G. A comparative study of transmembrane diffusion and permeation of ibuprofen across synthetic membranes using franz diffusion cells. Pharmaceutics. 2010 May;2(2):209–23.

156. Wagner H, Ulrich-Merzenich G. Synergy research: Approaching a new generation of phytopharmaceuticals. Phytomedicine. 2009;16:97–110.

157. Karniol IG, Shirakawa I, Kasinski N, Pfeferman A, Carlini EA. Cannabidiol interferes with the effects of Δ^9-tetrahydrocannabinol in man. Eur J Pharmacol. 1974;28:172–7.

158. Bettiol A, Lombardi N, Crescioli G, Maggini V, Gallo E, Mugelli A, et al. Galenic preparations of therapeutic Cannabis sativa differ in cannabinoids concentration: A quantitative analysis of variability and possible clinical implications. Front Pharmacol. 2019;9(JAN):1–7.

159. Citti C, Ciccarella G, Braghiroli D, Parenti C, Angela M, Cannazza G. Medicinal cannabis : Principal cannabinoids concentration and their stability evaluated by a high performance liquid chromatography coupled to diode array and quadrupole time of flight mass spectrometry method. J Pharm Biomed Anal [Internet]. 2016;128:201–9. Available

from: http://dx.doi.org/10.1016/j.jpba.2016.05.033

160. Pacifici R, Marchei E, Salvatore F, Guandalini L, Busardò FP, Pichini S. Evaluation of cannabinoids concentration and stability in standardized preparations of cannabis tea and cannabis oil by ultra-high performance liquid chromatography tandem mass spectrometry. Clin Chem Lab Med. 2017;55(10):1555–63.

161. Carcieri C, Tomasello C, Simiele M, De Nicolò A, Avataneo V, Canzoneri L, et al. Cannabinoids concentration variability in cannabis olive oil galenic preparations. J Pharm Pharmacol. 2018;70(1):143–9.

162. Office of Medicinal Cannabis. Medicinal Cannabis – Types of Medicinal Cannabis [Internet]. 2019 [Visited on 2019-09-18]. Available from: https://www.cannabisbureau.nl/english/medicinal-cannabis

163. Ahmed AIA, van den Elsen GAH, Colbers A, van der Marck MA, Burger DM, Feuth TB, et al. Safety and pharmacokinetics of oral delta-9-tetrahydrocannabinol in healthy older subjects: A randomized controlled trial. Eur Neuropsychopharmacol [Internet]. 2014;24(9):1475–82. Available from: http://dx.doi.org/10.1016/j.euroneuro.2014.06.007

164. Agenzia Italiana del Farmaco - AIFA. Foglio illustrativo: informazioni per il paziente Sativex Spray per mucosa orale [Internet]. [Visited on 2019-09-11]. Available from: https://farmaci.agenziafarmaco.gov.it/aifa/servlet/PdfDownloadServlet?pdfFileName=footer_003471_040548_FI.pdf&retry=0&sys=m0b1l3

165. Casiraghi A, Roda G, Casagni E, Cristina C, Musazzi UM, Franzè S, et al. Extraction method and analysis of cannabinoids in cannabis olive oil preparations. Planta Med. 2018;84(4):242–9.

166. Società Italiana Farmacisti Preparatori - SIFAP. Estrazione oleosa di infiorescenze femminili di Cannabis. 2017.

167. Politi M, Peschel W, Wilson N, Zloh M, Prieto JM, Heinrich M. Direct NMR analysis of cannabis water extracts and tinctures and semi-quantitative data on Δ^9-THC and Δ^9-THC-acid. Phytochemistry. 2008;69(2):562–70.

168. Peschel W. Quality control of traditional Cannabis tinctures: Pattern, markers, and stability. Sci Pharm. 2016;84(3):567–84.

169. Ibarguren M, López DJ, Escribá P V. The effect of natural and synthetic fatty acids on membrane structure, microdomain organization, cellular functions and human health. Biochim Biophys Acta-Biomembr [Internet]. 2014;1838(6):1518–28. Avail. from: http://www.sciencedirect.com/science/article/pii/S0005273613004604

170. Ptak M, Egret-Charlier M, Sanson A, Bouloussa O. A NMR study of the ionization of fatty acids, fatty amines and N-acylamino acids incorporated in phosphatidylcholine vesicles. Biochim Biophys Acta - Biomembr. 1980;600(2):387–97.

171. Gebicki JM, Hicks M. Ufasomes are stable particles surrounded by unsaturated fatty acid membranes. Nature. 1973;243(5404):232–4.

172. Salentinig S, Sagalowicz L, Glatter O. Self-assembled structures and pK_a value of oleic acid in systems of biological levance. Langmuir. 2010;26(14):11670–9.

173. Mally M, Peterlin P, Svetina S. Partitioning of oleic acid into phosphatidylcholine membranes is amplified by strain. J Phys Chem B. 2013;117(40):12086–94.

174. Shih L, Chung Y, Sriram R, Jue T. Interaction of myoglobin with oleic acid. Chem Phys Lipids [Internet]. 2015;191:115–22. Available from: http://www.sciencedirect.com/science/article/pii/S0009308415300153

175. Talló K, Moner V, De Cabo M, Cócera M, López O. Vesicular nanostructures composed of oleic acid and phosphatidylcholine: effect of pH and molar ratio. Chem Phys Lipids. 2018;213(April):96–101.

176. Mabrey S, Sturtevant JM. Incorporation of saturated fatty acids into phosphatidylcholine bilayers. Biochim Biophys Acta (BBA)/Lipids Lipid Metab. 1977;486(3):444–50.

177. Cistola DP, Hamilton JA, Jackson D, Small DM. Ionization and phase behavior of fatty acids in water: application of the Gibbs phase rule. Biochemistry. 1988;27(6):1881–8.

178. Cistola DP, Small DM, Hamilton JA. Ionization behavior of aqueous short-chain carboxylic acids: a carbon-13 NMR study. J Lipid Res [Internet]. 1982 Jul 1;23(5):795–9. Available from: http://www.jlr.org/content/23/5/795.abstract

179. Cistola DP, Small DM, Hamilton JA. Carbon 13 NMR studies of saturated fatty acids bound to bovine serum albumin. II. Electrostatic interactions in individual fatty acid binding sites. J Biol Chem. 1987;262(23):10980–5.

180. DeBacker B, Debrus B, Lebrun P, Theunis L, Dubois N, Decock L, et al. Innovative development and validation of an HPLC / DAD method for the qualitative and quantitative determination of major cannabinoids in cannabis plant material. J Chromatogr B. 2009;877:4115–24.

Acknowledgements

I would like to thank Professor Nicola Realdon for the great support throughout the entire project, as well as its expertise and advice. For the development of a PhD thesis on medical cannabis, special thanks are required for Professor Pietro Giusti and its knowledge of cannabinoids and endocannabinoids.

I want to thank Professor Giovanni Marzaro for the support and expertise in Medicinal Chemistry, as well as its laboratory group.

For the studies performed during the last year of this PhD project, I warmly thank Professor Elka Touitou and Doctor Hiba Natsheh for accepting me in their laboratory, for their patience and their valuable expertise on the development of soft, deformable vesicles.

I want to thank Doctor Antonella Casiraghi and Professor Stefano Dall'Acqua for their fundamental contribution to the studies over cannabis extraction and skin permeation experiments.

Thanks to Miss Martina Marcon, Miss Desiré Zanin, Miss Lucia Lequaglie, and Miss Marisa Fiordelisi for their contribution to the experimental activities.